A research on the drug discovery of tyrosine kinase inhibitors in hematological malignancies with animal model constructions

YOHEI NAKAYA

September 2014

A research on the drug discovery of tyrosine kinase inhibitors in hematological malignancies with animal model constructions

A dissertation submitted to

THE GRADUATE SCHOOL OF ENGINEERING SCIENCE

OSAKA UNIVERSITY

in partial fulfillment of the requirements for the degree of

DOCTOR OF PHILOSOPHY IN ENGINEERING

BY

YOHEI NAKAYA

September 2014

Abstract

Tyrosine kinases have been attracting considerable attention as target molecules for cancer therapy. Tyrosine kinases are enzymes which phosphorylate protein substrates, and they function as modulators of signal transduction pathways that induce cell proliferation. Tyrosine kinases can cause cancer when abnormally activated by gene mutations. Although various tyrosine kinase inhibitors have been created by many researchers and companies as drug candidates, only a few of them have been put to practical use in the treatment of cancer.

One of the challenges in the successful development of a tyrosine kinase inhibitor is an *in vivo* evaluation to select promising compounds. The subcutaneous tumor-bearing mouse model which is often used has several problems. One of the most important of these problems is that the model does not always accurately reflect the pathology of cancer patients. In order to evaluate compounds properly, disease model animals which closely mimic the pathology of the specific cancer are necessary. The purpose of the present study was to increase the probability of selecting promising compounds in two projects for developing selective tyrosine kinase inhibitors as cancer therapeutics, by constructing appropriate disease model animals and using them to evaluate the efficacy of drug candidates. To this end, (1) I constructed mouse models of hematological malignancies (a Ba/F3 transplant model, a bone marrow transplantation model, and a transgenic model), and used these model mice in exploratory research on (2) dual BCR-ABL/ LYN tyrosine kinase inhibitors for the treatment of drug-resistant chronic myeloid leukemia (CML) and (3) selective JAK2 tyrosine kinase inhibitors for the treatment of myeloproliferative neoplasms (MPN).

(1) I constructed a mouse model of drug-resistant CML by transplanting Ba/F3 cell lines which had been retrovirally transduced with the causative genes (mutated BCR-ABL genes). These mice exhibited the pathology of leukemia in a short period of time, and were resistant to existing drug (Ba/F3 transplant model). Similarly, I constructed a mouse model of MPN by transplanting donor bone marrow cells retrovirally transduced with the causative mutated JAK2 genes (bone marrow transplant model). I also adopted transgenic mice which expressed mutated JAK2 under the control of the $H2K_b$ promoter, as an animal model that reproduced the characteristic pathology of MPN (transgenic model). (2) A group of compounds including NS-187 has been found as a result of screening for dual BCR-ABL/ LYN tyrosine kinase inhibitors. I demonstrated that NS-187 substantially prolonged survival in Ba/F3 transplant model

mice. (3) A group of compounds including NS-018 was discovered by screening for potent and selective JAK2 inhibitors. I conducted repeat-dose tests of NS-018 in bone marrow transplant and transgenic model mice, and demonstrated that NS-018 had good efficacy with reduced hematological adverse effects.

In this study, I constructed animal models that accurately reflected patient pathology in two types of hematological malignancies that could not be reproduced in conventional models. As a result of improved screening of tyrosine kinase inhibitors using these animal models, it was possible to increase the probability of selecting promising compounds. The compounds selected, NS-187 and NS-018, are in clinical trial for the treatment of CML and MPN, respectively.

Contents

Chapter 1

General introduction

1-1 Molecularly targeted anticancer drugs

1-1-1 History of cancer research

Cancer research has a history of over 2000 years [1]. The ancient Greek physician Hippocrates, the “Father of Medicine”, described several kinds of cancer. He named it “cancer”, meaning crab or crayfish. In ancient Rome, Galen proposed that cancer occurred because of an imbalance in the four basic body fluids (Humorism). His theories dominated and influenced medical science in the Western and Islamic worlds for more than 1300 years. During the Renaissance, scientists developed a greater understanding of the human body and disease. Followers of René Descartes believed that all disease was the outcome of chemical processes, and that acidic lymph fluid was the cause of cancer (Lymph theory). In the 19th century, Johannes Müller demonstrated that cancer tissue was made of cells and not lymph, and proposed that cancer cells developed from budding elements between normal tissues (Blastema theory). His student Rudolph Virchow proposed that chronic irritation was the cause of cancer (Chronic irritation theory). Throughout the 17th and 18th centuries, some scientists believed that cancer was contagious (Infectious disease theory). In the 18th century, John Hill recognized tobacco as a substance that caused cancer (chemical carcinogen), while in 1911 Peyton Rous showed that certain viruses can increase the risk of developing cancer (viral carcinogen). The genetic basis of cancer was recognized by Theodor Boveri in 1902. He suggested that mutations of chromosomes could generate a cell with unlimited growth potential which could be passed on to its descendants (Chromosome theory).

Today scientists know that cancer is fundamentally a disease involving failure of the regulation of tissue growth. It usually results from changes in genetic or epigenetic factors, which could be caused by chemicals, radiation, or viruses, although there is a hereditary component to some cancers. However, the mechanisms of cancer

development have not been completely elucidated, and different researchers have different views on the mechanisms involved. The mainstream theory is that the degree of malignancy increases with the accumulation of genetic abnormalities within a cell (Multistep carcinogenesis). Some researchers have proposed that the different kinds of cells in a heterogeneous tumor arise from a single cell, which retains key stem cell properties (Cancer stem cell hypothesis). They advocate that the relapse of cancer and the emergence of metastasis are also attributable to cancer stem cells. There are many other concepts and ideas on oncogenesis. As described later, this thesis addresses the theme of molecularly targeted anticancer drugs, and employs a hypothesis called “driver mutation“ or “oncogene addiction” [2], which provides a rationale for molecularly targeted therapy.

1-1-2 Cancer epidemiology and treatment

The worldwide cancer patient population continues to grow. In Japan, the number of cancer cases in 2007 was approximately 704000, and the number of cancer deaths in 2011 was approximately 357000 [3]. It is estimated that one in two Japanese are diagnosed with cancer during their lifetime, and that one in four Japanese males and one in six Japanese females die from cancer. The incidence of cancer is expected to further increase in step with the aging of the population (Figure 1-1) [4].

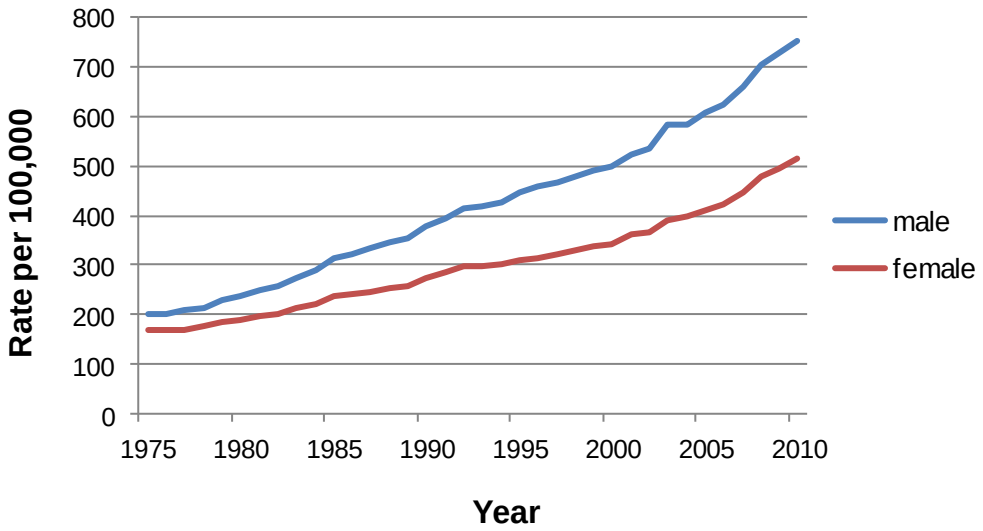

Figure 1-1. Incidence of cancer in Japan.
The crude incidence rate of cancer has been continuously increasing for both sexes since the 1980’s.

The main treatments for cancer include surgery, radiation therapy, and chemotherapy. In many types of cancer, including advanced-stage carcinomas and hematological malignancies, surgery and radiation therapy are not feasible. In such cases, chemotherapy with anticancer drugs is used. Although the treatment outcome of chemotherapy has improved, many patients still have recurrences of cancer. Furthermore, because most conventional anticancer drugs are cytotoxic not only to cancer cells but also to normal cells, side effects are inevitable. Cancer treatments with fewer side effects and a lower risk of cancer relapse are highly desirable.

1-1-3 Molecularly targeted anticancer drugs

Molecularly targeted anticancer drugs block a specific target molecule which is expressed specifically or excessively and is needed for the growth of the cancer cells. Molecularly targeted anticancer drugs differ from conventional anticancer drugs in several ways. Thus, molecularly targeted anticancer drugs act on specific molecular targets that are associated with cancer, whereas most conventional chemotherapeutic agents act on all rapidly dividing cells, both normal and cancer cells. In addition, molecularly targeted anticancer drugs are deliberately chosen or designed to interact with their target, whereas many conventional anticancer drugs were identified by their ability to kill cells. In principle, molecularly targeted anticancer drugs are expected to be more effective than conventional chemotherapeutic agents and less harmful to normal cells.

Molecularly targeted anticancer drugs include monoclonal antibodies and small-molecule inhibitors. Monoclonal antibodies are a good approach for targeting extracellular/cell surface molecules. On the other hand, small-molecule inhibitors have the advantages that they can be targeted to intracellular molecules and administered orally. This thesis concerns small-molecule inhibitors. Small-molecule compounds often inhibit non-target molecules as well as the target molecule, leading to unexpected adverse effects. Therefore, to increase the effectiveness of small-molecule compounds and decrease their side effects, rational drug design to increase target selectivity is important.

It is difficult to select an appropriate target molecule for a molecularly targeted anticancer drug. There are a lot of signaling pathways involved in the growth of cancer cells (Figure 1-2) [5]. Even if one pathway is inhibited, cancer cells can often survive by using other pathways. However, the inhibition of many pathways will increase not only

the efficacy but also the likelihood of adverse effects. Although the inhibition of a limited number of pathways is possible, it is unrealistic to try all combinations of a few pathways because of the large number of combinations. Recent studies indicate that there is a singular solution to certain types of cancer. The survival and proliferation of some cancer cells are almost completely dependent on a few pathways downstream of the mutated molecule (oncogene addiction) [2,6]. In this specific case, complete inhibition of the mutated molecule can eliminate the cancer cells. Mutated tyrosine kinases in certain types of hematological malignancy are such candidate target molecules.

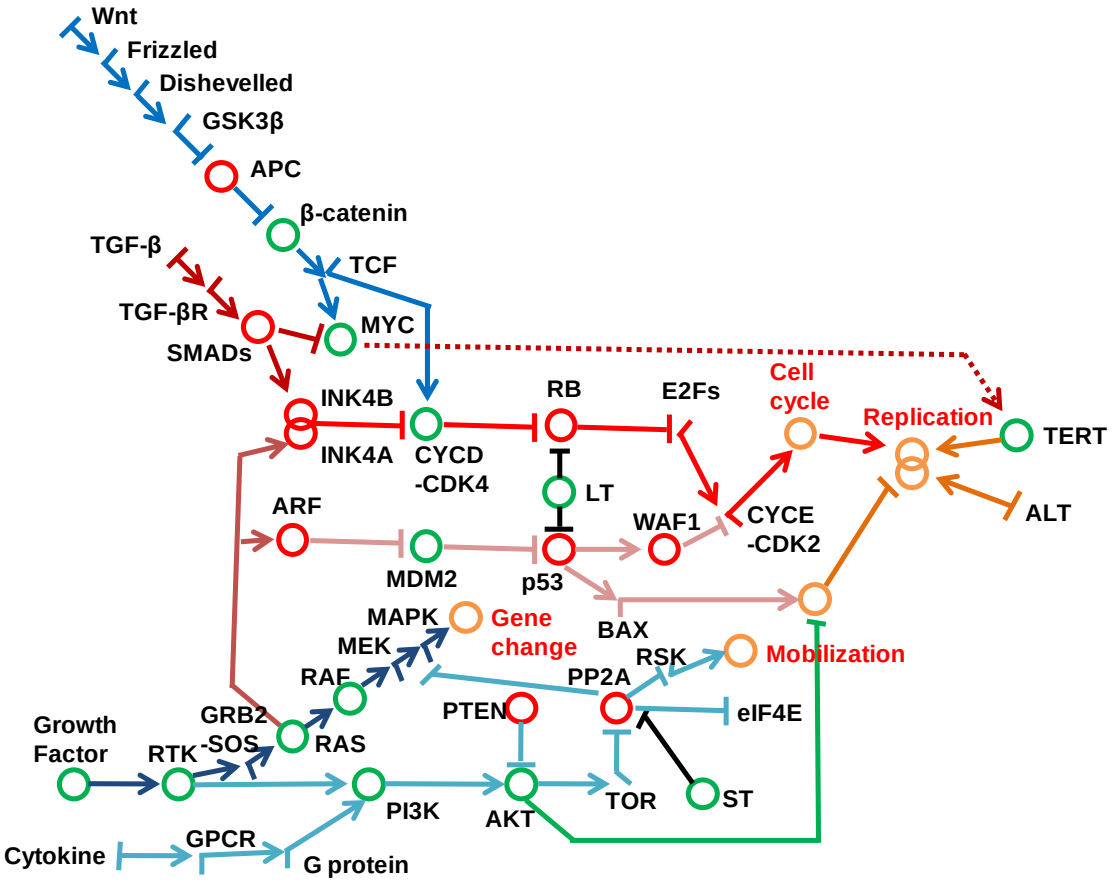

Figure 1-2. Signaling pathways in cancer.

During oncogenesis, gene mutations or expression changes accumulate in biological pathways such as those involved in the cell cycle, apoptosis, DNA damage repair, growth factor responses, cell adhesion, and angiogenesis.

1-2 Tyrosine kinase inhibitors

1-2-1 Function and categories of kinases

Kinases are enzymes that transfer phosphate groups from ATP to specific substrates, a process referred to as phosphorylation. Kinases function as regulators (on/off switches) of metabolic and signal-transduction pathways in cells.

Kinases are broadly classified into two types: (1) those that act on low-molecular-weight substrates in mainly metabolic pathways (e.g., creatine kinase, pyruvate kinase, hexokinase), and (2) those that act on protein substrates in intracellular signal-transduction pathways (protein kinases). This thesis concerns protein kinases. Eukaryotic protein kinases include tyrosine kinases and serine/threonine kinases, which phosphorylate the hydroxyl group of tyrosine residues or serine/threonine residues, respectively, of various proteins. There are at least 518 protein kinases in the human genome, and they are classified into nine groups by sequence homology (Figure 1-3) [7]. Of these protein kinases, 90 are tyrosine kinases, and the rest are serine/threonine kinases. Tyrosine kinases can be further divided into receptor tyrosine kinases and non-receptor tyrosine kinases. JAK-family and SRC-family kinases and ABL kinase, covered in this thesis, are non-receptor tyrosine kinases.

More than 99% of amino acids phosphorylated by kinases are serine/threonine, and the phosphorylated tyrosines represent less than 0.1%. However, the quantitatively less important phosphorylation of tyrosine plays an important physiological role. Tyrosine kinases function as regulators of signaling involved in cell differentiation, proliferation, adhesion, and immune reactions. Binding of growth factors and cytokines, such as insulin and interferon, to their receptors is converted to intracellular signals by tyrosine kinases. The phosphorylated protein changes its structure and relays signals downstream.

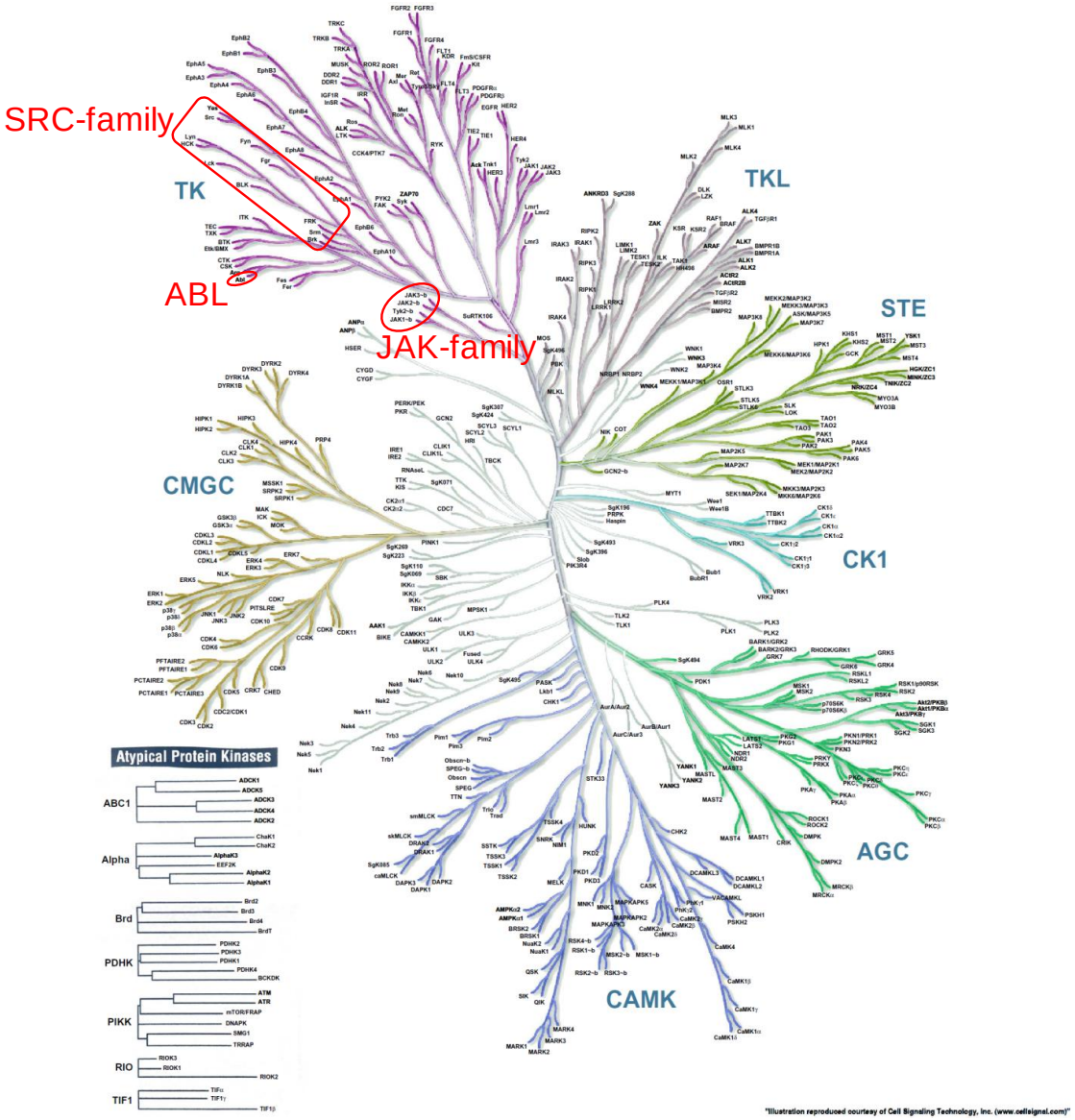

Figure 1-3. Phylogenetic tree of kinase family.

Human protein kinases are classified into nine major groups, and are subdivided into families, and sometimes subfamilies, based on the sequence of their kinase domains. Illustration reproduced courtesy of Cell Signaling Technology, Inc. (www.cellsignal.com).

1-2-2 Structure and activation of kinases

Although most protein kinases contain multiple domains, the kinase activity is associated with a kinase domain, which is highly conserved. The kinase domain can be

divided into subdomains: the N-terminal lobe, the C-terminal lobe, and the hinge region connecting them (Figure 1-4) [8]. The N-terminal lobe is mainly involved in the binding and placement of ATP via the phosphate-binding loop (P-loop). The C-terminal lobe is involved in the recognition and binding of the substrate protein and in part ATP-binding via the activation loop (A-loop), which changes its conformation greatly by phosphorylation. In the C-terminal lobe, there is a catalytic loop (C-loop) which contains an aspartic acid residue as the catalytic base in the phosphorylation reaction. A deep cleft between the two lobes is the active center, in which the binding of ATP and the protein substrate occur.

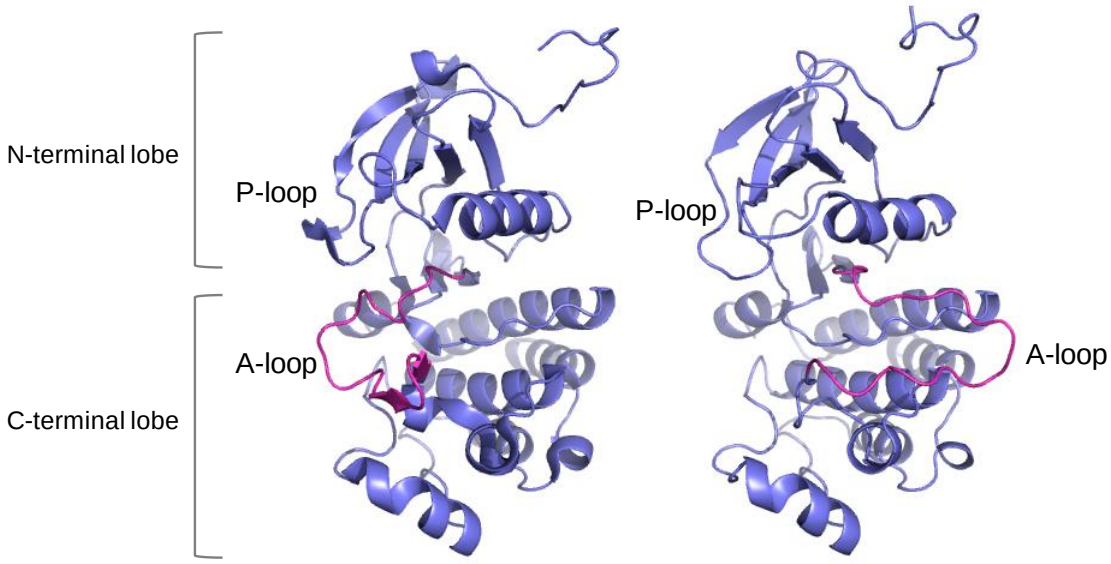

Figure 1-4. Structure of the kinase domain.
Left: Off (inactive) state of ABL. Right: On (activated) state of ABL. The activation loop (A-loop) is shown in pink. Protein Data bank IDs are 1IEP and 2GQG.

Kinase activation is highly regulated, and the kinase itself is turned on or off by phosphorylation. In the off (inactive) state, A-loop is folded and blocks the cleft between the lobes so that ATP cannot reach the catalytic center of the kinase. When it is converted to the on (activated) state by phosphorylation (sometimes by another kinase and sometimes by the kinase itself; *cis*-phosphorylation/autophosphorylation), the phosphorylated A-loop moves away from the cleft, and ATP and the substrate protein can reach the binding site in the active center.

1-2-3 Tyrosine kinase mutations in hematological malignancy

Kinase activation is usually tightly controlled, but kinases can be activated constitutively by gene mutations. The aberrant activation of kinases by mutations has been reported in some types of cancer, including hematological malignancies.

For example, BCR-ABL is an abnormal fusion kinase detected in virtually all patients with chronic myeloid leukemia (CML) [9]. As a result of chromosomal translocation, part of the BCR gene from chromosome 22 is fused with the ABL gene on chromosome 9 (Figure 1-5). Because ABL is a tyrosine kinase, the BCR-ABL fusion gene product is also a tyrosine kinase. The kinase domain of normal ABL tyrosine kinase is negatively regulated by the SH3 domain and does not show activity. However, in BCR-ABL kinase the suppressive function is released by the formation of a tetramer around the N-terminal portion of BCR. As a result of intermolecular phosphorylation, BCR-ABL kinase is constitutively active. BCR-ABL tyrosine kinase promotes aberrant cell growth and anti-apoptotic signaling mainly by activating the RAS, PI3K/AKT, and STAT pathways. Thus, BCR-ABL fusion is a driver mutation that gives a selective advantage to a clone cell and causes clonal expansions in CML.

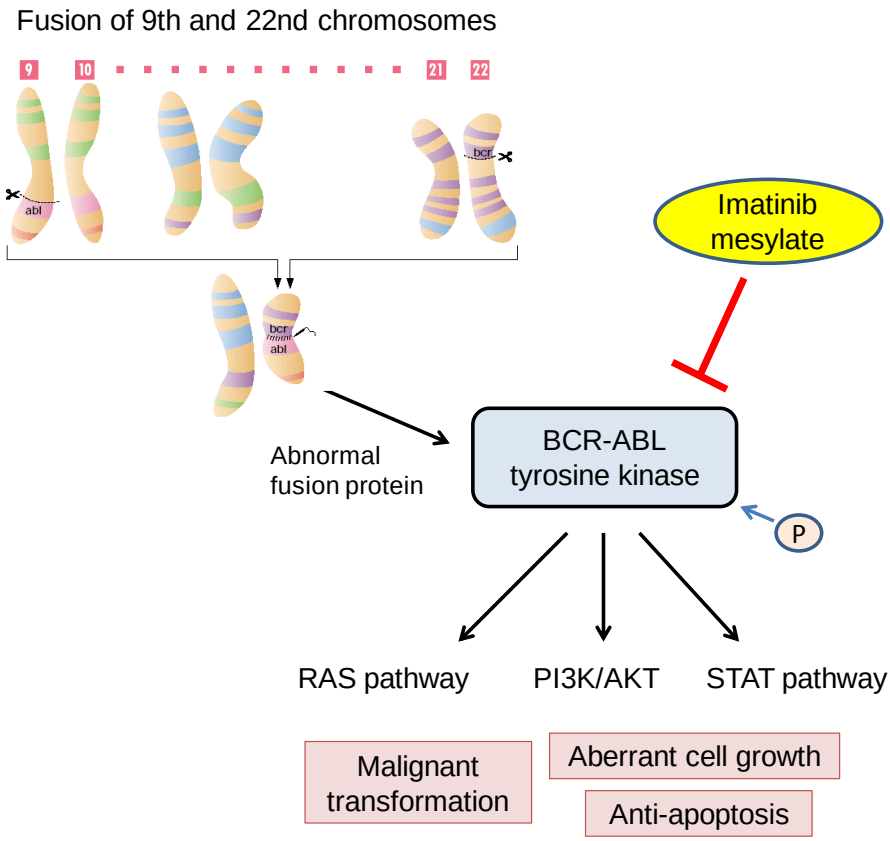

Figure 1-5. BCR-ABL tyrosine kinase in chronic myeloid leukemia.
The reciprocal translocation between the chromosomes 9 and 22 results in the generation of the abnormal tyrosine kinase BCR-ABL, which causes unregulated cell proliferation and malignant alteration.

Another example of the aberrant activation of a kinase by a mutation is a mutation of JAK2 tyrosine kinase observed in patients with myeloproliferative neoplasms (MPN) [10]. JAK2 tyrosine kinase has seven JH (Janus homology) domains (Figure 1-6). The JH1 domain at the C-terminal site has kinase activity. The JH2 domain is a pseudokinase domain that does not have kinase activity. JAK2 kinase is usually maintained in an inactive state by interaction of the JH1 and JH2 domains. A point mutation (V617F) in the JH2 domain suppresses the interaction with JH1, leading to constitutive JAK2 kinase activity. Mutated JAK2 tyrosine kinase promotes aberrant cell growth and anti-apoptotic signaling, mainly by activating the STAT, RAS/MAPK, and PI3K/AKT pathways. Thus, JAK2 V617F is a driver mutation in MPN.

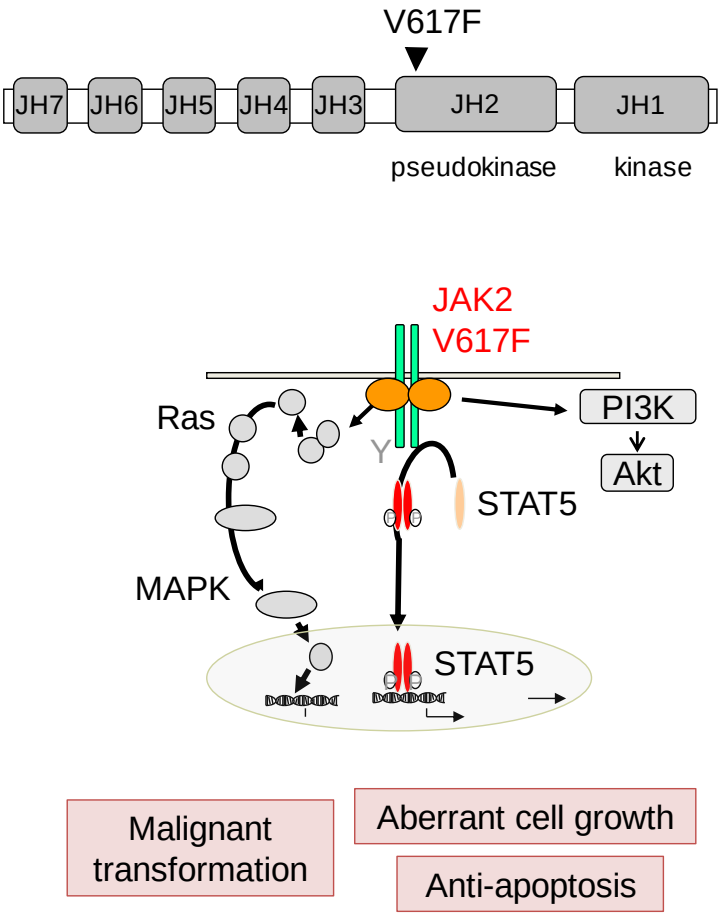

Figure 1-6. Mutation of JAK2 tyrosine kinase in myeloproliferative neoplasms.

A somatic point mutation in the JAK2 gene causes constitutive activation of the tyrosine kinase, which dysregulates cell growth and function.

1-2-4 Tyrosine kinase inhibitors

Because targeting the abnormally activated tyrosine kinase in cancer cells can be expected to suppress abnormal growth and induce apoptosis, tyrosine kinase inhibitors have been developed by many researchers and companies. Although kinase inhibitors have been studied since the early 1980's, the impetus for their development as drug candidates was the report about the kinase inhibitory effect of staurosporine in 1986 [11]. However, because staurosporine inhibits many kinases and shows little selectivity, clinical application of staurosporine was not possible in view of its side effects. For safety and high efficacy, excellent selectivity for the target kinase is required. The first

tyrosine kinase inhibitor put to practical use was imatinib mesylate (trade name, Gleevec), a selective ABL tyrosine kinase inhibitor [12]. As described in Chapter 2, imatinib showed excellent efficacy and safety in CML patients and became a breakthrough drug that drastically changed the treatment of CML.

More than 200 tyrosine kinase inhibitors are currently in clinical trials worldwide (Figure 1-7). To be approved as a therapeutic agent, a drug candidate must clear a number of hurdles such as efficacy, safety, pharmacokinetics, and physical properties. To date, only 13 tyrosine kinase inhibitors have been approved for the treatment of cancer. Many tyrosine kinase inhibitors have not shown a sufficient therapeutic effect in patients.

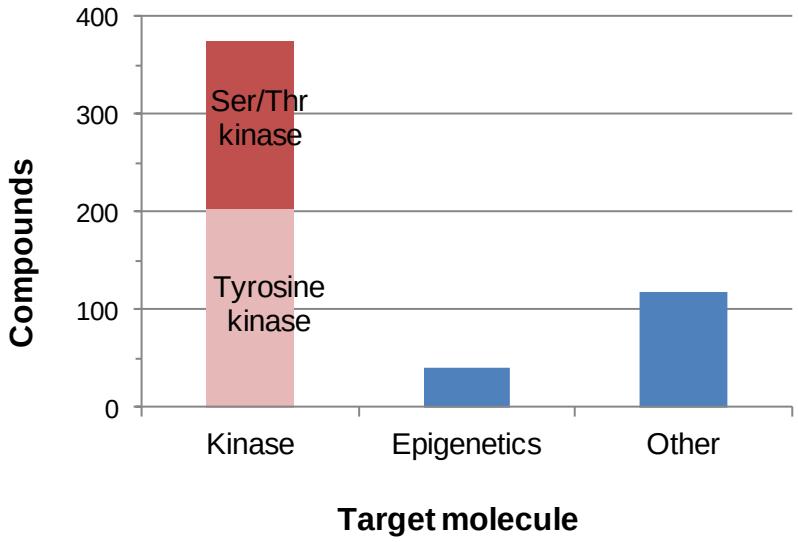

Figure 1-7. Molecularly targeted anticancer drugs in clinical trial.
Monoclonal antibodies, protein drugs, nucleic acid medicines, vitamin A derivatives, endocrine therapy agents, and thalidomide-based drugs are excluded. Abbreviation: Ser/Thr, serine/threonine.

1-3 The drug discovery process

The drug discovery process for molecularly targeted anticancer drugs is still in need of improvement, and there are many challenges. Figure 1-8 shows a simplified view of the flow from compound screening to clinical trial. First, compounds with activity against the target molecule are selected from a chemical library by high-throughput screening (HTS) with proteins or cells. Screening *in silico* is sometimes used. Chemical syntheses

and screening evaluations are repeated to increase the activity and selectivity of the compounds, and a relatively small number of which are selected. Finally, after evaluations such as *in vivo* efficacy, pharmacokinetics, and safety, one candidate is selected for clinical trial. However, as described in the previous section, a significant number of tyrosine kinase inhibitors in the pipeline have not shown a sufficient therapeutic effect in patients.

One of the most difficult parts of the drug discovery process is *in vivo* evaluation to select promising compounds [13]. In many cases, tumor-bearing model animals are used to evaluate the efficacy of compounds from point of the view of a high throughput (high numbers, short times, and convenience). In particular, cancer cell lines are often implanted subcutaneously into the backs of mice. However, there are several problems with this model [14,15]. Such model animals do not necessarily reflect the pathology of cancer patients accurately. The only outcome measure evaluated is tumor volume. In addition, the site of action of the drug is often different from the location of the original cancer. Compounds which decrease tumor volume in inappropriate model animals do not necessarily improve the clinical condition of patients. In order to evaluate compounds properly, it is necessary to use disease model animals which closely reflect the pathology of the cancer under study.

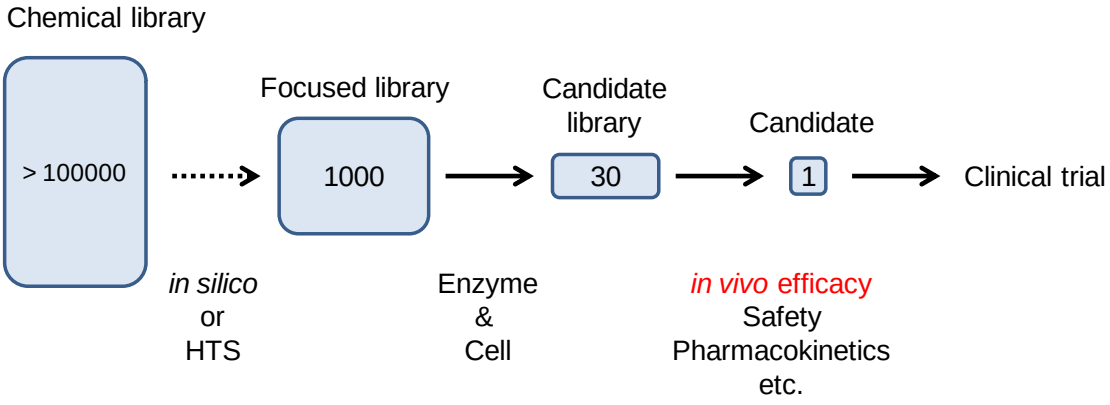

Figure 1-8. Drug discovery process for molecularly targeted anticancer drugs.

Once a target molecule is decided upon, various screening assays for promising compounds are done to evaluate their efficacy, metabolism, and safety.

1-4 Purpose of the work described in this thesis

The purpose of the study is to increase the probability of selecting promising compounds in two projects for developing selective tyrosine kinase inhibitors as cancer therapeutics, by constructing the appropriate disease model animals and performing the efficacy evaluation in these models. To this end, I introduced three mouse models of hematological malignancy (a Ba/F3 transplant model, a bone marrow transplantation model, and a transgenic model) for the screening processes. Specifically, I applied these model mice to exploratory research on dual BCR-ABL/LYN tyrosine kinase inhibitors for the treatment of drug-resistant CML (Chapters 2 and 3) and to research on selective JAK2 tyrosine kinase inhibitors for the treatment of MPN (Chapters 4 and 5) and myelodysplastic syndromes (Chapter 6).

Chapter 2

Discovery and characterization of a selective Bcr-Abl/Lyn tyrosine kinase inhibitor, NS-187, for the treatment of imatinib-resistant chronic myeloid leukemia

2-1 Introduction

The Philadelphia (Ph) chromosome results from a reciprocal translocation between chromosomes 9 and 22 that generates the breakpoint cluster region–Abelson (Bcr-Abl) chimeric protein, which in turn causes chronic myeloid leukemia (CML) and Ph^+ acute lymphoblastic leukemia (ALL) [16,17]. Imatinib mesylate (STI571, Gleevec) specifically inhibits the autophosphorylation of Abl tyrosine kinase and is not only highly efficacious in treating these diseases but also generally produces only mild side effects [18]. Within a few years of its introduction to the clinic, imatinib dramatically altered the first-line therapy for CML [19]. Most newly diagnosed CML patients in the chronic phase achieve durable responses when treated with imatinib [19]. However, a small percentage of these patients as well as most advanced-phase patients relapse on imatinib therapy [20,21]. Bcr-Abl–dependent mechanisms of resistance to imatinib include overexpression of Bcr-Abl and amplification of the *bcr-abl* gene and, most intriguingly, point mutations within the Abl kinase domain that interfere with imatinib binding [22-25].

To overcome imatinib resistance, higher doses of imatinib and combination therapy with other agents have been used with some efficacy. However, these strategies are limited in their application and effectiveness, especially for patients with Abl point mutations [26-28]. Therefore it is necessary to develop more effective Abl tyrosine kinase inhibitors. Several Src inhibitors from various chemical classes, including PD166326 [29], SKI-606 [30], AP23464 [31], and BMS-354825 [32], have been found to

be 100 to 300 times more effective than imatinib in blocking Bcr-Abl tyrosine kinase autophosphorylation, and these effects extend to point mutants of Bcr-Abl. However, while imatinib binds to only the inactive form of Abl, these dual Src-Abl inhibitors also bind to the active form, which shares considerable conformational similarity with the active forms of diverse tyrosine kinases, including the Src-family proteins [31,33]. This characteristic of dual Src-Abl inhibitors has some advantage with respect to Lyn kinase, a Src-family protein, because overexpression of Lyn is associated with imatinib resistance [34-36]. It has been shown that dual Src-Abl inhibitors can simultaneously inhibit Lyn [33] and this may enhance their ability to induce apoptosis in CML cells. However, the effect of lower specificity against Src-family kinases is not yet fully understood because these kinases play many important roles *in vivo* [37-41].

Thus we sought to identify a novel orally bioavailable compound for treating Ph^+ leukemias that (1) is more potent than imatinib in blocking Bcr-Abl kinase activity, including variants with point mutations in the kinase domain; (2) has fewer adverse effects; and (3) inhibits Lyn while otherwise remaining highly specific for Bcr-Abl. The crystal structure of the Abl kinase domain in complex with imatinib shows that some alterations to the structure of the drug are likely to be tolerated [42,43]. Chemical modifications made with the guidance of molecular modeling yielded several promising compounds. Among them, a potent and specific dual Abl-Lyn inhibitor, NS-187 (Figure 2-1A), was selected on the basis of its overall characteristics, including its pharmacokinetics and toxicity as determined in animal studies. NS-187 was found to be much more effective than imatinib and to inhibit Lyn at clinically relevant concentrations without affecting the phosphorylation of Src, Blk, or Yes. Its inhibitory effect extended to almost all Bcr-Abl point mutants tested.

2-2 Materials and Methods

2-2-1 Reagents and cell lines

NS-187 and imatinib were synthesized and purified at Nippon Shinyaku (Kyoto, Japan). The compounds were dissolved as 10 mM aliquots in dimethyl sulfoxide (Sigma-Aldrich, St Louis, MO) and stored at -80°C until required for use. K562 (chronic myeloid leukemia), U937 (histiocytic lymphoma), NCI-H526 (small cell lung cancer), and A431 (epidermoid carcinoma) cells were obtained from the American Type Culture Collection (Manassas, VA). KU812 (chronic myeloid leukemia) and NHDF (normal

fibroblast) cells were obtained from the Japanese Collection of Research Biosources (Osaka, Japan) and Kurabo (Osaka, Japan), respectively. Ba/F3-wt, Ba/F3-E255K, and Ba/F3-T315I cells were kindly provided by Dr Martin Ruthardt of Frankfurt University. K562, KU812, U937, Ba/F3-wt, Ba/F3-E255K, and Ba/F3-T315I cells were cultured in RPMI-1640 (Nissui, Tokyo, Japan) with 2 mM L-glutamine (Nacalai Tesque, Kyoto, Japan) and 10% fetal bovine serum (FBS; Vitromex, Vilshofen, Germany). NCI-H526 cells were cultured in RPMI-1640 with 2 mM L-glutamine, 4.5 g/L glucose (Nacalai Tesque), 10 mM HEPES (*N*-2-hydroxyethylpiperazine-*N*'-2-ethanesulfonic acid; Sigma-Aldrich), 1.0 mM sodium pyruvate (ICN Pharmaceuticals, Costa Mesa, CA), and 10% FBS. A431 and NHDF cells were cultured in Dulbecco modified Eagle medium (DMEM; Nissui) with 4 mM L-glutamine and 10% FBS. All cell lines were maintained at 37°C in a fully humidified atmosphere of 5% CO2. Cells undergoing exponential growth were used in the experiments.

2-2-2 Generation and purification of Abl kinase domains

The Abl kinase domain, which consists of c-Abl amino acids 229-515, was amplified by polymerase chain reaction with K562 cDNA as a template and subcloned into the pENTR/D-TOPO vector (Invitrogen, Carlsbad, CA). Each mutation (E244V, G250E, Q252H, Y253F, E255K, E255V, T315I, F317L, M351T, E355G, F359V, H396P, and F486S) was introduced by using the QuikChange Site-Directed Mutagenesis Kit (Stratagene, La Jolla, CA). The presence of the mutations was confirmed by sequencing. The wild-type (wt) and mutated kinase domains in the pENTR/D-TOPO vector were transferred to the pDEST10 vector (Invitrogen) by recombination with Gateway LR clonase (Invitrogen). Sf9 cells were infected with baculovirus generated from each kinase domain pDEST10 by using the Bac-to-Bac Baculovirus Expression System (Invitrogen). After inoculation, Sf9 cells were lysed and the kinase domain was purified on a Q-Sepharose Fast Flow anion-exchange column (Amersham Biosciences, Piscataway, NJ) and a HisTrap HP column (Amersham Biosciences). The protein concentration of each kinase domain was determined by sodium dodecyl sulfate–polyacrylamide gel electrophoresis (SDS-PAGE) followed by staining with Coomassie Brilliant Blue.

2-2-3 Kinase assay

Bcr-Abl kinase assays were performed in 25 μL of reaction mixture containing 250 μM

peptide substrate, 740 Bq/μL [γ-^{33}P]ATP, and 20 μM cold adenosine triphosphate (ATP) by using the SignaTECT protein tyrosine kinase assay system (Promega, Madison, WI). Each Bcr-Abl kinase was used at a concentration of 10 nM. Kinase assays for Abl, Src, and Lyn were carried out with an enzyme-linked immunosorbent assay (ELISA) kit from Carna Biosciences (Kobe, Japan). The inhibitory effects of NS-187 against 79 tyrosine kinases were tested with KinaseProfiler (Upstate, Dundee, United Kingdom).

2-2-4 Inhibition of intracellular tyrosine kinases

K562 cells, BaF3/wt cells, BaF3/E255K cells, and BaF3/T315I cells were treated with serial dilutions of the compounds for 1.5 hours. Serum-starved NHDF cells, NCI-H526 cells, and A431 cells were treated with serial dilutions of the compounds for 1.5 hours followed by stimulation with 50 ng/mL platelet-derived growth factor (PDGF; Upstate), 100 ng/mL stemcell factor (SCF; R&D Systems, Minneapolis, MN), or 100 ng/mL epidermal growth factor (EGF; R&D Systems) for 10 minutes. Cells were harvested and lysed with radioimmunoprecipitation assay (RIPA) buffer, and equal amounts of cell lysate protein were analyzed by Western blotting with antiphosphotyrosine antibody PY20 conjugated with horseradish peroxidase (BD Transduction Laboratories, San Jose, CA) and anti–c-Abl antibody, anti–c-Kit antibody, anti–CT10 regulator of kinaselike (anti-CrkL) antibody, anti–EGF receptor (anti-EGFR) antibody, anti–extracellular signal-related kinase 1 (anti-ERK1) antibody (Santa Cruz Biotechnology, Santa Cruz, CA), or anti-PDGFR type A/B (Upstate).

2-2-5 Cell proliferation assays

K562, BaF3/wt, BaF3/E255K, and BaF3/T315I cells were plated in triplicate at 1 x 10^3 cells/well in 96-well plates, whereas KU812 and U937 cells were plated in triplicate at 5 x 10^3 cells/well in 96-well plates. Cells were incubated with serial dilutions of the compounds for 3 days. Cell proliferation was measured by MTT (3-(4,5-dimethylthiazol-2-yl)-2,5-diphenyltetrazolium bromide; Nacalai Tesque) assay, and the 50% inhibitory concentration (IC_{50}) values were calculated by fitting the data to a logistic curve.

2-2-6 Subcutaneous xenograft model and BaF3 leukemia models

Approvals for the following in vivo studies were obtained from the institutional review

board at Kyoto University Hospital. Balb/c-nu/nu female mice 8 weeks of age were purchased from Japan Clea (Osaka, Japan). KU812 xenograft was established by subcutaneous injection of 2.5 x 10^7 cells into the right flank of the mice. Seven days after inoculation, the mice were randomized into groups of 5, and NS-187, imatinib, or vehicle (0.5% methylcellulose) was administered orally twice a day by gavage for 10 consecutive days. Tumor sizes were assessed at least twice a week by caliper measurement and their volumes calculated from the formula, tumor size (cm^3) = (d^2 x D)/2/1000, where d and D are the shortest and longest diameter of the tumor, respectively. Significant differences between samples were determined with the Dunntt test.

Ba/F3-wt leukemia was established by intravenous injection of 1 x 10^6 cells into the tail vein of Balb/c-nu/nu mice. The next day the mice were randomized into groups of 7, and NS-187, imatinib, or vehicle (0.5% methylcellulose) was administered orally twice a day for 11 consecutive days. Ba/F3-E255K leukemia was established by intravenous injection of 5 x 10^4 cells into the tail vein of Balb/c mice. The next day the mice were randomized into groups of 3, and NS-187, imatinib, or vehicle was administered orally twice a day for 26 consecutive days. Survival analysis was performed by the Kaplan-Meier method and statistical significance was assessed by the log-rank test.

2-2-7 Molecular modeling

All computations were performed with Molecular Operating Environment (MOE) version 2003.01 (Chemical Computing Group, Montreal, QC, Canada). Sequence alignment and homology modeling of Src-family proteins were performed with MOE-Align and MOE-Homology, respectively. The X-ray coordinates of the imatinib/Abl cocrystal structure [43] were used as the template. NS-187 was manually docked into the binding site. Because of the structural similarity between NS-187 and imatinib, the mode of binding of NS-187 was assumed to be very similar to that of imatinib, and typical hydrogen-bonding interactions were retained: the nitrogen of the terminal pyrimidine ring with the backbone-NH of Met318, the nitrogen of the anilino group with the OH of Thr315, the amide-NH with the side-chain carboxylate of Glu286, and the amide-CO with the backbone-NH of Asp381. The energy of the models thus obtained was minimized by using the Merck Molecular Force Field (MMFF94s) method [44]. The amino acids within 0.7 nm (7 Å) of NS-187 were fully minimized, and changes in the structures of NS-187 and around the amino acids were small. Figures were prepared with PyMOL version 0.97 (DeLano Scientific, South San Francisco, CA).

2-3 Results

2-3-1 NS-187 blocks the wild-type Bcr-Abl autophosphorylation and its downstream signaling

NS-187, *N*-[3-(4,5'-bipyrimidin-2-ylamino)-4-methylphenyl]-4-{[3S]-3-(dimethylamino)pyrrolidin-1-yl}methyl)-3-(trifluoromethyl)benzamide (Figure 2-1A), was discovered by screening for potent and selective Bcr-Abl kinase inhibitors. We compared the ability of NS-187 and imatinib to inhibit the tyrosine kinase activity of wild-type (wt) Bcr-Abl by first testing by Western blot analysis whether the protein is autophosphorylated in Bcr-Abl–positive K562 cells and Ba/F3 cells transfected with wt Bcr-Abl (Ba/F3-wt) when the cells are treated with either drug (Figure 2-1B-C). Its autophosphorylation status in 293T cells transfected with wt Bcr-Abl was also examined. The IC_{50} values of NS-187 against wt Bcr-Abl in K562 and 293T cells were 11 and 22 nM, respectively (Table 2-1). The corresponding values for imatinib were 280 and 1200 nM. Thus, NS-187 was 25 and 55 times more potent than imatinib, respectively, in blocking Bcr-Abl autophosphorylation (Table 2-1).

The effect of NS-187 and imatinib on the tyrosine kinase activity of platelet-derived growth factor receptor (PDGFR), c-Kit, and epidermal growth factor receptor (EGFR) were also examined. NS-187 suppressed PDGFR and c-Kit phosphorylation with IC_{50} values very similar to those of imatinib (Figure 2-1E-F). The ranking of IC_{50} with respect to imatinib is PDGFR > c-Kit > Bcr-Abl, whereas the ranking with respect to NS-187 is Bcr-Abl > PDGFR > c-Kit (Table 2-1). Neither NS-187 nor imatinib inhibited EGFR at clinically relevant concentrations (Figure 2-1G).

The downstream mediators of Bcr-Abl, CrkL, and ERK are dephosphorylated on treatment with imatinib [45]. Examination of the intracellular phosphorylation status of CrkL and ERK revealed that NS-187 inhibited the phosphorylation of CrkL and ERK in K562 cells at much lower concentrations than did imatinib (Figure 2-2A-B). The inhibition of phosphorylation was also observed in Ba/F3-wt cells (Figure 2-2C-D). Thus, NS-187 was more potent Bcr-Abl inhibitor than was imatinib.

Table 2-1. Ability of NS-187 and imatinib to inhibit the phosphorylation of Bcr-Abl and other tyrosine kinases at the cellular level.

Tyrosine kinase	Cell line	IC_{50}, nM	
		NS-187	Imatinib
Bcr-Abl			
Wild type	293T (transfected cells)	22	1200
E255K	293T (transfected cells)	98	> 10 000
T315I	293T (transfected cells)	>10 000	> 10 000
Bcr-Abl			
Wild type	BaF3 (transfected cells)	63	491
E255K	BaF3 (transfected cells)	340	6800
T315I	BaF3 (transfected cells)	> 10 000	> 10 000
Bcr-Abl	K562	11	280
PDGFR	NHDF	56	100
c-Kit	NCI-H526	840	210
EGFR	A431	3300	> 10 000

K562 cells were examined for Bcr-Abl phosphorylation after treatment with NS-187 or imatinib by Western blot analysis with Bcr-Abl–specific antibodies, as were 293T or Ba/F3 cells transfected with wt or point mutants of Bcr-Abl. NHDF, NCI-H526, and A431 cells were examined for PDGFR, c-Kit, or EGFR phosphorylation, respectively, after treatment with first NS-187 or imatinib and then PDGF, SCF, or EGF, respectively, by Western blot analysis with the corresponding antibodies.

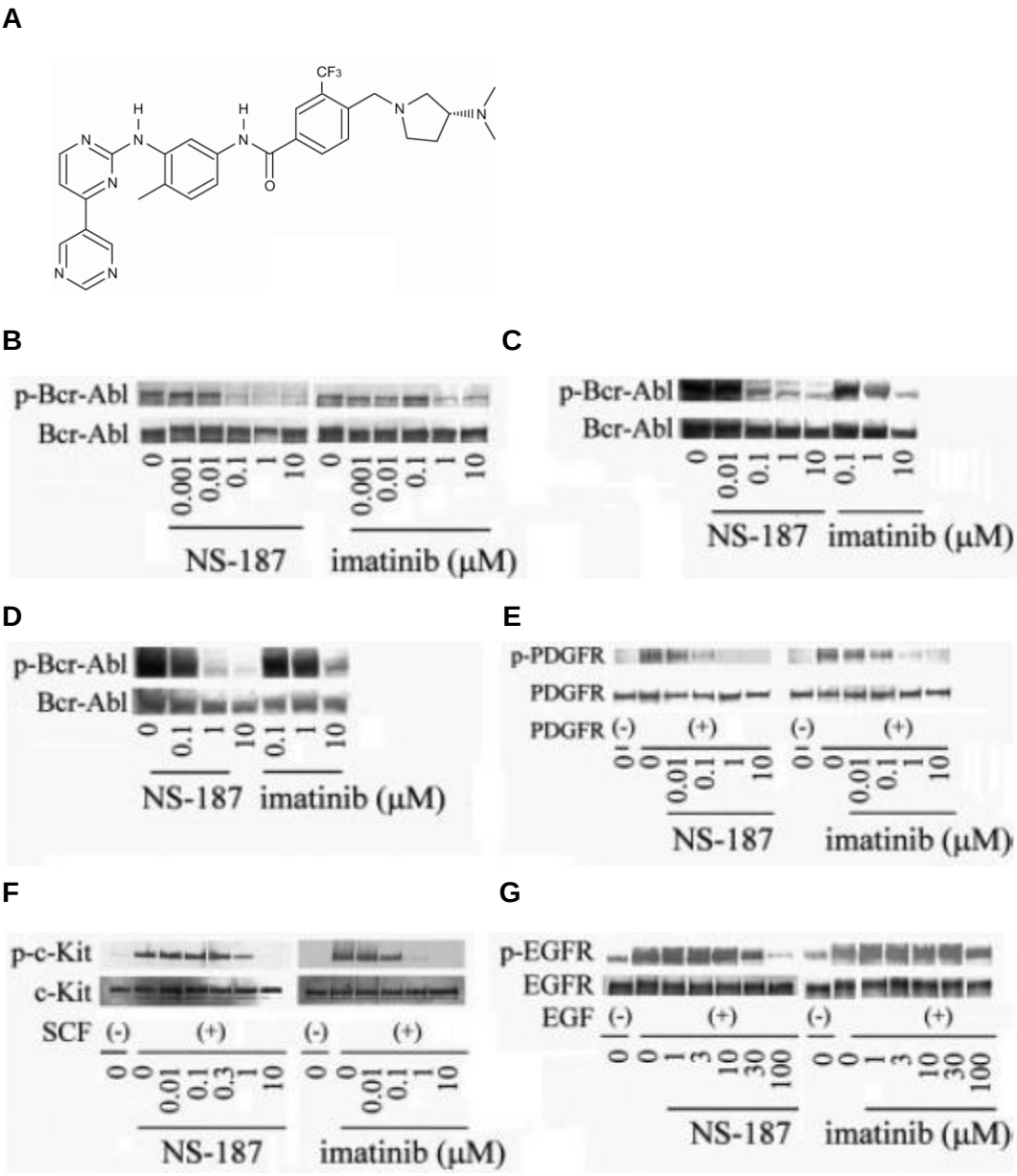

Figure 2-1. Structure and activity of NS-187.

Chemical structures of NS-187 (A). K562 cells (B), Ba/F3-wt cells (C), and Ba/F3-E255K cells (D) were incubated for 1.5 hours with the indicated concentrations of each compound. Serum-starved NHDF cells (E), NCI-H526 cells (F), and A431 cells (G) were incubated for 1.5 hours with each compound prior to stimulation for 10 minutes with PDGF, SCF, or EGF, respectively. Cells were then lysed and subjected to Western blot analysis with antiphosphotyrosine antibody (B-G), anti–c-Abl antibody (B-D), anti-PDGFR antibody (E), anti–c-Kit antibody (F), or anti-EGFR antibody (G). p indicates phosphorylated.

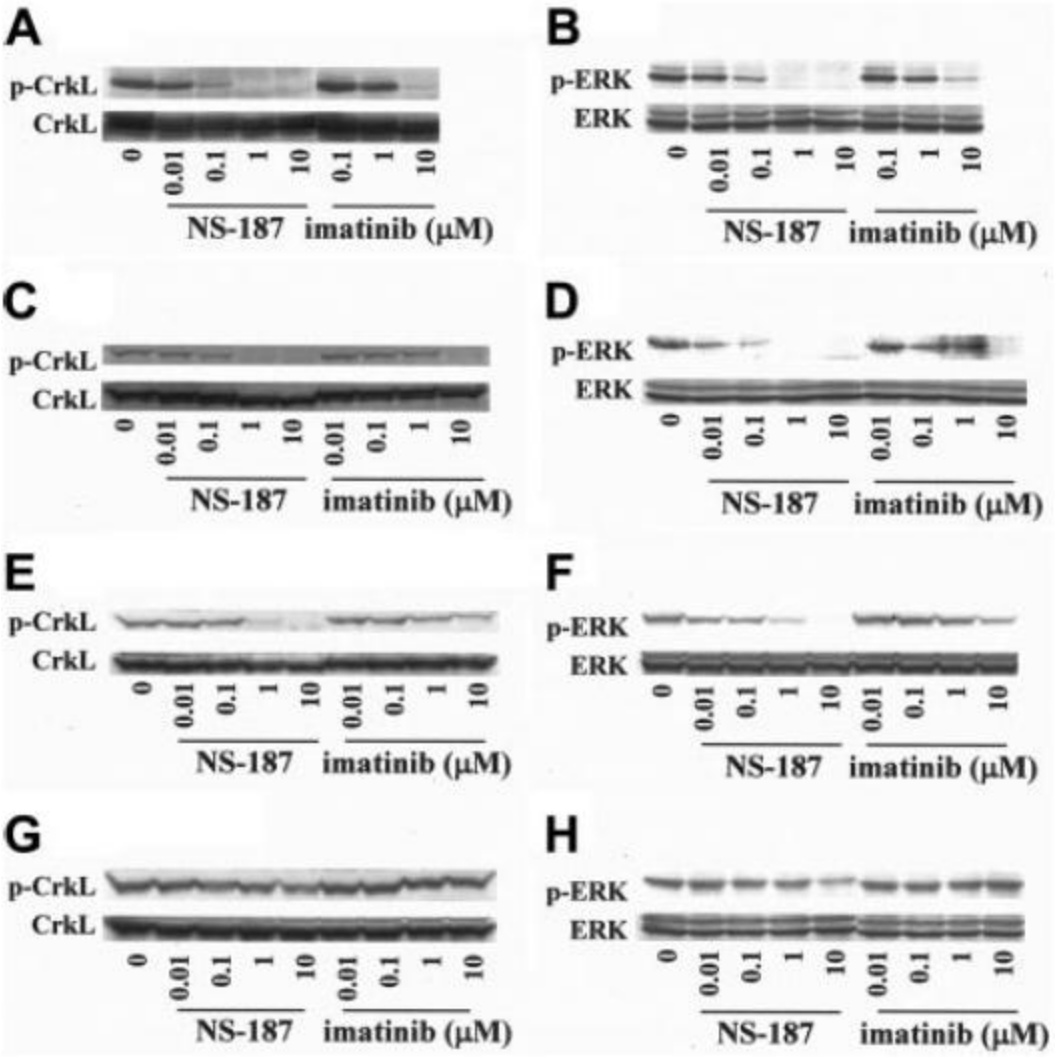

Figure 2-2. Effect of NS-187 on intracellular phosphorylation of CrkL and ERK.

NS-187 inhibits the phosphorylation of CrkL and ERK in cells expressing wt Bcr-Abl or the E255K Bcr-Abl mutant but not in cells expressing the T315I Bcr-Abl mutant. K562 (A-B), Ba/F3-wt (C-D), Ba/F3-E255K (E-F), or Ba/F3-T315I (G-H) cells were incubated for 1.5 hours with the indicated concentrations of each compound. Cells were then lysed and subjected to Western blot analysis with antiphosphotyrosine antibody (A-H), anti-CrkL antibody (A,C,E,G), or anti-ERK1 antibody (B,D,F,H). The phosphorylated forms of CrkL (p) migrate more slowly than the unphosphorylated forms.

2-3-2 NS-187 inhibits the tyrosine phosphorylation of 12 of 13 known kinase domain point mutants

More than 30 point mutations within the Abl kinase domain have been reported [46]. The ability of NS-187 to inhibit 13 of these mutant Bcr-Abl kinases was tested by constructing and purifying the mutant kinase domains and then subjecting them to *in vitro* kinase assays in the presence of NS-187 or imatinib. NS-187 at physiologically obtainable concentrations inhibited the phosphorylation of Bcr-Abl harboring the M244V, G250E, Q252H, Y253F, E255K, E255V, F317L, M351T, E355G, F359V, H396P, or F486S mutations but it did not inhibit the phosphorylation of the T315I mutant (Table 2-2). For all mutants except T315I, the IC_{50} for imatinib was at least 5 times as high as the corresponding value for NS-187.

The effect of NS-187 on 2 of the mutants was also examined in whole cells by assessing the phosphorylation of Bcr-Abl with the E255K or the T315I mutation in Ba/F3 cells (Ba/F3-E255K and Ba/F3-T315I). Unlike imatinib, NS-187 inhibited the phosphorylation of the E255K mutant at clinically relevant concentrations (Figure 2-1D). However, neither imatinib nor NS-187 had any effect on the phosphorylation of the T315I mutant (data not shown).

Table 2-2. Effect of NS-187 and imatinib on the *in vitro* phosphorylation of purified wt and point mutated Abl kinase domains.

	IC_{50}, nM	
Abl kinase	**NS-187**	**Imatinib**
Wild type	72	1 100
M244V	240	3 500
G250E	160	2 000
Q252H	410	2 100
Y253F	81	1 500
E255K	540	5 800
E255V	1 400	> 10 000
T315I	> 10 000	> 10 000
F317L	760	1 900
M351T	150	3 900
E355G	580	7 100
E359V	1 300	> 10 000
H396P	95	1 400
F486S	470	9 500

The purified Abl kinase domains were subjected to *in vitro* kinase assays as described in “Materials and methods.” The enzyme concentration was 10 nM.

2-3-3 NS-187 is a dual Bcr-Abl/Lyn tyrosine kinase inhibitor

To test the ability of NS-187 to inhibit other tyrosine kinases, 79 tyrosine kinases were assayed with KinaseProfiler (Upstate). These included the 5 Src-family kinases Blk, Src, Fyn, Lyn, and Yes. The effects of 0.1 μM NS-187 and 10 μM imatinib were tested because these concentrations gave equal inhibition of Abl. At a concentration of 0.1 μM, NS-187 inhibited 4 of the 79 tyrosine kinases, that is, Abl, Abl-related gene (Arg), Fyn, and Lyn. Notably, at 0.1 μM, NS-187 did not inhibit PDGFRα, PDGFRβ, Blk, Src, or Yes (Figure 2-3). In contrast, 10 μM imatinib inhibited 9 tyrosine kinases, that is, Abl, Arg, Blk, FMS-like TK-3 (Flt3), Fyn, Lyn, PDGFRα, PDGFRβ, and p70S6K (data not shown), indicating that NS-187 inhibited Abl more specifically than did imatinib. To confirm the specificity of NS-187 against Lyn, the inhibitory effects of NS-187 against Abl, Src, and Lyn were tested. The IC_{50} values of NS-187 for these kinases were 5.8 nM, 1700 nM, and 19 nM, respectively, and those of imatinib were 106 nM, greater than 10000 nM,

and 352 nM, respectively. These findings suggest that NS-187 acts as an Abl-Lyn inhibitor while otherwise remaining highly specific for Bcr-Abl.

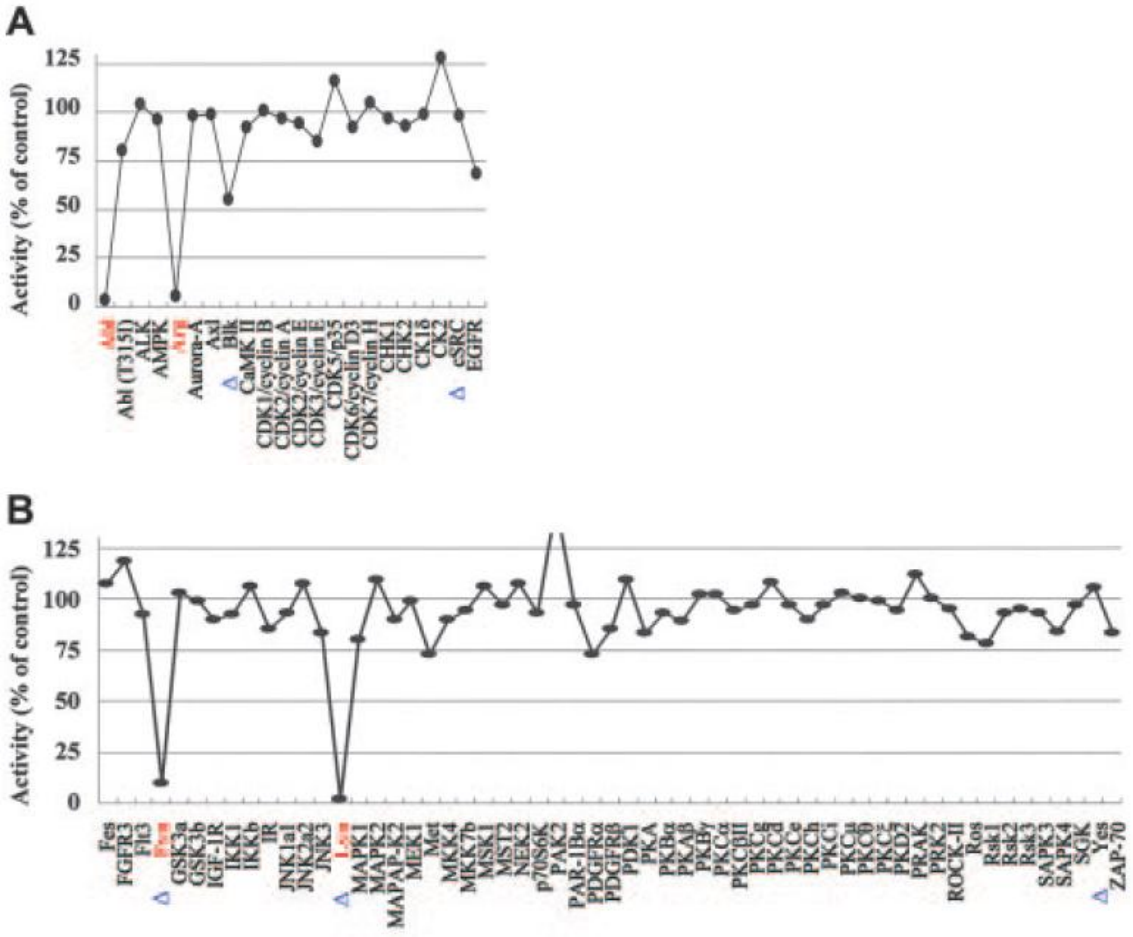

Figure 2-3. Kinase inhibition profile and the docking model.

Kinase inhibition profile of NS-187 and Abl (panel B is the continuation of panel A). Seventy-nine tyrosine kinases, including 5 Src-family kinases (Blk, Src, Fyn, Lyn, and Yes; indicated by on the x-axis) were assayed by KinaseProfiler. At 0.1 μM, NS-187 inhibited 4 of the 79 tyrosine kinases, namely, Abl, Arg, Fyn, and Lyn (indicated by red on the x-axis).

2-3-4 NS-187 suppresses the growth of leukemic cell lines expressing wild-type Bcr-Abl or E255K mutant

NS-187 suppressed the growth of the Bcr-Abl–positive cell lines K562 (Figure 2-4A), KU812 (Figure 2-4B), and Ba/F3-wt (Figure 2-4D) much more potently than did imatinib, but neither drug affected the proliferation of the Bcr-Abl–negative U937 cell line (Figure

2-4C). As to Bcr-Abl point mutants, NS-187 exhibited a concentration-dependent antiproliferative effect against Ba/F3-E255K (Figure 2-4E) but had no effect on Ba/F3-T315I cells within the concentration range tested (Figure 2-4F). Imatinib was less effective against all of the point mutants tested (Figure 2-4E-F).

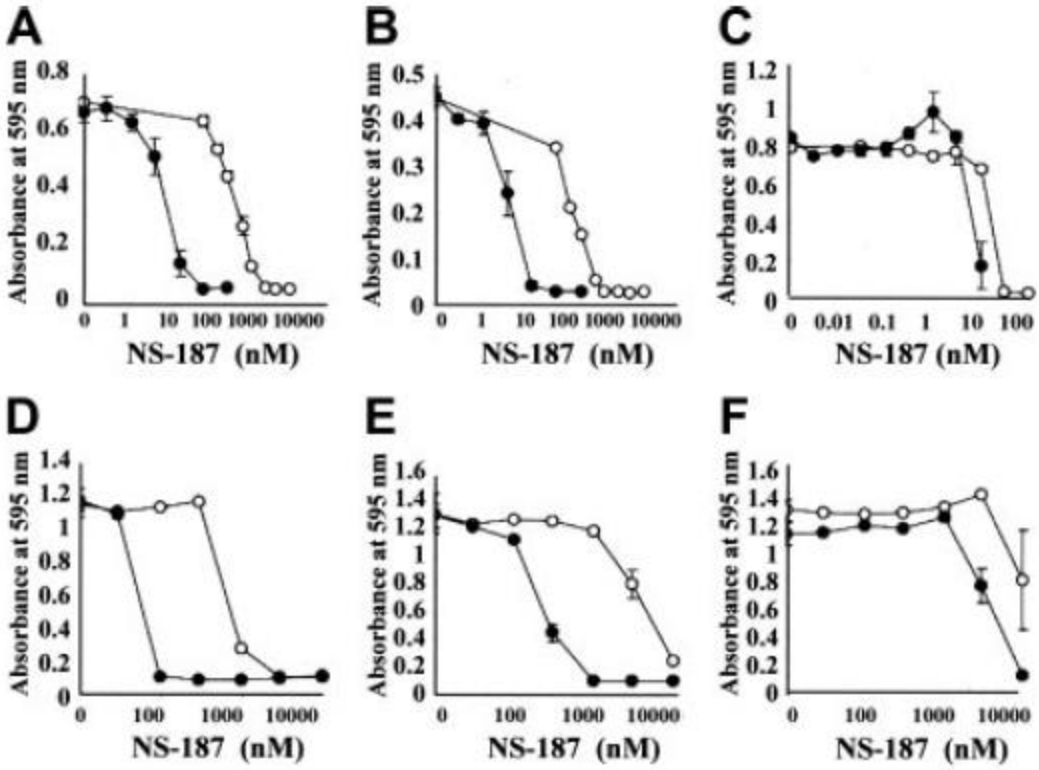

Figure 2-4. Effect of NS-187 on *in vitro* growth of cell lines harboring Bcr-Abl.

(A) Bcr-Abl–positive K562 cells, (B) Bcr-Abl–positive KU812 cells, (C) Bcr-Abl–negative U937 cells, (D) Ba/F3-wt cells, (E) Ba/F3-E255K cells, and (F) Ba/F3-T315I cells were treated with serial dilutions of NS-187 (●) or imatinib (○) for 3 days. Cell proliferation was assessed by means of the MTT assay.

2-3-5 *In vivo* effects of NS-187

In our preliminary experiments, when Balb/c mice were given NS-187 orally at a dose of 30 mg/kg, the pharmacokinetic parameters were as follows: T_{max}, 2 hours; maximum concentration (C_{max}), 661 ng/mL; area under the curve $(AUC)_{0-\infty}$, 2294 ng·h/mL; $T_{1/2}$, 1.0 hour; and bioavailability value (BA), 32%. The maximal tolerated dose (MTD) of NS-187 in Balb/c or Balb/c-nu/nu mice was 200 mg/kg/d (100 mg/kg twice a day). C_{max} for

NS-187 was estimated at 2226 ng/mL (4.0 μM) when mice were treated twice a day orally with 100 mg/kg of NS-187.

To test the effect of NS-187 on in vivo tumor growth, Balb/c-nu/nu mice were injected subcutaneously with Bcr-Abl–positive KU812 cells on day 0 and given NS-187 or imatinib orally twice a day from day 7 to day 17. At 20 mg/kg/d, imatinib inhibited tumor growth slightly, whereas at 200 mg/kg/d, it inhibited tumor growth almost completely. In contrast, at only 0.2 mg/kg/d NS-187 significantly inhibited tumor growth, whereas at 20 mg/kg/d it completely inhibited tumor growth without any adverse effects (Figure 2-5A). When mice were treated with 0.2 or 20 mg/kg/d of NS-187, the estimated C_{max} was 4 nM or 400 nM, respectively, suggesting that the *in vivo* effects of NS-187 were comparable to its *in vitro* effects (Figure 2-4B). The body weights of the treated tumor-bearing mice were not significantly different from those of untreated mice, even at a dosage of 200 mg/kg/d NS-187 (data not shown). Thus, NS-187 was at least 10-fold more potent than imatinib *in vivo* with complete inhibition of tumor growth as the end point and at least 100-fold more potent with partial inhibition as the end point. NS-187 was well tolerated by the mice.

We also tested the ability of NS-187 to suppress tumor growth in another murine tumor model, namely, Balb/c-nu/nu mice that received Ba/F3-wt cells intravenously. The mice were treated orally with NS-187 or imatinib for 11 days starting on day 1. All 7 untreated mice had died by day 23 due to leukemic cell expansion, whereas all mice treated with 400 mg/kg/d imatinib had died by day 25. Thus, imatinib had little effect on tumor growth in this model, whereas NS-187 significantly prolonged the survival of the mice in a dose-dependent manner compared with untreated mice (Figure 2-5B). We also examined the effect of longer exposure to NS-187 (25 days) in mice inoculated with 5×10^4 instead of 1×10^6 Ba/F3-wt cells. NS-187 also prolonged the survival of these mice in a dose-dependent manner (data not shown).

We next examined the ability of NS-187 to block the *in vivo* growth of Ba/F3-E255K cells in Balb/c-nu/nu mice. Ba/F3-E255K-bearing mice were treated with NS-187 or imatinib for 26 days starting on day 1. The untreated mice and mice treated with 200 mg/kg/d imatinib had all died by day 28 (Figure 2-5C). In contrast, NS-187 at 120 mg/kg/d significantly prolonged survival compared with untreated mice (Figure 2-5C). NS-187 was also well tolerated by the mice. Thus, NS-187 was more potent than imatinib and could override the point mutation–based imatinib-resistance mechanism *in vivo*.

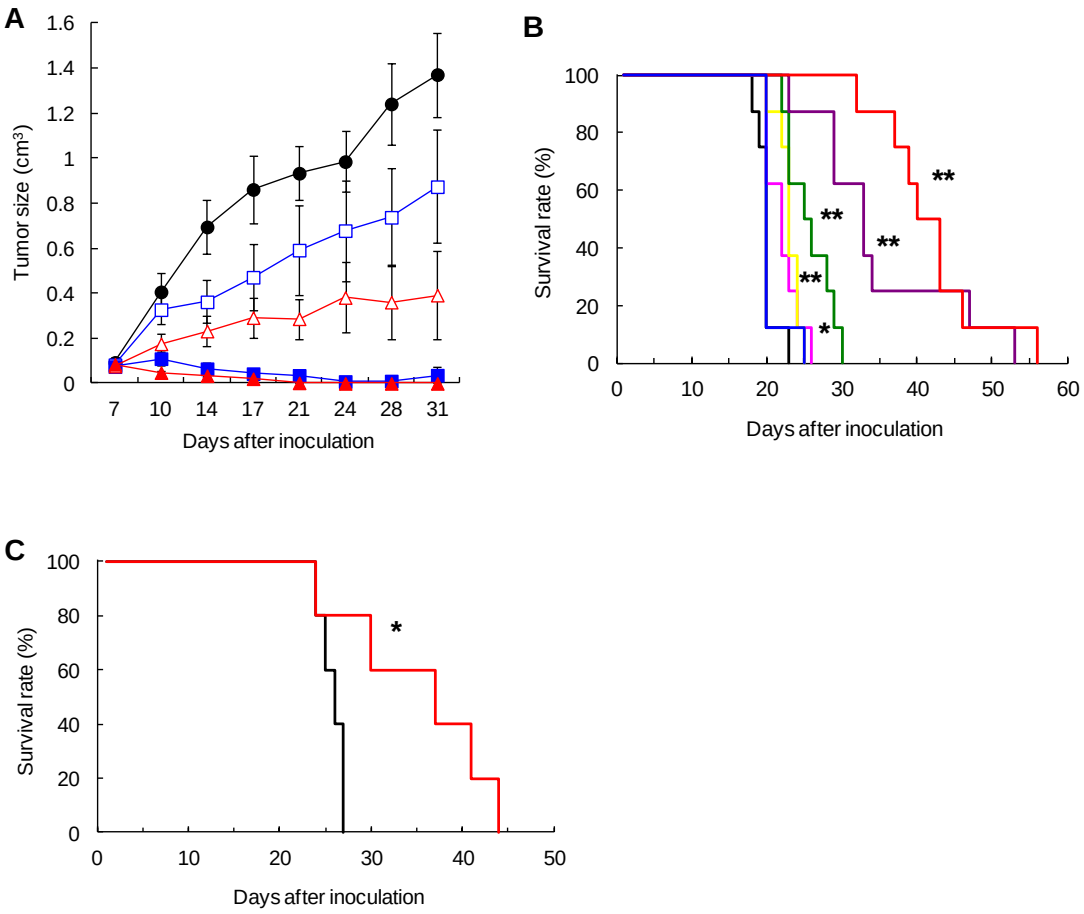

Figure 2-5. Effect of NS-187 on *in vivo* tumor growth.

(A) Balb/c-nu/nu mice received subcutaneous transplants of KU812 cells (day 0) and were given vehicle (●), NS-187 (Δ, 0.2 mg/kg/d; ▲, 20 mg/kg/d), or imatinib (□, 20 mg/kg/d; ■, 200 mg/kg/d) daily from day 7 to day 17. Data points represent the mean standard deviation calculated for 7 mice. Effect of NS-187 in Ba/F3-leukemia model. (B) Survival of Balb/c-nu/nu mice that received transplants of Ba/F3-wt cells and given vehicle (black), NS-187 (pink, 6 mg/kg/d; yellow, 20 mg/kg/d; green, 60 mg/kg/d; purple, 120 mg/kg/d; red, 200 mg/kg/d), or imatinib (blue; 400 mg/kg/d) daily from day 1 to day 11. (C) Survival of Balb/c-nu/nu mice that received transplants of Ba/F3-E255K cells and given vehicle (black), NS-187 (red; 120 mg/kg/d), or imatinib (blue; 200 mg/kg/d) daily from day 1 to day 26. *P < .05; **P < .01.

2-4 Discussion

In view of the frequent development of imatinib resistance during the treatment of Ph^+ leukemia, we sought to develop a novel agent to treat this disease that fulfills the following requirements for a ”post-imatinib” drug: (1) it inhibits Bcr-Abl, including variants with point mutations in the kinase domain, more effectively than does imatinib; (2) it has at most mild toxicity; and (3) it simultaneously inhibits another kinase whose activity is associated with imatinib resistance while remaining at least as specific for Bcr-Abl as is imatinib. With the aid of Bcr-Abl–docking modeling we have identified a candidate drug, NS-187, that inhibited the autophosphorylation of wt Bcr-Abl in K562 and 293T/wt cells more potently than did imatinib (Table 2-1). It also inhibited the phosphorylation of CrkL and ERK in K562 and BaF3/wt cells more strongly than did imatinib (Figure 2-2A-D; Table 2-1). Moreover, it suppressed the in vitro growth of Bcr-Abl–positive KU812 and K562 cells at much lower concentrations than did imatinib (Figure 2-4A-B). Significantly, NS-187 was at least 10-fold more potent than imatinib in mice bearing Bcr-Abl–positive tumors (Figure 2-5A-B) and had no adverse effects. Furthermore, not only was NS-187 effective against wt Bcr-Abl but it also blocked the activity of Bcr-Abl with point mutations in the kinase domain (Figure 2-1D, 2-2E-F; Table 2-1, 2-2). In addition, it inhibited the *in vitro* growth of cells expressing mutant Bcr-Abl proteins (Figure 2-4E) and prolonged the survival of mice engrafted with Ba/F3-E255K cells (Figure 2-5C). The only point mutant that NS-187 failed to significantly inhibit was the T315I Bcr-Abl mutant. Imatinib failed to inhibit any of the point mutants tested. These findings show that NS-187 fulfills the first 2 requirements of a post-imatinib drug that were listed above.

Other post-imatinib agents such as PD166326 [29], SKI-606 [30], AP23464 [31], and BMS-354825 [32,33] were developed from Src inhibitors on the basis of the similarity between Abl and the Src-family proteins [47,48]. It has been shown that the simultaneous inhibition of any 2 of the Ras, signal transducers and activators of transcription 5 (STAT5), and phosphatidylinositol 3–kinase (PI3K) pathways leads to a synergistic enhancement of apoptosis in CML cells [49-51]. At present, research aimed at the development of effective therapies for Ph^+ leukemias is focused not only on these signaling pathways but also on Lyn kinase, since acquired imatinib resistance may be mediated in part through the overexpression of Lyn [34,35]. Moreover, short interfering RNA (siRNA) targeting Lyn induces apoptosis in imatinib-resistant Ph^+ leukemia cells [36]. Imatinib minimally inhibits Lyn (IC_{50}, 352 nM). However, the dual Src-Abl inhibitor BMS-354825 significantly suppresses Lyn phosphorylation, and this is consistent with its greater antitumor activity in CML samples [33]. These observations suggest that the

ability of an agent to act simultaneously against Lyn and Abl will be advantageous in Ph^+ leukemia therapy. However, it may be important for the activity of such a therapeutic agent to be limited to Abl and Lyn to avoid the possibility of adverse effects. It is well known that imatinib inhibits not only Abl but also PDGFR and c-Kit, and this may be responsible for adverse effects such as bone marrow suppression, periorbital edema, and hypopigmentation [52]. In addition, Src proteins are known to play important roles in osteoclastogenesis [37], the regulation of Ca^{2+} signaling [38], the modulation of vascular adaptations [39], and signaling through a variety of cell surface receptors [40]. For example, the vascular permeability activity of vascular endothelial growth factor (VEGF) specifically depends on the Src-family proteins Src or Yes [41]. These observations suggest that inhibition of PDGFR, c-Kit, or Src-family proteins could cause unpredictable adverse effects. We set out to discover a compound that would inhibit Lyn and Abl while inhibiting as few other kinases as possible. Although another novel Abl-specific inhibitor, AMN107, which like NS-187 is a 2-phenylaminopyrimidine–class compound, does not inhibit Lyn [53,54], we found that NS-187 inhibited Lyn in addition to Fyn but did not inhibit PDGFR, Src, Blk, or Yes at 0.1 μM, a concentration that adequately inhibits Abl kinase activity (Figure 2-3).

To investigate why NS-187 inhibited Lyn without simultaneously inhibiting Src, docking studies were performed using the cocrystal structure of imatinib bound to Abl [43]. Our proposed docking model of the NS-187/Abl complex is shown in Figure 2-6. The cocrystal structure reveals that the P-loop of Abl moves toward imatinib upon binding of imatinib to the protein [43]. This induced fit contributes to increased van der Waals interactions and stabilization of the inactive conformation of the complex. Such an induced fit is also likely to occur with NS-187 due to its structural similarity to imatinib. Moreover, as with imatinib, the NS-187/Abl complex is likely to be stabilized by the hydrogen-bonding interaction between the OH of Tyr253 and the side-chain NH2 of Asn322 as well as the water-mediated hydrogen-bonding interaction between the side-chain CO of Gln252 and the side-chain carboxylate of Asp325 (Figure 2-6). As to the variable binding of NS-187 to different Src-family proteins, it seems to be significant that while the amino acids at positions 253 and 325 are always Phe and Asp, respectively, the amino acid at position 252 is either Gln or Cys (Table 2-3). NS-187 inhibited the Gln252-bearing proteins Abl, Fyn, and Lyn but had lower activity against the Cys252-bearing Src and Yes. This is probably because Gln, unlike Cys, readily forms hydrogen bonds [55]. As a result, the stabilization of the NS-187/Src complex by the induced movement of the P-loop is weaker when Cys252 is present than when Gln252 is present. Thus, induced fit of NS-187 to the kinase is likely to be important for

its ability to block the activity of the kinase. Our docking models support the notion that NS-187 is more specific for Lyn than for Src.

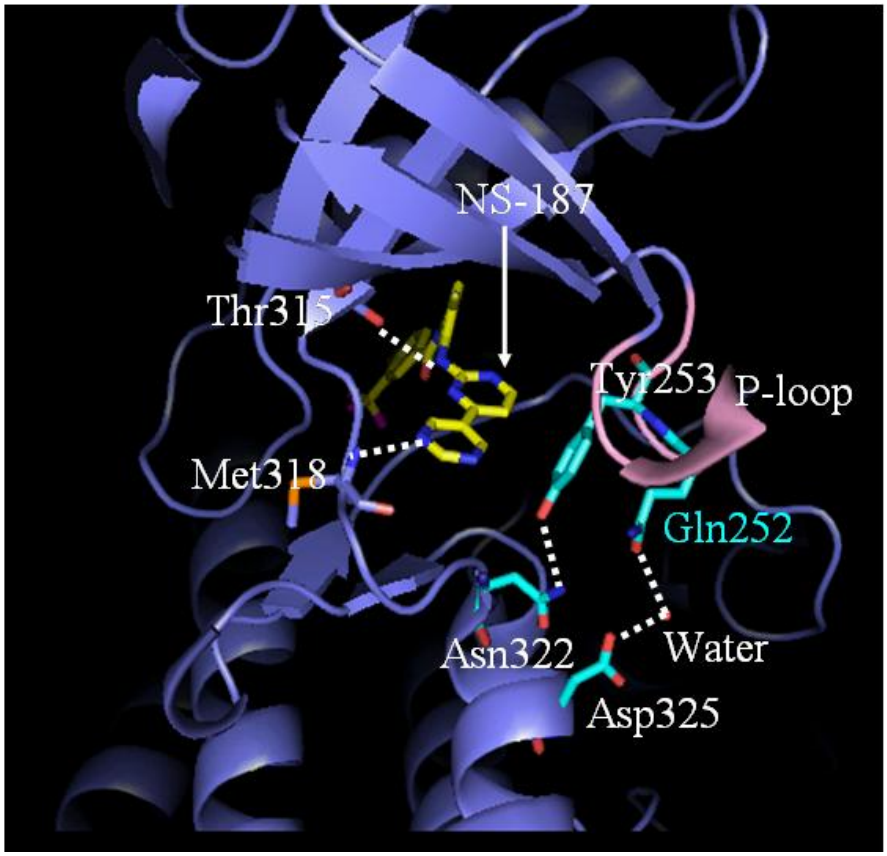

Figure 2-6. Close view of the docking model of NS-187 and Abl.
Hydrogen-bonding interactions are shown as white broken lines. Movement of the P-loop shown in pink and the hydrogen-bonding interactions of the amino acids shown in sky blue contribute to stabilize the complex.

Table 2-3. Relationship between the amino acid at position 252 in Src-family proteins and the ability of NS-187 to inhibit its phosphorylation.

Family	Kinase	Amino acid 252	NS-187 inhibitory activity
Abl	Abl	Gln	High
Src-A	Yes	Cys	Low
Src-A	Src	Cys	Low
Src-A	Fyn	Gln	High
Src-B	Lyn	Gln	High

NS-187 is therefore an excellent candidate for an antileukemia agent. However, NS-187 is limited in one respect; that is, it cannot inhibit the phosphorylation of T315I Bcr-Abl. To our knowledge, an ATP-competitive inhibitor that can inhibit the phosphorylation of T315I Bcr-Abl has not yet been developed. This is probably because the T315I mutation eliminates a crucial hydrogen bond and sterically blocks the imatinib-binding site. According to our docking model, there is little space around T315, suggesting that it would be difficult for an ATP-competitive inhibitor of Bcr-Abl to inhibit the T315I mutant (data not shown). Only ON012380, a non–ATP-competitive inhibitor of Bcr-Abl, is effective against Bcr-Abl/T315I [56]. In addition, such non–ATP-competitive inhibitors may be less specific for Abl than are ATP-competitive inhibitors like NS-187. A compound that specifically inhibits Bcr-Abl/T315I is desirable even if it is difficult to develop.

In conclusion, NS-187 more potently inhibits Abl kinase activity than does imatinib, and its inhibitory activity is less affected by point mutations in the Abl kinase domain. Moreover, NS-187 also inhibits Lyn while otherwise maintaining a high specificity for Bcr-Abl. The efficacy and safety of NS-187 for Ph^+ leukemias is expected to be verified by early-phase clinical trials.

Chapter 3

Evaluation of NS-187 in mice models of imatinib-resistant chronic myeloid leukemia

3-1 Introduction

Efficacy of imatinib mesylate is limited in accelerated/ blastic-phase chronic myeloid leukemia (CML) and Philadelphia-chromosome-positive acute lymphoblastic leukemia (Ph^+ ALL) [20,21]. More than half of the cases of resistance to imatinib are attributable to the point mutations in the Abl kinase domain [19]. Recently, the overexpression of Lyn kinase has been suggested as another mechanism of imatinib-resistance [34].

We have developed NS-187, which has a 25–55-fold greater potency than imatinib to inhibit Abl kinase and which simultaneously inhibits Lyn kinase. We have shown that NS-187 inhibits the kinase activity of 12 of 13 variant Abl kinases with clinically relevant mutations and suppresses the proliferation of cells expressing Bcr-Abl/E255K [57]. However, its *in vitro* and *in vivo* antiproliferative effects against other mutant Abl kinases have not yet been reported. Because *in vitro* results do not always correlate with *in vivo* efficacy, we herein examined the *in vitro* and *in vivo* effects of NS-187 on seven mutated Bcr-Abl proteins and shown that NS-187 had excellent *in vivo* anti-leukemic activity which correlated well with its *in vitro* effects.

3-2 Materials and Methods

3-2-1 Reagents and cell lines

NS-187 and imatinib was synthesized by Nippon Shinyaku Co. Ltd. (Kyoto, Japan) [58]. Ba/F3 cell lines expressing p210 Bcr-Abl/wild-type, M244V, G250E, Q252H, Y253F, T315I, M351T or H396P were established as previously described [57].

3-2-2 Cell viability, immunoblotting and kinase assay

Cells under exponential growth were treated with serial dilutions of the compounds, and incubated for 3 days. Cell viability was determined by assay with MTT (Nacalai Tesque, Kyoto, Japan). Cells treated with serial dilutions of NS-187 for 3 h, were lysed and equal amounts of cell lysates were analysed by Western blotting as described elsewhere [57]. Tyr393-phosphorylated Abl was determined by immunoblotting with anti-phospho-c-Abl (Tyr412) (Cell Signaling Technology, Beverly, MA) (Tyr412 in c-Abl corresponds to Tyr393 in Bcr-Abl). Each mutant form of Abl at a concentration of 10nM was subjected to *in vitro* kinase assays with the SignaTECT^{TM} PTK assay system (Promega, Madison, WI).

3-2-3 Ba/F3 leukemia model

All procedures involving animals were approved by the institutional review board at Nippon Shinyaku. BALB/cA Jcl-nu mice were injected intravenously with 1 x 10^6 cells and randomized into groups of five on day 1. The mice were administered orally with NS-187 (100 mg/kg/dose), imatinib (200 mg/kg/dose) or vehicle (0.5% methylcellulose) twice daily from day 2 through day 12. Survival analysis was performed by the Kaplan–Meier method and statistical significance was assessed by the log-rank test. The prolongation of survival was calculated as the mean survival of mice treated with NS-187 or imatinib as a percentage of the mean survival of vehicle-treated control mice, and denoted T/C (%).

3-3 Results and discussion

3-3-1 *In vitro* effects of NS-187 in imatinib-resistant cell lines

We herein examined the effects of NS-187 or imatinib on intracellular Bcr-Abl tyrosine phosphorylation which have not been previously reported. NS-187 inhibited both wild-type and mutated Bcr-Abl intracellular phosphorylation with a mean IC_{50} value of 140 nM, except Bcr-Abl/T315I (Figure 3-1A). Bcr-Abl/wild-type, Q252H and M351T were especially sensitive to NS-187. Furthermore, NS-187 potently suppressed the growth of these cells, especially cells expressing Bcr-Abl/wild-type, Q253H, Y253F or M351T, though it did not suppress the growth of cells expressing Bcr-Abl/T315I (Figure 3-1B). Imatinib, meanwhile, was much less active against all cell lines tested (Figure 3-1C). These data indicate that NS-187 greatly inhibited not only the intracellular phosphorylation of most mutated Bcr-Abl kinases, but also the proliferation of cells expressing those kinases.

Since phosphorylation on Tyr393 is considered to stabilize the activation loop in the open conformation seen in the active kinase [43,59], the stronger efficacy of NS-187 compared to imatinib could be explained by its effects on the Tyr393-phosphorylated form of Bcr-Abl. Imatinib inhibited the Tyr393-unphosphorylated form of Bcr-Abl with an IC_{50} value of 35 nM but had little effect on the phosphorylated form (Figure 3-1D–F). In contrast, NS-187 effectively inhibited the kinase activity of both Tyr393-phosphorylated and Tyr393-unphosphorylated forms of Bcr-Abl with respective IC_{50} values of 72 and 30 nM, suggesting that NS-187 may have a sufficiently high affinity for Bcr-Abl to enable it to bind even to an unfavourable conformation.

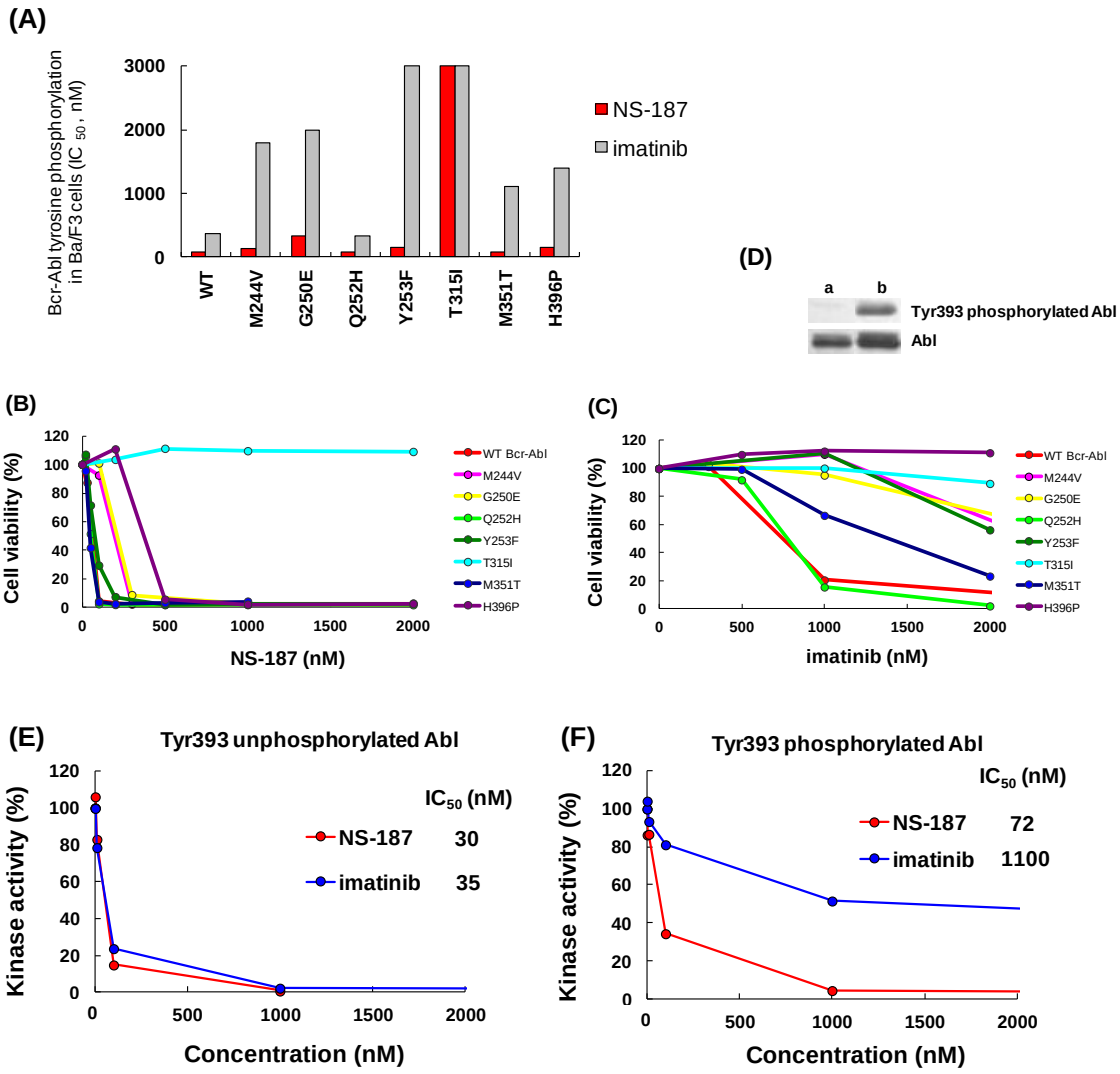

Figure 3-1. *In vitro* effects of NS-187.

(A) Ba/F3 cells expressing the indicated mutant forms of Bcr-Abl were incubated with NS-187 or imatinib for 3 h. Cells were lysed and equal amounts of protein were analysed by immunoblotting with an anti-phosphotyrosine antibody. The amounts of phosphorylated protein were assessed by band densitometry. (B and C) Ba/F3 cells expressing the indicated mutant forms of Bcr-Abl were treated for 3 days with serial dilutions of NS-187 (B) or imatinib (C). Cell proliferation was determined by MTT analysis. (D) The Tyr393 unphosphorylated (lane a) and phosphorylated (lane b) forms of Abl kinase domain. (E and F) Inhibitory effects of NS-187 or imatinib on the kinase activity of the Tyr393-unphosphorylated (E) and the Tyr393-phosphorylated (F) forms of Abl. The data shown are representative of three independent experiments.

3-3-2 *In vivo* activity of NS-187 in an imatinib-resistant mouse leukemia model

To determine whether the *in vitro* inhibition of the growth of imatinib-resistant cells by NS-187 would be observed in an *in vivo* mouse leukemia model, mice were injected intravenously with Ba/F3 cells expressing either wild-type or mutant forms of Bcr-Abl. Mice which received Ba/F3 cells expressing Bcr-Abl/wild-type or any mutant form of Bcr-Abl except Bcr-Abl/T315I showed significant prolongation of survival by NS-187 at a dosage of 200 mg/kg/day without any apparent signs of toxicity (Figure 3-2A–H). This is consistent with the *in vitro* results. In contrast, imatinib even at a dosage of 400 mg/kg/day was much less effective.

To assess the in vivo activity of NS-187 against mutated Bcr-Abl, the prolongation of survival, T/C (%), due to NS-187 or imatinib was calculated and is shown together with the IC_{50} values for NS-187 in the *in vitro* inhibition of cell growth (Figure 3-2I). NS-187 resulted in the highest observed T/C (%) values in Ba/F3 leukemia cells expressing Bcr-Abl/wild-type, Q252H or M351T, in good agreement with the *in vitro* data. Moreover, the rank-order of the IC_{50} values for cell growth inhibition was clearly inversely correlated with T/C (%) in NS-187-treated mice (Figure 3-2I). Thus, the *in vitro* activity of NS-187 mirrored its efficacy in the *in vivo* mouse model of leukemia, a result which suggests that NS-187 will be clinically effective.

In conclusion, NS-187, which inhibited both Tyr393-phosphorylated and Tyr393-unphosphorylated forms of Bcr-Abl, suppressed the intracellular phosphorylation of mutated Bcr-Abl proteins and significantly prolonged the survival of mice which had received leukemic cells expressing mutated Bcr-Abl proteins. These data suggest that NS-187 is a promising agent for CML and Ph^+ ALL which will extent to the treatment of imatinib-resistant patients with Bcr-Abl mutations.

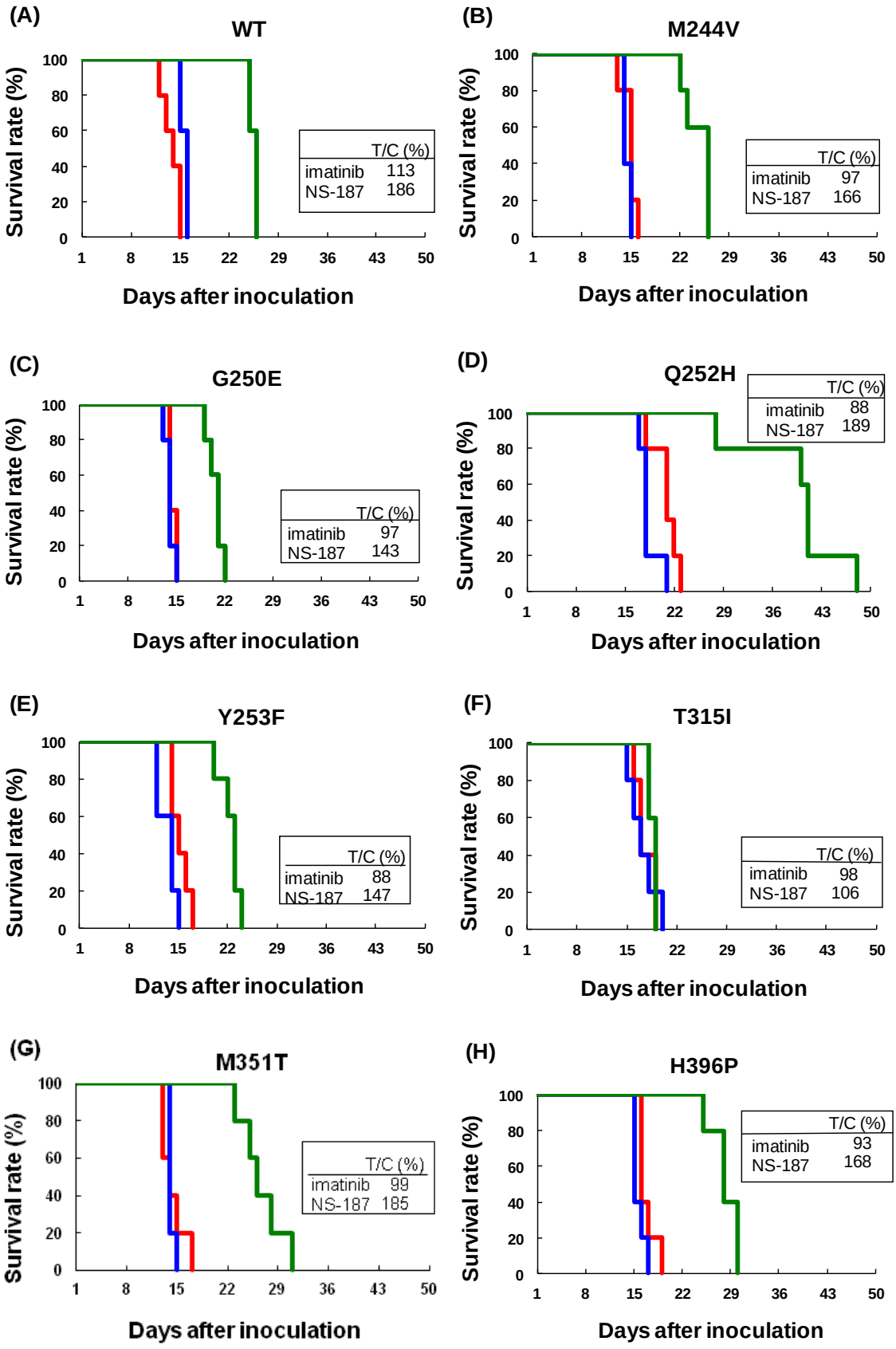
(A)
WT
Survival rate (%)
Days after inoculation
T/C (%)
imatinib 113
NS-187 186
(B)
M244V
Survival rate (%)
Days after inoculation
T/C (%)
imatinib 97
NS-187 166
(C)
G250E
Survival rate (%)
Days after inoculation
T/C (%)
imatinib 97
NS-187 143
(D)
Q252H
Survival rate (%)
Days after inoculation
T/C (%)
imatinib 88
NS-187 189
(E)
Y253F
Survival rate (%)
Days after inoculation
T/C (%)
imatinib 88
NS-187 147
(F)
T315I
Survival rate (%)
Days after inoculation
T/C (%)
imatinib 98
NS-187 106
(G)
M351T
Survival rate (%)
Days after inoculation
T/C (%)
imatinib 99
NS-187 185
(H)
H396P
Survival rate (%)
Days after inoculation
T/C (%)
imatinib 93
NS-187 168

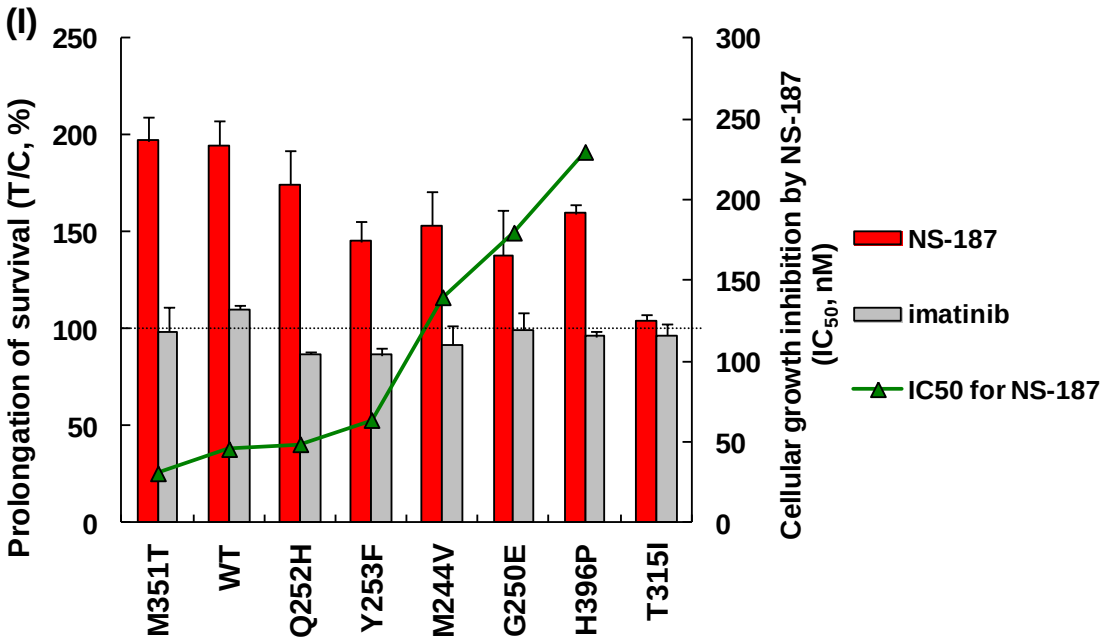

Figure 3-2. ***In vivo*** **activity of NS-187 in an imatinib-resistant mouse leukemia model.**

(A–H) BALB/cA-nu mice were intravenously injected with Ba/F3 cells expressing the indicated mutant forms of Bcr-Abl on day 1. The mice were orally administered twice daily with NS-187 (green), imatinib (blue) or vehicle (red) from day 2 through day 12. The survival of the mice was assessed by the method of Kaplan and Meier. Each group contained five mice. (I) T/C (%) for NS-187 or imatinib. T/C (%) is shown as the average for three independent Ba/F3 clones expressing the same Bcr-Abl mutant. The Bcr-Abl mutants on the horizontal axis are aligned in ascending order of the IC_{50} values for NS-187 for the inhibition of cell growth. Data are presented as means ± S.D. of at least three independent experiments.

Chapter 4

Discovery and characterization of NS-018, a selective JAK2 tyrosine kinase inhibitor, for the treatment of myeloproliferative neoplasms

4-1 Introduction

The breakpoint cluster region-abelson (BCR-ABL) negative myeloproliferative neoplasms (MPNs) include polycythemia vera (PV), essential thrombocythemia (ET), and primary myelofibrosis (PMF) [60.61]. Current treatment options for MPNs, and especially for PMF, are limited and largely palliative with the notable exception of allogeneic stem cell transplantation [62]. A somatic point mutation at codon 617 of Janus kinase 2 (JAK2) tyrosine kinase (JAK2V617F) has been shown to occur in approximately 95% of patients with PV and approximately 50% of patients with ET and PMF [63-67]. JAK2V617F is a constitutively activated kinase that activates the JAK/STAT signaling pathway and dysregulates cell growth and function. Expression of JAK2V617F transforms hematopoietic cells to cytokine-independent growth *in vitro* and causes MPN-like diseases in mice after bone marrow transplantation [64,68-71]. Transgenic mice expressing JAK2V617F also develop MPN-like diseases [72-77]. In addition, other somatic mutations leading to aberrant JAK2 activation, that is, activating mutations in exon 12 of JAK2 and mutations at codon 515 of the thrombopoietin receptor (MPLW515L/K), have been identified in JAK2V617F-negative MPN patients [78,79]. These findings suggest that the inhibition of aberrant JAK2 activation would have a therapeutic benefit, and several JAK2 inhibitors are currently in clinical trials for patients with MPNs [80,81].

NS-018 is a newly discovered, orally bioavailable, small-molecule inhibitor of JAK2 that is competitive with adenosine triphosphate (ATP). In the present study, we describe the preclinical characterization of NS-018 and report on its potent and selective inhibitory activity against JAK2 and Src-family kinases and promising *in vitro* and *in vivo*

activity against constitutively active JAK2 mutants.

4-2 Materials and Methods

4-2-1 *In vitro* kinase assay

The kinase domains of human JAK1, JAK2, JAK3, and TYK2 were purchased from Carna Biosciences. Each kinase was incubated in a reaction medium containing serial dilutions of NS-018, biotinylated-peptide substrate, ATP, and $MgCl_2$ in a streptavidin-coated plate for 1 h at 30°C. Phosphorylated substrates were spectrophotometrically detected with horseradish peroxidase-linked antibody (PY-20; BD Bioscience) and TMB (3,3',5,5'-tetramethylbenzidine) solution (Sigma Aldrich). The concentrations required to give 50% inhibition (IC_{50}) were estimated by fitting the absorbance data to a logistic curve with SAS version 8.2 (SAS Institute). The inhibitory effect of NS-018 was tested against a panel of 53 kinases by Carna Biosciences according to their internal protocol.

4-2-2 Cell lines

The human JAK2V617F and MPLW515L genes were generated by site-directed mutagenesis and cloned into the pDON-AI-2-Neo retroviral vector (Takara Bio), and the TEL-JAK2 and TEL-JAK3 genes were cloned into the pMYs retroviral vector (Cell Biolabs). Ba/F3 cells (Riken BRC Cell Bank) were cultured in RPMI-1640 medium supplemented with 10% fetal bovine serum (FBS) and 10% murine Interleukin-3 (IL-3) Culture supplement (BD Biosciences). Ba/F3-JAK2V617F, Ba/F3-MPLW515L, Ba/F3-TEL-JAK2, and Ba/F3-TEL-JAK3 cells were generated by retroviral infection with the pDON-AI-2-Neo/φMP34 or pMYs/Plat-E packaging system followed by selection for IL-3-independent growth. The clones used were confirmed to show exogenous gene expression by reverse transcriptase polymerase chain reaction and sequencing. SET-2 and CMK cells were from the German Collection of Microorganisms and Cell Cultures (DSMZ), and K-562, U-937, and SKM-1 cells were from Health Science Research Resources Bank. All cell lines were cultured in RPMI-1640 containing 10% or 20% FBS.

4-2-3 Cellular assay

Cell lines were used after reaching 70–90% confluence. For cell growth assay, cells were seeded in 96-well plates at densities optimized for growth rate (transformed Ba/F3 cell lines at 1×10^3 cells/well, SET-2 cells at 1×10^4 cells/well, MV4-11 cells at 2×10^4 cells/well, and other cell lines at 5×10^3 cells/well). The next day, cells were treated with serial dilutions of NS-018, and incubated for 72 h at 37°C with 5% CO_2. Viability was measured by MTT (3-(4,5-dimethylthiazol-2-yl)-2,5-diphenyltetrazolium bromide) assay. IC_{50} values were estimated with SAS version 8.2.

For western blot analysis, Ba/F3-JAK2V617F cells were treated with increasing concentrations of NS-018 for 3 h and total cell lysates were prepared. Lysate samples were subjected to sodium dodecyl sulfate polyacrylamide gel electrophoresis (SDS-PAGE), transferred to a polyvinylidene difluoride (PVDF) membrane, and probed with antibody specific for phospho-STAT5 (Tyr694), phospho-STAT3 (Tyr705), phosphor-p44/42 MAPK (ERK), STAT5, STAT3, or p44/42 MAPK (ERK) (Cell Signaling Technology). Antibodies were detected with the appropriate horseradish peroxidase-linked secondary antibodies (GE Healthcare) and membranes were developed with the ECL Plus western blotting detection system (GE Healthcare). Images were acquired with the ChemiDoc imaging system and analyzed with Quantity One software (Bio-Rad Laboratories).

For apoptosis assay, Ba/F3-JAK2V617F cells were treated with increasing concentrations of NS-018 for 48 h, stained with annexin V and propidium iodide (BD Biosciences), and analyzed with a FACSCalibur flow cytometer (BD Biosciences). For the DNA fragmentation assay, Ba/F3-JAK2V617F cells were treated with NS-018 for 29 h and DNA was extracted with the ApopLadder Ex Kit (Takara Bio). DNA fragmentation was assessed by agarose gel electrophoresis with ethidium bromide staining and analyzed with ChemiDoc Quantity One.

4-2-4 Colony formation assay

Peripheral blood mononuclear cells from PV patients with the JAK2V617F mutation or healthy volunteers were collected with informed consent and Institutional Review Board approval. A total of 2×10^5 cells were treated with increasing concentrations of NS-018 in MethoCult H4534 methylcellulose medium (StemCell Technologies) supplemented with or without 3 U/mL erythropoietin. Experiments were performed in triplicate. Burst forming unit-erythroid (BFU-E) were counted on day 14. IC_{50} values were estimated with SAS version 8.2.

4-2-5 Mouse Ba/F3-JAK2V617F disease model

The study was conducted in compliance with the Law for the Humane Treatment and Management of Animals (Law No. 105, 1973, as revised on 1 June 2006). Female BALB/c nude mice (Japan SLC) were placed in blanket cages in an environment maintained at 21–25°C and 45–65% relative humidity, with artificial illumination for 12 h and a ventilation frequency of at least 15 times per hour. They were allowed free access to food pellets and tap water. Ba/F3-JAK2V617F cells (10^6 per mouse) were inoculated intravenously into seven-week-old mice. Administration of vehicle (0.5% methylcellulose) or NS-018 twice daily by oral gavage began the day after cell inoculation. Survival was monitored daily, and moribund mice were humanely killed and their time of death was recorded for purposes of survival analysis. In a parallel study, all mice were humanely sacrificed after eight days of administration, and their spleens were removed and weighed.

4-2-6 JAK2V617F transgenic mice

The generation and genotyping of transgenic mice (BDF1 strain) were carried out as previously described [74]. At 12 weeks after birth, treatment with vehicle or NS-018 was begun by oral gavage and was continued twice a day on weekdays for 24 weeks. The body weight of the mice was measured weekly. Peripheral blood was drawn monthly into heparin-coated glass capillary tubes, and hematological parameters were determined with a Celltac α hematology analyzer (Nihon Kohden). For fractional analysis of white blood cells, nucleated cells were stained with fluorescently conjugated antibodies specific for Mac1, Gr1, B220, and CD3 (BD Biosciences) and the percentage of each fraction was determined with a FACSCalibur. The fractional cell number was computed by multiplying the percentage by the total white blood cell count.

All mice were humanely sacrificed at the end of treatment, and terminal blood samples and organs were taken. For flow cytometric analysis of spleen and bone marrow, cells were treated with hemolysis buffer, washed in phosphate-buffered saline (PBS) containing 2% FBS, and treated with biotinylated antibodies specific for lineage-antigens (CD3, CD4, CD8, Gr1, Mac1, B220, CD19, and Ter119) for 30 min on ice. After washing, cells were treated with fluorescently conjugated antibodies (BD Biosciences) for 90 min. Antibodies for hematopoietic stem cell staining were APC-conjugated c-Kit, FITC-conjugated CD34, and PE-conjugated Sca-1. Antibodies for myeloid progenitor staining were biotin-conjugated IL7Rα, APC-conjugated c-Kit,

FITC-conjugated CD34, PE-conjugated Sca-1, and PE-Cy7-conjugated FcγR. Antibodies for megakaryocytic progenitor staining were APC-conjugated c-Kit, PE-conjugated CD9, PE-Cy7-conjugated FcγR, and FITC-conjugated CD41. Antibodies for erythrocyte progenitor staining were FITC-conjugated CD71 and PE-conjugated TER119. After washing, cells were resuspended in PBS containing 2% FBS and propidium iodide, and analyzed with a MACSQuant flow cytometer (Miltenyi Biotec) and FlowJo software (Tree Star).

For histological evaluation, tissues samples from liver, spleen, lung and femur were fixed in formalin, embedded in paraffin and cut for hematoxylin-eosin staining or Gomori silver staining according to standard protocols (Biopathology Institute). Histological slides were viewed under a BX50 microscope and photographed with an Olympus FX380 digital camera.

4-2-7 Structural analysis

The kinase domain of human JAK2 was expressed in Sf9 cells infected with recombinant virus and purified as described elsewhere [82]. The NS-018/protein complex was concentrated and crystallized by the hanging-drop method at 4°C. Diffraction data from flash-frozen crystals were collected at the BL32B2 beamline of the SPring-8 synchrotron facility (Hyogo, Japan) and processed with the HKL-2000 package [83]. The structure was solved by molecular replacement with the program Phaser [84]. All computations were performed with Molecular Operating Environment (MOE) version 2009.10 (Chemical Computing Group). Figure 4-1 was prepared with PyMOL version 1.3 (Schrödinger, LLC).

4-3 Results

4-3-1 NS-018 is a potent and selective JAK2 kinase inhibitor *in vitro*

NS-018, (*N*-[(1S)-1-(4-fluorophenyl)ethyl]-4-(1-methyl-1H-pyrazol-4-yl)-*N'*-(pyrazin-2-yl)pyridine-2,6-diamine maleate), was discovered by screening for potent and selective JAK2 inhibitors. In *in vitro* kinase assays, NS-018 was highly active against JAK2 with an IC_{50} of 0.72 nM, and it had 30–50-fold greater selectivity for JAK2 over other Jak-family kinases such as JAK1, JAK3, and TYK2 (Table 4-1). The ability of NS-018 to inhibit other kinases was tested with a panel of 53 kinases in the presence of ATP at concentrations close to their respective Km values. NS-018 showed potent inhibition of Src-family kinases, notably SRC and FYN, as well as weak inhibition of ABL and FLT3 with 45- and 90-fold selectivity for JAK2, respectively (Table 4-2). NS-018 showed a high degree of selectivity for JAK2 over many other tyrosine kinases (Table 4-2) and serine/threonine kinases (Table 4-3).

Table 4-1. *In vitro* effects of NS-018 on Jak-family enzyme activity.

	IC_{50}, nM	**Fold selectivity over JAK2**
JAK2	0.72	1
JAK1	33	46
JAK3	39	54
TYK2	22	31

Table 4-2. Tyrosine kinase selectivity profile of NS-018.

Tyrosine kinase	Family name	Inhibition at 100 nM, %	Fold selectivity over JAK2
JAK2	Jak	101.6	1
FYN	Src	100.0	4
SRC	Src	100.6	5
YES	Src	100.1	11
LYNa	Src	91.2	25
FGR	Src	92.6	26
LCK	Src	97.5	29
HCK	Src	87.0	49
ABL	Abl	90.7	45
FLT3	PDGFR	82.5	90
CSK	Csk	8.6	ND
EGFR	EGFR	-8.5	ND
EPHB4	Eph	19.3	ND
FGFR1	FGFR	4.8	ND
IGF1R	InsR	12.0	ND
ITK	Tec	8.5	ND
KDR	VEGFR	-2.2	ND
MET	Met	-8.7	ND
PDGFRa	PDGFR	6.3	ND
RET	Ret	51.2	ND
TIE2	Tie	-0.1	ND
TYRO3	Axl	-6.9	ND
ZAP70	Syk	16.4	ND

The ability of NS-018 to inhibit 23 tyrosine kinases was tested at one concentration (100 nM) in the presence of ATP at concentrations close to their respective K_m values. IC_{50} values were separately determined against the kinase which were shown to be inhibited more than 80% at 100 nM NS-018. ND, not done.

Table 4-3. Serine/threonine kinase selectivity profile of NS-018.

Serine/threonine kinase	Kinase group	Inhibition at 100 nM, %
AKT1	AGC	-5.1
AMPKa1/b1/g1	CAMK	-1.1
AurA	Other	18.6
CaMK4	CAMK	-1.4
CDK2	CMGC	12.6
CHK1	CAMK	-14.5
CK1e	CK1	-3.3
DAPK1	CAMK	-53.0
DYRK1B	CMGC	-1.7
Erk2	CMGC	-1.9
GSK3b	CMGC	-1.4
IKKb	CAMK	-3.6
IRAK4	TKL	-4.0
JNK2	CMGC	2.3
MAP2K1	STE	12.6
MAPKAPK2	CAMK	1.9
MLK2	TKL	-14.6
MST2	STE	11.0
NEK2	Other	-5.9
p38a	CMGC	-3.4
p70S6K	AGC	-2.6
PAK4	STE	16.8
PDK1	AGC	-2.0
PIM1	CAMK	-9.8
PKACa	AGC	2.5
PKCa	AGC	3.7
PKD2	CAMK	0.1
RAF1	TKL	-4.1
ROCK1	AGC	4.8
SGK	AGC	-6.8

4-3-2 Structural analysis of JAK2 kinase in complex with NS-018

Phosphorylation of the activation loop (A-loop) is one of the most common mechanisms for regulating protein kinase activity, and it leads to the relocation of an Asp-Phe-Gly (DFG) motif located adjacent to the N-terminus of the A-loop [85]. The X-ray co-crystal structure of JAK2 in complex with NS-018 revealed that (1) Tyr residues at positions 1007 and 1008 in the A-loop were phosphorylated, (2) the phosphorylated A-loop lay outside the active-site cleft, and (3) NS-018 bound to JAK2 in the “DFG-in” active conformation (Figure 4-1).

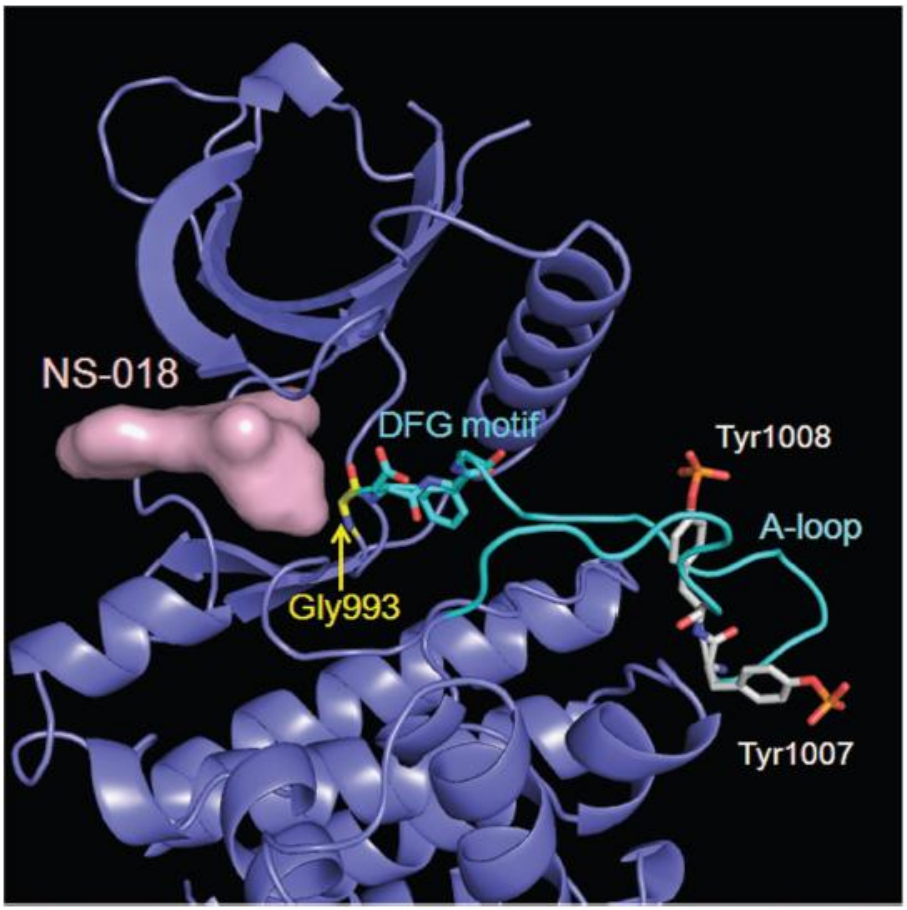

Figure 4-1. X-ray co-crystal structure of NS-018 bound to JAK2 kinase.
The surface of NS-018 is shown in pink, the backbone of JAK2 in slate, and the activation loop (A-loop) in cyan. Gly993 is located immediately N-terminal to the DFG motif. For clarity, only key residues are shown.

4-3-3 NS-018 inhibits JAK2-mediated signaling and proliferation and induces apoptosis

To evaluate the effects of NS-018 on JAK2-mediated signaling, we exposed Ba/F3 cells expressing JAK2V617F (Ba/F3-JAK2V617F) to increasing concentrations of NS-018 for 3 h and measured the level of phosphorylation of JAK2-mediated signaling components by Western blotting (Figure 4-2a). NS-018 inhibited the phosphorylation of STAT5, STAT3, and ERK in a dose-dependent manner, with maximal effects at approximately 100, 30, and 300 nM, respectively.

We next assessed the antiproliferative activity of NS-018 against hematopoietic cell lines (Table 4-4). NS-018 suppressed the growth of Ba/F3-JAK2V617F cells with an IC_{50} of 60 nM and the JAK2V617F-positive cell line SET-2 with an IC_{50} of 120 nM. NS-018 also inhibited the growth of Ba/F3-MPLW515L cells, which is dependent on JAK2-mediated signaling due to an activating mutation of the thrombopoietin receptor, at similar concentrations. Ba/F3-TEL-JAK2 cells were highly sensitive to NS-018, but Ba/F3-TEL-JAK3 cells were less sensitive. CMK cells, which are dependent on both JAK1 and JAK3 due to an activating mutation of JAK3 that signals through wild-type JAK1 [86], were also insensitive to NS-018. NS-018 showed weak antiproliferative activity against K-562 cells, which carry BCR-ABL, and MV4-11 cells, which carry an internal tandem duplication of FLT3. This selective antiproliferative activity was roughly consistent with the kinase inhibitory profile of NS-018. Additionally, NS-018 showed only minimal cytotoxicity against other hematopoietic cell lines such as SKM-1 and U-937.

To determine whether the antiproliferative activity of NS-018 was accompanied by an increase in apoptosis, we exposed Ba/F3-JAK2V617F cells to various concentrations of NS-018 and determined the percentages of apoptotic cells by flow cytometry with annexin V/propidium iodide staining and assessed DNA fragmentation. NS-018 treatment increased both the percentage of annexin V positive cells (Figure 4-2b) and the extent of DNA fragmentation (Figure 4-2c) in a dose-dependent manner. Thus, NS-018 both inhibited the phosphorylation of components of JAK2-mediated signaling and induced apoptosis in cell lines whose growth depended on JAK2 activation.

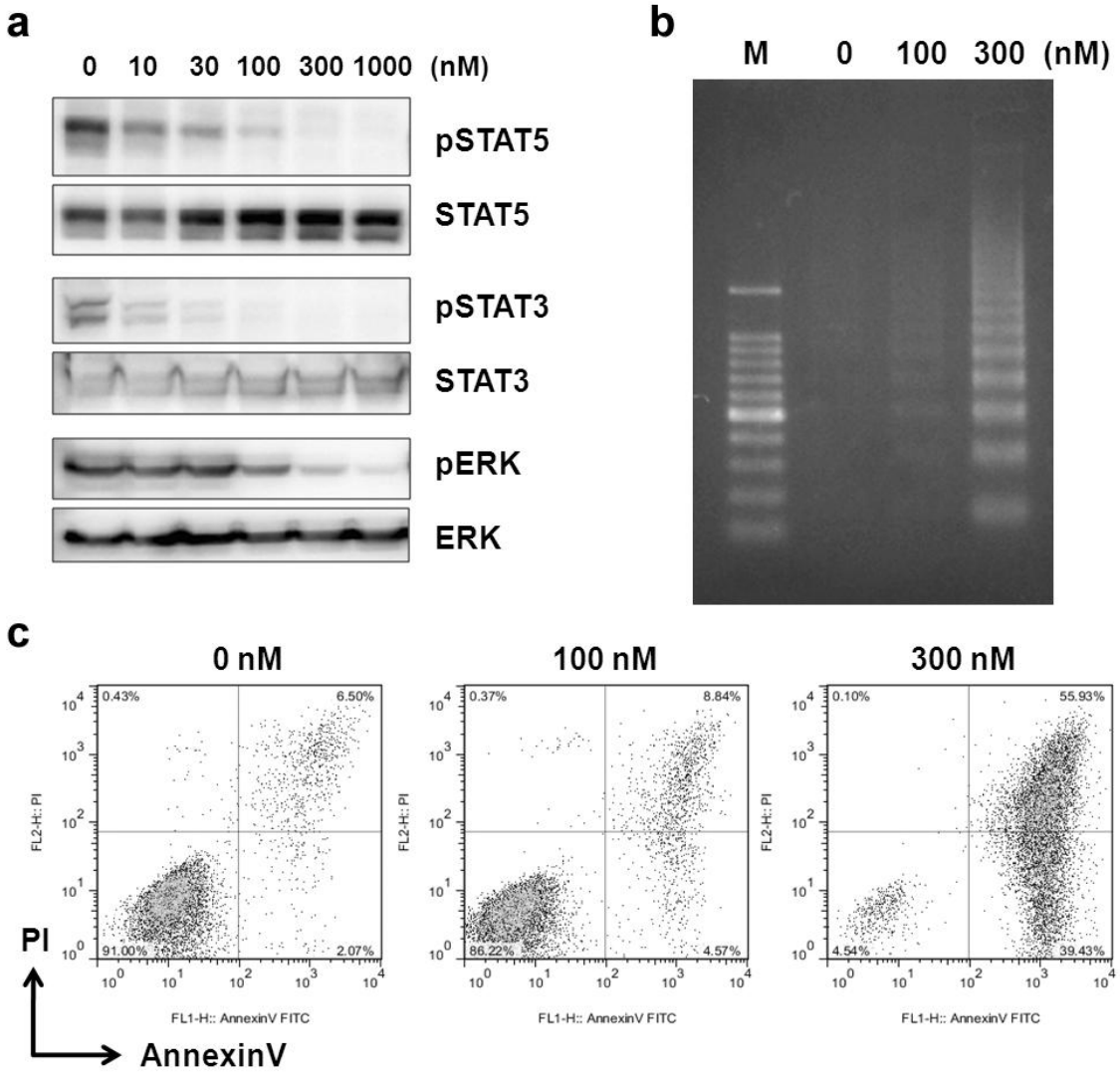

Figure 4-2. Inhibition of JAK2-mediated signaling and induction of apoptosis in Ba/F3-JAK2V617F cells by NS-018.

(a) Ba/F3-JAK2V617F cells were treated with increasing concentrations of NS-018 for 3 h and then lysed. Lysate was subjected to SDS-PAGE, transferred to a PVDF membrane and probed with the indicated antibodies. (b) Ba/F3-JAK2V617F cells were treated with 0–300 nM NS-018 for 48 h and tested for apoptosis by staining with annexin V/propidium iodide (PI). (c) Ba/F3-JAK2V617F cells were treated with NS-018 for 29 h prior to DNA extraction and DNA fragmentation was assessed by agarose gel electrophoresis. M indicates the DNA size marker.

Table 4-4. Antiproliferative activity of NS-018 against hematopoietic cell lines.

Cell line	Origin	Activated kinase	IC_{50}, nM
Ba/F3-JAK2V617F	Murine pro-B cell	JAK2V617F	60
Ba/F3-TEL-JAK2	Murine pro-B cell	TEL-JAK2	11
Ba/F3-TEL-JAK3	Murine pro-B cell	TEL-JAK3	800
Ba/F3-MPLW515L	Murine pro-B cell	MPLW515L	61
SET-2	ET	JAK2V617F	120
CMK	AML	JAK3A572V	1100
K-562	CML	BCR-ABL	1600
MV4-11	AML	FLT3-ITD	730
SKM-1	AML	nk	4100
U-937	Lymphoma	nk	5800

nk, not known; TEL, translocation ets leukemia; MPL, myeloproliferative leukemia virus oncogene; ET, essential thrombocythemia; AML, acute myelogenous leukemia; CML, chronic myelogenous leukemia; BCR-ABL, breakpoint cluster region-abelson leukemia virus; FLT3-ITD, fms-like tyrosine kinase 3-internal tandem duplication.

4-3-4 NS-018 inhibits erythroid progenitor cell growth in primary PV patient samples

To evaluate the efficacy of NS-018 against primary MPN patient cells, we performed colony formation assays with mononuclear cells from the peripheral blood of PV patients with the JAK2V617F mutation or of healthy volunteers. NS-018 inhibited the formation of BFU-E from healthy controls and PV patients in a dose-dependent manner, but the degree of inhibition was significantly greater for the PV patients ($P = 0.011$). Specifically, for three healthy controls, NS-018 inhibited erythroid colony growth with a mean IC_{50} of 952 ± 118 nM, while for four PV patients the corresponding IC_{50} was 529 ± 36 nM (Figure 4-3a). We also assessed the efficacy of NS-018 in inhibiting the growth of erythropoietin-independent, endogenous erythroid colony (EEC) formation, a hallmark of JAK2V617F-positive MPN. NS-018 inhibited EEC formation with a mean IC_{50} of 224 ± 26 nM (Figure 4-3b). Thus, NS-018 effectively inhibited erythroid progenitor cell growth in PV patient samples.

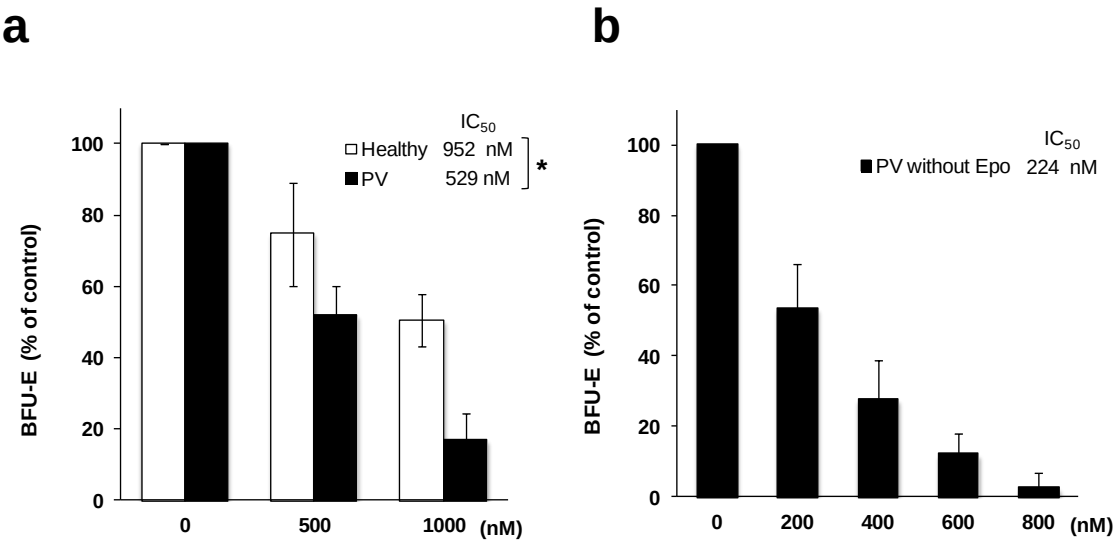

Figure 4-3. Effect of NS-018 on erythroid colony formation by PV patient cells.

Mononuclear cells isolated from the peripheral blood of PV patients with the JAK2V617F mutation (n = 4) or healthy volunteers (n = 3) were treated with increasing concentrations of NS-018 in methylcellulose-based media with erythropoietin (a) or without erythropoietin (b). Burst forming unit-erythroid (BFU-E) were counted on day 14. Values represent the mean ± SEM. Statistical significance was assessed by the t-test (* $P<0.05$).

4-3-5 NS-018 is effective in a mouse Ba/F3-JAK2V617F disease model

We next evaluated the in vivo efficacy of NS-018 in a mouse acute disease model. Mice inoculated with Ba/F3-JAK2V617F cells showed marked splenomegaly and died within 2–3 weeks due to penetrant hematopoietic disease progression. NS-018, administered by oral gavage twice a day, significantly prolonged survival of the mice at dosages of 12.5 mg/kg or higher (Figure 4-4a). Although vehicle-treated mice had all died by day 19, all mice treated with 100 mg/kg NS-018 were still alive even on day 25. NS-018 also significantly reduced splenomegaly at dosages of 1.5 mg/kg or higher (Figure 4-4b). The weight and appearance of the spleens of mice treated with 50 mg/kg NS-018 were similar to those of uninoculated control mice. Thus, NS-018 was highly efficacious in this mouse model of acute disease.

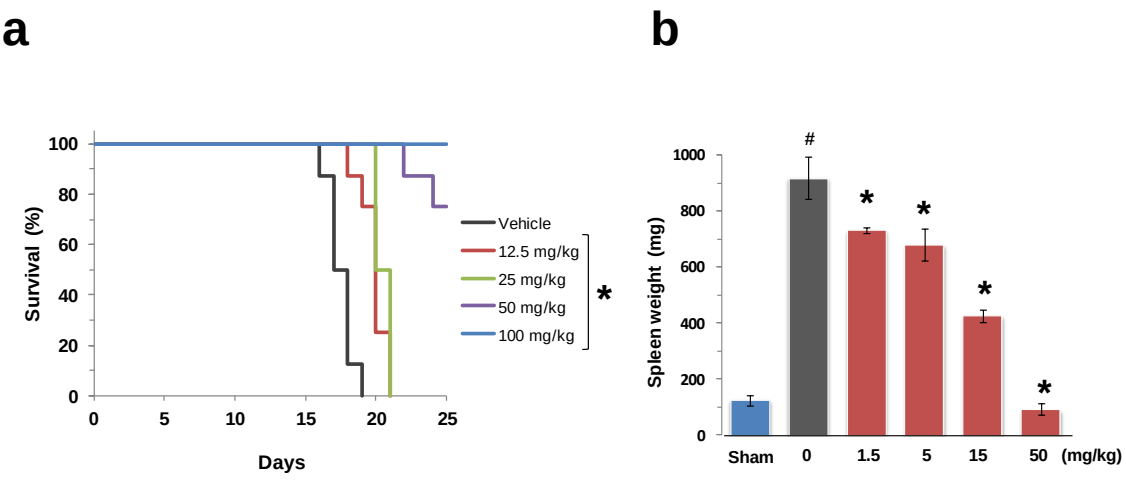

Figure 4-4. Effect of NS-018 on survival and splenomegaly in a mouse Ba/F3-JAK2V617F disease model.

Disease was established in BALB/c nude mice by intravenous injection of 1 × 10^6 Ba/F3-JAK2V617F cells. (a) Survival curves. NS-018 was administered by oral gavage twice a day for 11 days at the indicated doses. Statistical significance was assessed by the log-rank test (* P<0.01 vs vehicle, eight mice per group). (b) Mice inoculated with Ba/F3-JAK2V617F were orally administered with the indicated doses of NS-018 twice a day. Uninoculated control mice (sham) received vehicle only. The day after the completion of eight days of administration, spleens were removed and weighed. Values represent the mean ± SEM. Statistical significance was assessed by the t-test (# P<0.01 vs sham) and Dunnett's test (* P<0.01 vs vehicle, five mice per group).

4-3-6 Efficacy of NS-018 in mouse MPN model (JAK2V617F transgenic mice)

Mice expressing JAK2V617F under the control of the H2Kb promoter (V617F-TG mice) show an MPN phenotype, including leukocytosis, thrombocytosis, progressive anemia, hepatosplenomegaly with extramedullary hematopoiesis, megakaryocyte hyperplasia and fibrosis in the bone marrow [74]. They also exhibit body weight loss and high mortality compared to wild-type controls. Their bone marrow cells show constitutive activation of STAT5 and cytokine-independent erythroid colony formation. In the present study, we tested the efficacy of NS-018 in this chronic MPN model. Before starting long-term administration, we confirmed that NS-018 inhibited constitutive

JAK2-mediated signaling *in vivo*. As expected, NS-018 inhibited the phosphorylation of STAT5 in Mac1+/Gr1+ myeloid cells from bone marrow of V617F-TG mice following a single oral administration at a dosage of 50 mg/kg (Figure 4-5).

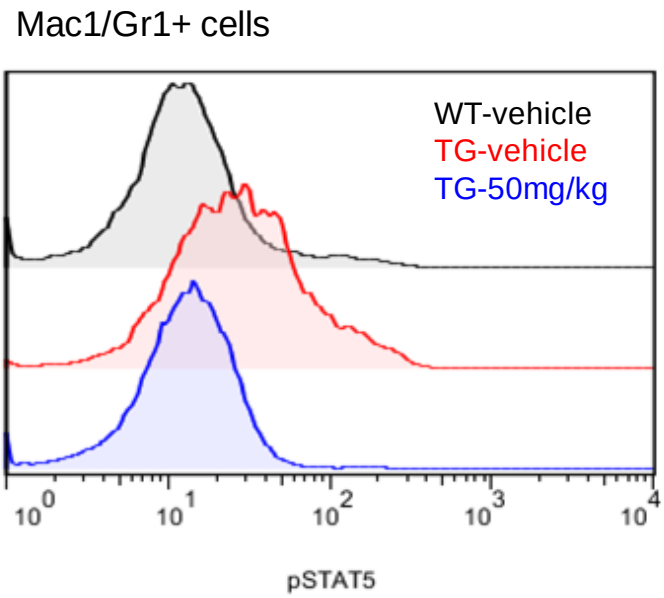

Figure 4-5. Inhibition of STAT5 phosphorylation in JAK2V617F transgenic mice by NS-018.

Wild-type (WT) or JAK2V617F transgenic (TG) mice were orally administered with NS-018 (50 mg/kg) or vehicle once. One hour after administration, bone marrow cells were collected and fixed immediately, and stained with fluorescently conjugated antibodies specific for Mac1, Gr1, and phospho-STAT5. The levels of phosphorylation of STAT5 in Mac1/Gr1- positive cells were determined by flow cytometry.

After disease was established at 12 weeks after birth, V617F-TG mice were randomly assigned to treatment with NS-018 or vehicle. NS-018 was administered by oral gavage twice a day for 24 weeks at doses of 25 or 50 mg/kg, and the control groups received vehicle only. No signs of gross toxicity were observed during the 24 weeks of treatment. During the study, the peripheral blood count of the mice was monitored monthly (Figure 4-6A-D). V617F-TG mice showed marked leukocytosis. After four weeks of NS-018 treatment, the white blood cell count was reduced to 59% in the 25 mg/kg group and 39% in the 50 mg/kg group compared to the vehicle-treated group, and the effect was maintained until the end of the study (Figure 4-6A). To determine which kinds of white blood cell increased, we performed a fractional analysis by flow cytometry. At eight

weeks, the numbers of Mac1+/Gr1+ myeloid cells, B220+ B cells, and CD3+ T cells in V617F-TG mice were respectively 370-, 5.4-, and 8.8-fold greater than in wild-type mice (Figure 4-6B). In the 50 mg/kg group, the respective numbers fell to 98-, 3.3-, and 5.3-fold. Although NS-018 reduced the numbers of all white blood cell types, the reduction in Mac1+/Gr1+ myeloid cells was the greatest. V617F-TG mice also showed progressive anemia (Figure 4-6C). The 25 mg/kg group followed the same course of reduction in red blood cell count as the vehicle-treated group. However, the 50 mg/kg group showed no reduction in red blood cell count even after 20 weeks, although the count was lower than that of wild-type mice. This indicated that treatment with 50 mg/kg NS-018 prevented the progression of anemia. V617F-TG mice showed thrombocytosis in the early stages, but the platelet count declined with time (Figure 4-6D). Platelet aggregation and giant platelets were observed in the peripheral blood of these mice.15 NS-018 treatment resulted in sustained thrombocytosis.

NS-018 treatment also reduced hepatosplenomegaly in a dose-dependent manner (Figure 4-6E). In the spleen, NS-018 treatment significantly decreased Mac1+/Gr1+ myeloid cells associated with extramedullary hematopoiesis and significantly increased B220+ B cells (Figure 4-6F). Consistent with the reduction in organ weights and infiltrating myeloid cells, the histopathological results showed that NS-018 markedly reduced cell invasion and restored normal architecture (Figure 4-6G). In the spleen of V617F-TG mice, the white pulp was blended throughout and partially preserved, and the red pulp was expanded by mainly myeloid cell invasion. However, NS-018 treatment resulted in a marked reduction in cell invasion and a restored architecture of the spleen (Figure 4-6Ga-d). In the liver and lung, extramedullary hematopoiesis consisting of myeloid cells and megakaryocytes was reduced in a dose-dependent manner (Figure 4-6Ge-l) and almost completely disappeared in the 50 mg/kg group (Figure 4-6Gh, l). In contrast to the pathological improvement in these organs, NS-018 treatment had little impact on the progression of fibrosis and megakaryocyte hyperplasia in the bone marrow.

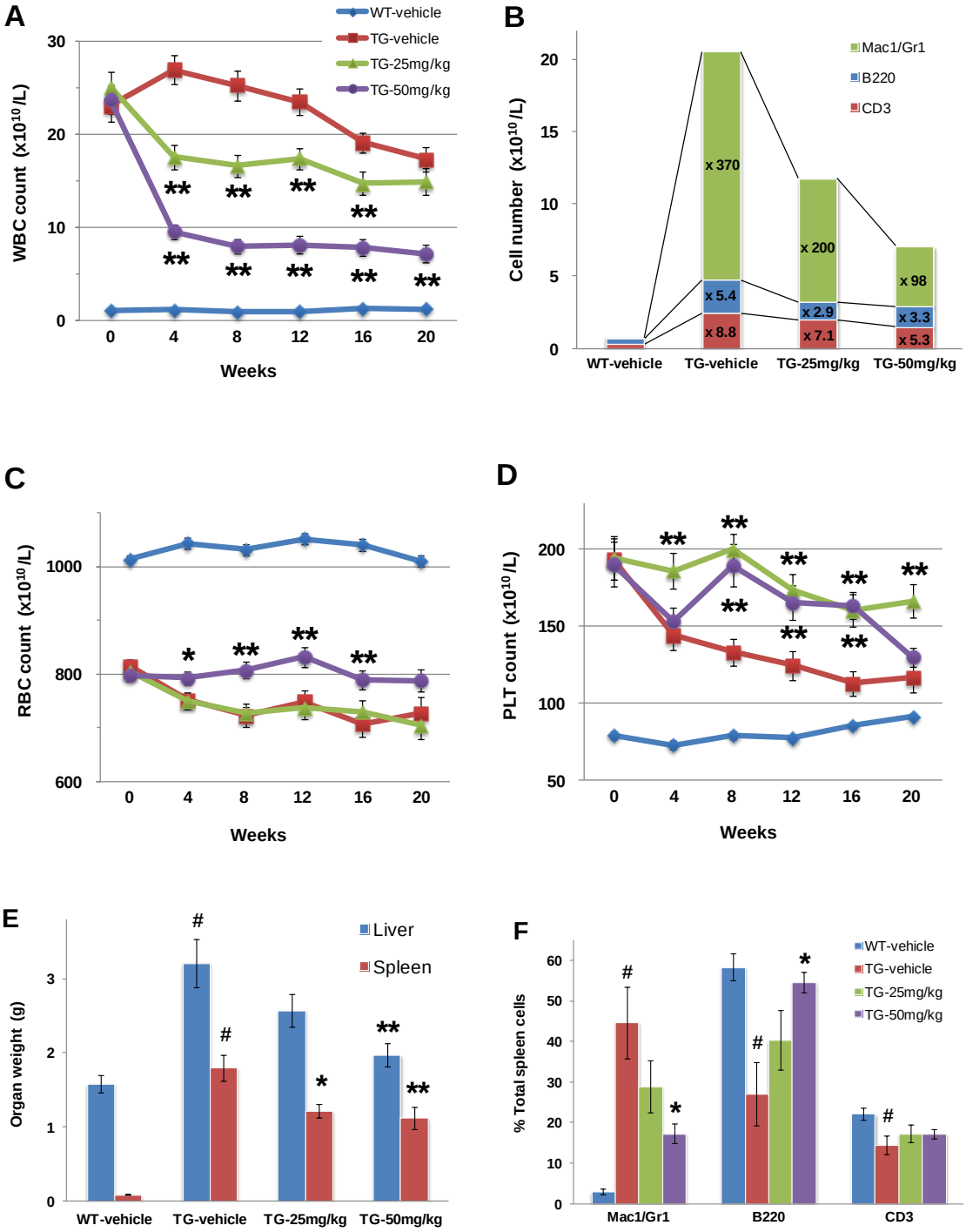
A
WT-vehicle
TG-vehicle
TG-25mg/kg
TG-50mg/kg
WBC count (x10^10/L)
Weeks
B
Mac1/Gr1
B220
CD3
Cell number (x10^10/L)
x 370
x 5.4
x 8.8
x 200
x 2.9
x 7.1
x 98
x 3.3
x 5.3
WT-vehicle
TG-vehicle
TG-25mg/kg
TG-50mg/kg
C
RBC count (x10^10/L)
Weeks
D
PLT count (x10^10/L)
Weeks
E
Liver
Spleen
Organ weight (g)
WT-vehicle
TG-vehicle
TG-25mg/kg
TG-50mg/kg
F
WT-vehicle
TG-vehicle
TG-25mg/kg
TG-50mg/kg
% Total spleen cells
Mac1/Gr1
B220
CD3

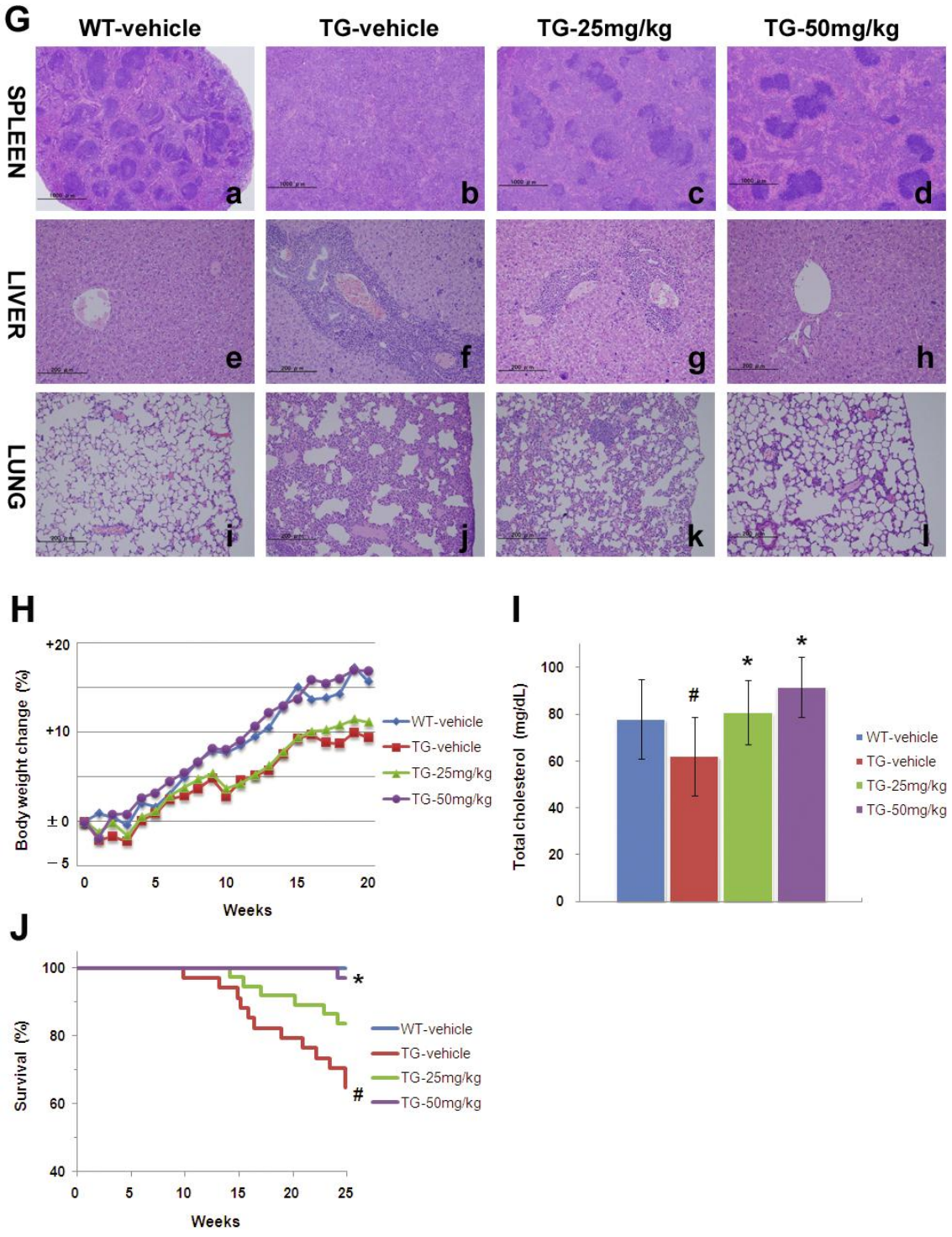

Figure 4-6. Effect of NS-018 in JAK2V617F transgenic mice.

JAK2V617F transgenic mice (TG) were divided into three groups and orally administered with vehicle, 25 mg/kg NS-018, or 50 mg/kg NS-018 (n = 34, 37, and 36, respectively) twice a day for 24 weeks. Wild-type mice (WT) received vehicle only (n = 27). (A) White blood cell (WBC), (C) red blood cell (RBC), and

(D) platelet (PLT) counts were monitored monthly. Values represent the mean ± SEM. Statistical significance was assessed by the t-test (* P<0.05, ** P<0.01 vs TG-vehicle). (B) Differences in cellular composition. Nucleated cells from peripheral blood were stained with fluorescently conjugated antibodies specific for Mac1/Gr1 (myeloid cells), B220 (B cells), and CD3 (T cells) and analyzed by flow cytometry. (E) The weight of liver and spleen were measured at the end of the treatment period. Values represent the mean ± SEM. Statistical significance was assessed by the t-test (# P < 0.01 vs WT-vehicle) or Dunnett's test (* P<0.05, ** P<0.01 vs TG-vehicle). (F) Spleen cells were stained with fluorescently conjugated antibodies specific for Mac1/Gr1 (myeloid cells), B220 (B cells), and CD3 (T cells) and analyzed by flow cytometry. (G) After NS-018 treatment, tissue sections were prepared from spleen (a-d; original magnification ×40), liver (e-h; magnification ×200), and lung (i-l; magnification ×200) for staining with hematoxylin and eosin. (H) The body weight of the mice was monitored weekly. (I) Total cholesterol in the serum at the end of the study. Values represent the mean ± SEM. Statistical significance was assessed by the t-test (# P<0.01 vs WT-vehicle) or Dunnett's test (* P<0.01 vs TG-vehicle). (J) Survival curves of mice. Statistical significance was assessed by the log-rank test (# P<0.01 vs WT-vehicle, * P<0.01 vs TG-vehicle).

4-3-7 NS-018 improves survival and compromised nutritional status in a mouse MPN model

V617F-TG mice exhibited reduced body weight gain and high mortality compared to wild-type controls (Figure 4-6H, J). However, mice treated with 50 mg/kg NS-018 progressively gained more weight than vehicle-treated mice, and their body weight was comparable to that of wild-type mice (Figure 4-6H). Total cholesterol was significantly decreased in the serum of V617F-TG mice compared with wild-type mice, indicating compromised nutritional status. However, in accordance with the body weight gain, total cholesterol was increased in the NS-018-treated groups at the end of the study (Figure 4-6I). NS-018 also improved the survival of V617F-TG mice. During the 24-week study, 12 of 34 mice died in the vehicle group, whereas 1 of 36 mice died in the 50 mg/kg group (Figure 4-6J). This corresponds to a statistically significant prolongation of survival in the 50 mg/kg group (P<0.01). Taken together, these results suggest that NS-018 reduced leukocytosis, anemia progression, hepatosplenomegaly, and extramedullary hematopoiesis, improved nutritional status, and prolonged survival in

V617F-TG mice.

4-4 Discussion

In view of the lack of satisfying treatment options for patients with BCR-ABL-negative MPNs, we sought to develop an orally bioavailable small-molecule therapeutic agent to treat these diseases. The discovery of the JAK2V617F and MPLW515L mutations in MPN patients suggests that the inhibition of aberrant JAK2 activation would have a therapeutic benefit for MPN patients. Our novel JAK2 inhibitor, NS-018, was found to be highly active against JAK2 with an IC_{50} of less than 1 nM and to have high selectivity for JAK2 over many other kinases.

In addition to JAK2, NS-018 inhibited Src-family and ABL kinases with up to almost 50-fold selectivity for JAK2 (Table 4-2). To investigate the structural factors determining the selectivity of NS-018, we carefully explored the binding site of the X-ray co-crystal structure of the complex of the human JAK2 kinase domain and NS-018 (Figure 4-1). Gly at position 993, which is located immediately N-terminal to the activation loop DFG motif, tightly fixed the position of NS-018. Because Gly is the smallest amino acid, we hypothesized that NS-018 effectively inhibites kinases with small amino acids at this position. In keeping with this hypothesis, NS-018 was active against Abl and Src-family kinases, which have Ala, the second smallest natural amino acid, at this position.28 However, kinases belonging to the Axl, FGFR, InsR, Met, and Tie families have Gly or Ala at this position, yet NS-018 did not inhibit them. These kinases may have amino acids at other positions that prevent NS-018 binding. The remaining kinases listed in Table 4-2 have larger amino acids such as Cys, Ser, or Thr at this position, and NS-018 did not inhibit these kinases. Furthermore, the Ser/Thr kinases listed in Table 4-3 also have larger amino acids such as Cys, Ser, Thr, Val, Leu, or Ile at the corresponding position, and NS-018 also did not inhibit these kinases. These results provide evidence that the selectivity of NS-018 is largely determined by the size of the amino acid at position 993.

JAK and Src-family kinases work in concert to activate many signaling molecules [88]. Cooperation between SRC and JAKs is required for full activation of STAT3 [89]. Potent inhibition of STAT3 phosphorylation in Ba/F3-JAK2V617F cells by NS-018 (Figure 4-2a) may be explained by the simultaneous inhibition of JAK2 and Src-family kinases. Several reports have indicated the involvement of Src-family kinases in the pathogenesis of MPNs. For example, a TEL-lyn fusion gene has been identified in a

patient with primary myelofibrosis [90]. The Src-family kinase inhibitors dasatinib and PP2 have been shown to suppress erythropoietin-independent erythroid colony growth from PV [91,92]. Furthermore, SRC kinase preactivation is associated with platelet hypersensitivity in ET and PV patient samples [93]. On the other hand, LYN, FGR, and HCK have been reported to be independent of JAK2V617F-induced polycythemia in a murine retroviral bone marrow transplantation model [71]. Although the involvement of Src-family kinases in MPNs has not yet been fully clarified, simultaneous inhibition of JAK2 and some Src-family kinases is expected to be advantageous in preventing aberrant JAK2-STAT signaling and thereby curing the disease.

NS-018 inhibited the growth of cells which depended on JAK2 activation with IC_{50} values of 11–120 nM. Consistent with the selective inhibition by NS-018 of the enzymatic activity of JAK2 over that of JAK1 and JAK3, Ba/F3-TEL-JAK3 and CMK cells were less sensitive to NS-018. Weak inhibition of ABL and FLT3 kinases by NS-018 is the most likely explanation for its weak antiproliferative activity against K-562 cells (which express BCR-ABL) and MV4-11 cells (which express an internal tandem duplication of FLT3). The difference between the selectivity of NS-018 in the enzyme-inhibition assay and in the cell growth assay may arise from a difference in the extent to which cell growth depends on kinase activation in these cell lines. The fact that NS-018 did not inhibit other Tyr or Ser/Thr kinases might explain its low general cytotoxicity against nontarget cells.

The efficacy of several JAK2 inhibitors has been evaluated in an acute mouse Ba/F3-JAK2V617F disease model [94-96]. In the present study, NS-018 seemed as effective as these inhibitors in this model (Figure 4-4). These results demonstrate the *in vivo* potency of NS-018. To further evaluate the efficacy of NS-018 in a chronic MPN model, we performed long-term administration of NS-018 to transgenic mice expressing JAK2V617F. In contrast to other reports that several JAK2V617F transgenic mice tend to show polycythemia [72,73,75-77], our transgenic mice showed progressive anemia [74]. Although the reason for this is unclear, any impairments in the differentiation of erythrocyte progenitors to mature erythrocytes and the progression of bone marrow fibrosis are supposed to be related to anemia (unpublished data). Treatment with 50 mg/kg NS-018 prevented the progression of anemia in these mice (Figure 4-6C). To assess the causes of differences in the peripheral blood count, we examined the effects of NS-018 on hematopoietic cellular compartments and differentiation in bone marrow and spleen by flow cytometric analysis. No significant differences were observed in the proportion of hematopoietic stem cells (CD34+/Kit+/Sca1+/Lineage-), common myeloid progenitors (CD34+/Kit+/Sca1-/FcγRlow/Lineage-), granulocyte/macrophage

progenitors (CD34+/Kit+/Sca1-/FcγRhigh/Lineage-), megakaryocytic/erythroid progenitors (CD34low/Kit+/Sca1-/FcγRlow/Lineage-), erythrocyte progenitors (CD71+/Ter119+), or megakaryocytic progenitors (CD41+/Kit+/CD9+/FcγRlow/Lineage-) in the NS-018-treated group compared with the vehicle-treated group (data not shown). Because the proportions of stem cells and progenitors in the spleen and bone marrow were not changed by NS-018 administration, it was assumed that erythrocyte progenitors did not increase. Additionally, serum levels of erythropoietin and thrombopoietin were not significantly different in NS-018-treated and vehicle-treated V617F-TG mice. Thus, the reason for the NS-018-dependent reduction in anemia progression remains unclear.

V617F-TG mice also showed thrombocytosis in the early stages, but the platelet count slowly decreased with time. Because the megakaryocyte number in bone marrow in these mice was remained higher than in wild-type mice, platelet production was assumed not to have decreased. One possible explanation for the reduction in platelet count is enhancement of platelet trapping due to progressive splenomegaly. The sustained thrombocytosis caused by NS-018 treatment (Figure 4-6D) was considered to be the result of reduced splenomegaly. Another possible explanation for the platelet-count reduction in V617F-TG mice is a reduced platelet life span due to the enhanced platelet aggregation. It has been hypothesized that, in patients with MPNs, continuous leukocyte degranulation due to leukocyte activation might result in the consumption of factor V and protein S, leading to activated protein C resistance and increased risk of thrombosis [97]. Platelet aggregation has also been observed in V617F-TG mice [74]. Although NS-018 has been shown not to affect the clotting function of blood from normal rats (unpublished data), treatment with NS-018 might reduce platelet aggregation by suppressing leukocyte activation, thereby prolong platelet life span in these mice.

Loss of appetite and deterioration in nutritional status are observed in patients with MPNs, especially myelofibrosis [98]. V617F-TG mice also exhibited reduced body weight gain and reduced total serum cholesterol levels, and NS-018 markedly increased both their body weight gain and their cholesterol levels (Figure 4-6H, I). These effects may have been brought about by an improvement in appetite through a reduction in the mechanical compression of the gastrointestinal tract resulting from hepatosplenomegaly, as well as inhibition of leptin signaling through JAK2. Improvement in nutritional status by NS-018 seemed to contribute to the prolonged survival of these mice.

In summary, NS-018 significantly reduced leukocytosis, hepatosplenomegaly, and extramedullary hematopoiesis, and improved nutritional status in V617F-TG mice. All

these effects of NS-018 may contribute to the survival benefits observed in V617F-TG mice. Additionally, NS-018 inhibited erythroid colony formation by peripheral blood mononuclear cells from PV patients at concentrations significantly lower than those required for healthy controls (Figure 4-3). Examination of the X-ray co-crystal structure showing NS-018 bound to JAK2 in the “DFG-in” active conformation strongly suggests that NS-018 may inhibit constitutively activated JAK2 with the V617F mutation as well as or better than it inhibits activated wild-type JAK2. Overall, our results suggest that NS-018 will be effective in treating patients with MPNs. The efficacy and safety of NS-018 for MPNs is expected to be verified by early-phase clinical trials to begin in early 2011.

Chapter 5

Analysis of NS-018 for JAK2V617F mutant kinase selectivity

5-1 Introduction

Janus kinase 2 (JAK2) is a tyrosine kinase which plays an essential role in the cytokine signaling pathways that regulate hematopoiesis. Germline deletion of JAK2 in mice results in embryonic lethality due to a lack of hematopoiesis [99,100], and conditional JAK2 deletion in young adult mice severely impairs erythropoiesis and thrombopoiesis [101].

A somatic point mutation at codon 617 of JAK2, V617F, occurs in the BCR-ABL-negative myeloproliferative neoplasms (MPN), including polycythemia vera, essential thrombocythemia, and primary myelofibrosis [63-67]. The resulting mutant protein, JAK2V617F, is a constitutively activated kinase that activates multiple downstream signaling pathways, such as the signal transducer and activator of transcription (STAT), extracellular signal-regulated kinases (ERK) and Akt signaling pathways, and it transforms hematopoietic cells to cytokine-independent growth. The expression of JAK2V617F causes MPN-like diseases in mice after bone marrow transplantation (BMT) [68-71]. Transgenic mice expressing JAK2V617F also develop MPN-like diseases [72-77]. These findings suggest that the inhibition of aberrant JAK2 activity would have therapeutic benefit, and accordingly several JAK2 inhibitors have been developed for the treatment of MPN [80,81,102-106].

JAK2 inhibitors show significant therapeutic benefit by reducing spleen size, relieving debilitating symptoms, and improving overall survival in clinical trials of these compounds in the treatment of myelofibrosis [105-107]. Although current JAK2 inhibitors are therapeutically effective, they are reported to have hematologic adverse events, including anemia and thrombocytopenia [105-107].

NS-018,

(N-[(1S)-1-(4-fluorophenyl)ethyl]-4-(1-methyl-1H-pyrazol-4-yl)-N'-(pyrazin-2-yl)pyridine-2,6-diamine maleate) is a potent and selective inhibitor of JAK2 and Src-family kinases which is currently in early-phase clinical trials for MPN. In a previous study, NS-018 prevented the progression of anemia in JAK2V617F transgenic mice as well as improving splenomegaly and survival [108]. However, the effect has not yet been confirmed in other animal models. Furthermore it remains unclear which characteristic feature of NS-018 contributes to this effect. In this study, we confirmed the effect of NS-018 on red blood cells in another myelofibrosis model mouse. We also report that NS-018 suppressed the growth of cells harboring JAK2V617F more strongly than that of cells harboring wild-type JAK2.

5-2 Materials and Methods

5-2-1 Production of retroviruses

Murine JAK2WT (wild-type) and murine JAK2V617F cDNA [74] were cloned into the retroviral vector pMCs-IRES-GFP (Cell Biolabs, San Diego, CA, USA). Transient transfection of Platinum-E retroviral packaging cells (Cell Biolabs) was performed by using the FuGENE6 transfection agent (Promega, Madison, WI, USA) according to the manufacturer's protocol. Retroviral supernatants were harvested after 48 h and used to transduce the murine interleukin-3 (IL-3) dependent pro-B cell line Ba/F3 or bone-marrow cells.

5-2-2 JAK2V617F BMT mice

Murine BMT experiments were performed as previously described [68,69]. Briefly, female BALB/c donor mice (Japan SLC, Hamamatsu, Shizuoka, Japan) were treated with 5-fluorouracil (150 mg/kg, intraperitoneal injection) to increase the number of cycling stem cells for retroviral transduction. Three days after injection, bone-marrow cells were harvested by flushing the femurs and tibias of the donor mice with phosphate-buffered saline. Mononuclear cells were isolated by Ficoll-Paque density gradient centrifugation and cultured for 24 h in αMEM medium supplemented with 20% fetal bovine serum and recombinant murine interleukin-6, stem cell factor, FMS-like tyrosine kinase 3 (flt3) ligand, and thrombopoietin (PeproTech; 50 ng/ml each). The cells were treated with retroviral supernatants in RetroNectin-coated dishes (Takara Bio,

Otsu, Shiga, Japan) for 72 h. The cells were then injected into the lateral tail vein of BALB/c recipient mice that had been irradiated with 2.5 Gy of gamma rays (2×10^5 cells per mouse).

Ten days after transplantation, NS-018 was orally administered twice daily for 40 days at 50 mg/kg. After treatment, all mice were humanely killed and terminal blood samples and organs were collected. Hematological parameters were determined with an ADVIA 120 hematology system (Siemens Healthcare, Erlangen, Germany). For survival analysis, the statistical significance of differences between vehicle and NS-018 groups was assessed by the log-rank test with SAS version 9.1.3. For blood count and spleen weight analyses, the statistical significance of differences between control and vehicle groups was assessed by the Welch test. If the control and vehicle groups were significantly different, the statistical significance of differences between the vehicle and NS-018 groups was assessed by the Welch test. For histological evaluation, tissues samples from spleens and femurs were fixed in formalin, embedded in paraffin and cut for hematoxylin–eosin staining or Watanabe silver staining according to standard protocols (KAC, Kyoto, Japan). Histological slides were viewed under an Olympus BX50 microscope and photographed with an Olympus FX380 digital camera. Studies were conducted in compliance with the Law for the Humane Treatment and Management of Animals (Law No. 105, 1 October 1973, as revised on 1 June 2006).

5-2-3 Cell culture and growth assay

Ba/F3 cells (Riken BRC Cell Bank, Tsukuba, Ibaraki, Japan) were cultured in RPMI-1640 medium supplemented with 10% fetal bovine serum and 20 ng/ml recombinant murine IL-3 (PeproTech, Rocky Hill, NJ, USA). Ba/F3-JAK2WT and Ba/F3-JAK2V617F cells were generated by retroviral infection with polybrene.

For growth assays, cells were seeded in 96-well plates at 1×10^3 cells/well, treated with serial dilutions of compound, and incubated for 90 h at 37°C in 5% CO_2. Viability was measured by WST-8 assay (Cell Counting Kit-8; Dojindo Laboratories, Kumamoto, Japan). The concentration required to give 50% inhibition (IC_{50}) was estimated with SAS version 9.1.3 (SAS Institute, Cary, NC, USA).

For colony formation assay, bone-marrow cells were harvested by flushing the femurs and tibias of JAK2V617F transgenic mice or WT control mice with phosphate-buffered saline. A total of 2×10^5 cells were treated with increasing concentrations of NS-018 in MethoCult M3334 methylcellulose medium (StemCell Technologies, Vancouver, BC, Canada) in the presence of 3 U/ml erythropoietin. Experiments were performed in

triplicate. Erythroid colony-forming units (CFU-E) were counted on day 3 and a two-way factorial analysis of variance was performed with SAS version 9.1.3.

5-2-4 Structural analysis

The acquisition of the X-ray co-crystal structure of NS-018 bound to JAK2 was described previously [108]. All published X-ray crystal structures were taken from the Protein Data Bank (http://www.rcsb.org/pdb/home/home.do). Figure 3-5 and 3-6 were prepared with PyMOL version 1.3 (Schrödinger, New York, NY, USA).

5-3 Results

5-3-1 Efficacy of NS-018 in JAK2V617F BMT mice

To assess the effect of NS-018 in a mouse model with a myelofibrosis-like disease, we established a JAK2V617F BMT mouse model. BALB/c mice were subjected to BMT with bone marrow donor cells retrovirally transduced to express JAK2WT or JAK2V617F. Only JAK2V617F BMT mice developed myelofibrosis-like disease, including leukocytosis, splenomegaly, and bone marrow fibrosis (Figure 5-1). They also exhibited higher mortality than control or JAK2WT BMT mice.

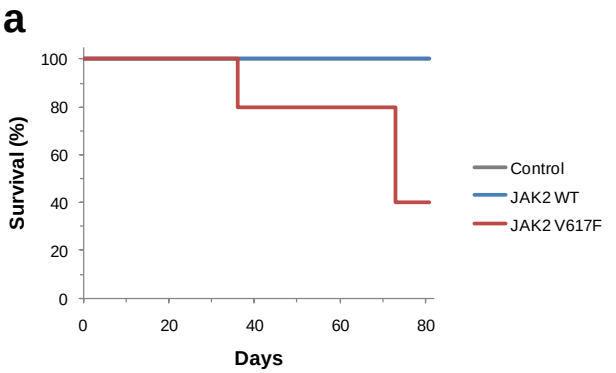

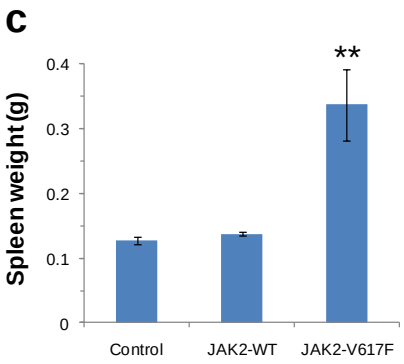

b

Mice	WBC ($\times 10^9$/l)	RBC ($\times 10^{10}$/l)	RETIC ($\times 10^{10}$/l)	PLT ($\times 10^{10}$/l)
Control	7.0	1110	31.4	153
JAK2WT BMT	6.9	1180	40.1	108
JAK2V617F BMT	178	1250	158	120

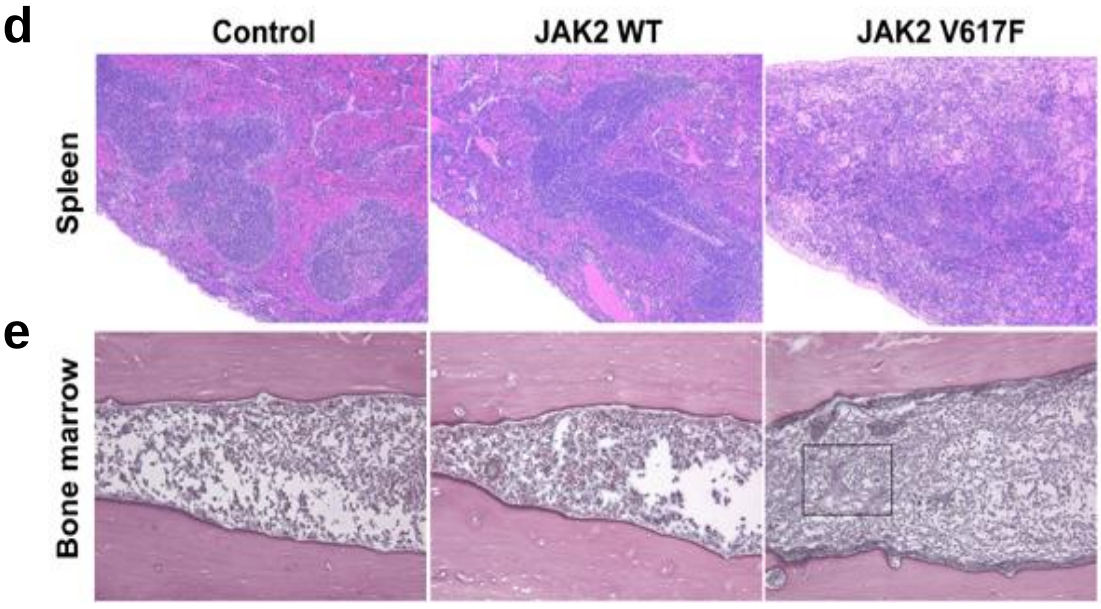

f 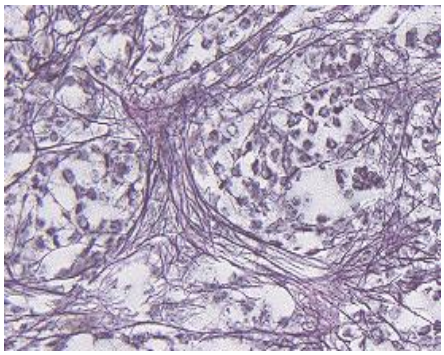

Figure 5-1. Development of myelofibrosis-like disease in JAK2V617F BMT mice.

BALB/c mice were subjected to BMT with bone marrow donor cells retrovirally transduced to express JAK2V617F or JAK2WT. Eighty days after BMT, peripheral blood samples and organs were collected. (a) Survival. (b) Peripheral blood count. (c) Spleen weight. (d) Spleen sections. Hematoxylin and eosin. (e) Bone marrow. Reticulin staining (original magnification ×200). (f) Inset from (d), right panel.

We next evaluated the efficacy of NS-018 in this model. When disease was established at 10 days after transplantation, JAK2V617F BMT mice were randomly assigned to either of two groups for treatment with NS-018 or vehicle. NS-018 was administered by oral gavage twice a day for 40 days at a dose of 50 mg/kg, while the control group received vehicle only. No signs of gross toxicity were observed during the 40 days of treatment.

During the total of 50 days of the study, four of eight mice in the vehicle-treated group died, whereas no mice in the NS-018-treated group died (Figure 5-2a). This represents a statistically significant prolongation of survival in the NS-018-treated group ($P<0.05$).

Vehicle-treated JAK2V617F BMT mice showed marked leukocytosis (Figure 5-2b), as evidenced by a 47-fold increase in the mean white blood cell (WBC) count in the peripheral blood of vehicle-treated mice to 359 × 10^9/L (compared to 7.6 × 109/L in control mice). NS-018 treatment achieved a 95% suppression of this increase to 17.4 × 10^9/L. In vehicle-treated JAK2V617F BMT mice, the differential WBC count showed that the neutrophils had increased to 80.0%, compared to 7.5% in control mice (Figure 5-2c). Conversely, the percentage of lymphocytes in vehicle-treated JAK2V617F BMT mice was 10.7%, compared to 88.8% in control mice. NS-018 treatment partially suppressed both the increase in neutrophils and the decrease in lymphocytes, giving 47.9%

neutrophils and 42.2% lymphocytes. JAK2V617F BMT mice showed a higher reticulocyte (RETIC) count than control mice but about the same red blood cell (RBC) count. NS-018 treatment did not decrease the RBC and only marginally decreased the RETIC count (Figure 5-2d). JAK2V617F BMT mice showed a 78% decrease in the platelet (PLT) count compared with control mice (Figure 5-2e), and NS-018 treatment did not further decrease the count.

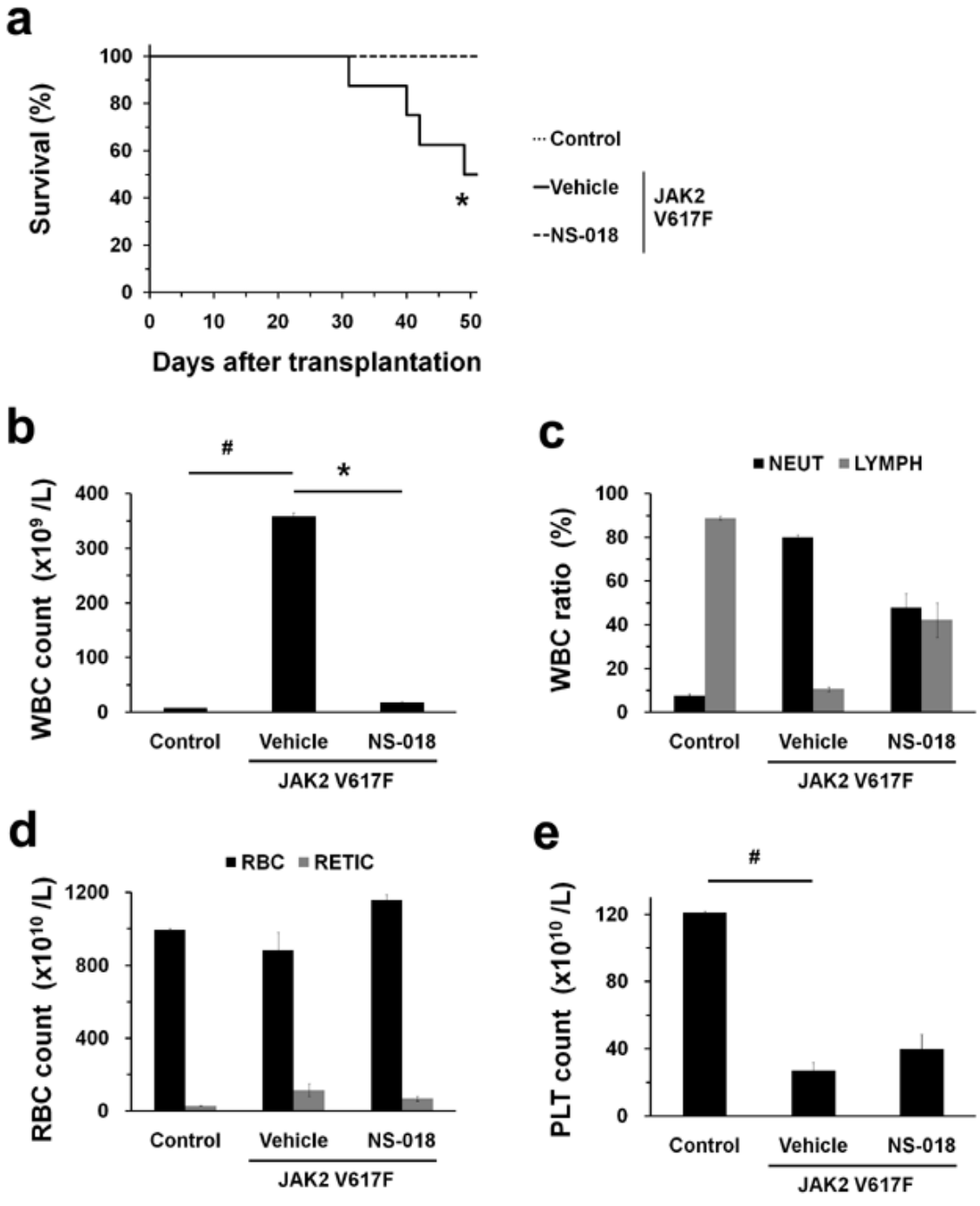

Figure 5-2. Effect of NS-018 on survival and peripheral blood counts in JAK2V617F BMT mice.

(a) Kaplan-Meier plot of untransplanted control mice treated with vehicle (Control) and JAK2V617F BMT mice treated with vehicle (Vehicle) or 50 mg/kg NS-018 (NS-018) for 40 days. Statistical significance in survival between the Vehicle and NS-018 groups was assessed by the log-rank test (*P<0.05, eight mice per group). (b) White blood cell (WBC), (c) neutrophil (NEUT) and lymphocyte (LYMPH), (d) red blood cell (RBC) and reticulocyte (RETIC) and (e) platelet (PLT) counts. Bars represent the mean ± s.e.m. The statistical significance of differences between the Control and Vehicle groups (#P<0.05) and between the Vehicle and NS-018 groups (*P<0.05) were assessed by the Welch test.

Vehicle-treated JAK2V617F BMT mice also showed marked splenomegaly, with higher average spleen weights (2.07 ± 0.08 g) than control mice (0.10 ± 0.01 g) (Figure 5-3a). NS-018-treated JAK2V617F BMT mice had a spleen weight of 0.49 ± 0.08 g, or 24% of that of vehicle-treated mice, so that NS-018 largely prevented the development of splenomegaly. The histopathological results also provide evidence that NS-018 treatment suppressed the development of splenomegaly. Spleen sections from vehicle-treated JAK2V617F BMT mice exhibited complete disruption of the normal splenic architecture (Figure 5-3b,c). The white pulp was partially preserved but blended throughout, and the red pulp was expanded, mainly by myeloid-cell invasion. NS-018 treatment resulted in markedly reduced myeloid-cell invasion and a less disrupted splenic architecture (Figure 5-3d).

Finally, NS-018 partially suppressed bone marrow fibrosis in JAK2V617F BMT mice (Figure 5-3e–g). There was mild-to-moderate reticulin fibrosis in all vehicle-treated mice that survived to the study endpoint (n = 4), whereas in seven of eight mice treated with NS-018 there was only slight-to-little reticulin fibrosis. Only one NS-018-treated mouse showed mild fibrosis. Taken together, these results show that NS-018 reduced leukocytosis and splenomegaly, suppressed bone marrow fibrosis, and prolonged survival in JAK2V617F BMT mice without reducing the RBC or PLT counts.

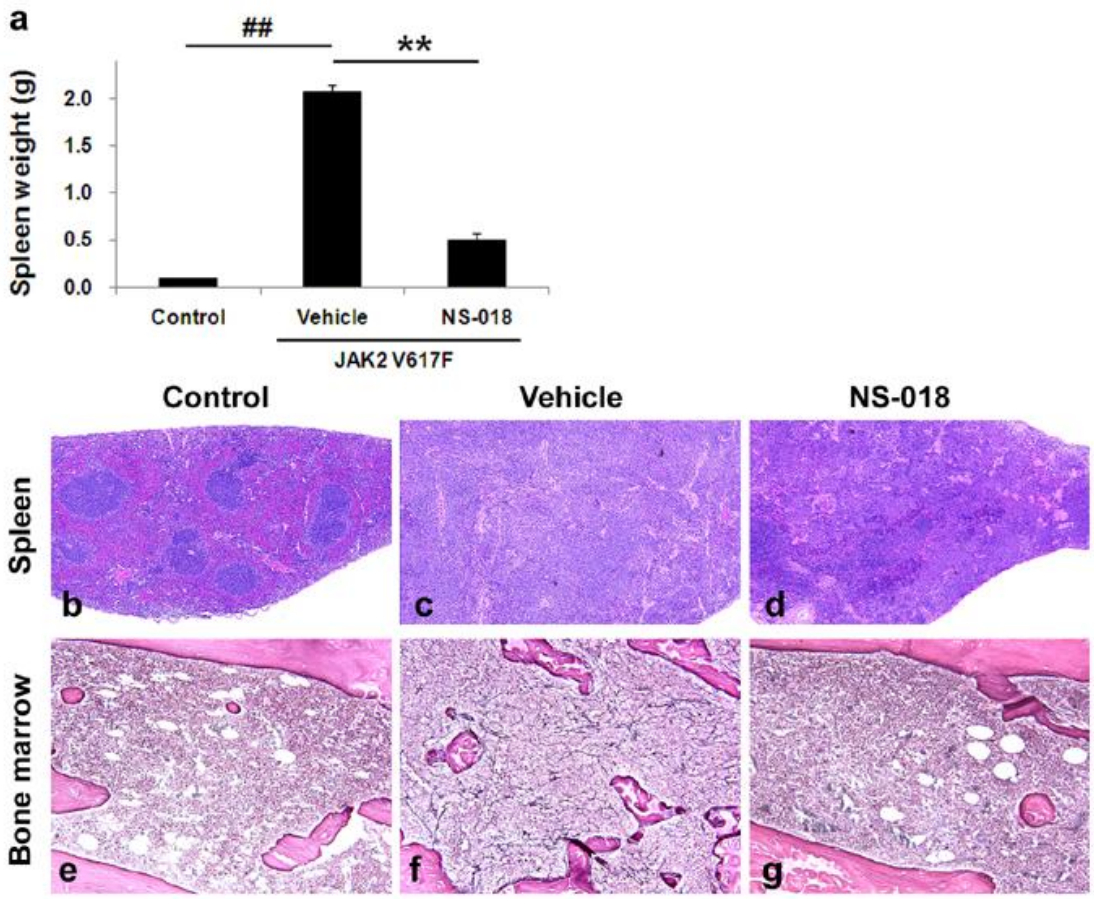

Figure 5-3. Effect of NS-018 on spleen weight and bone marrow fibrosis in JAK2V617F BMT mice.

NS-018 was orally administered for 40 days at 50 mg/kg twice a day. After treatment, spleens and femurs were removed. (a) Spleen weight. Bars represent the mean ± s.e.m. The statistical significance of differences between the Control and Vehicle groups (##P<0.01) and between the Vehicle and NS-018 groups (**P<0.01) were assessed by the Welch test. (b–d) Spleen sections stained with hematoxylin and eosin (original magnification ×40). (e–g) Bone-marrow tissue sections prepared from femur and stained for reticulin (original magnification ×200).

5-3-2 Preferential inhibition by NS-018 of the growth of cells harboring JAK2V617F

Inhibition of JAK2WT can decrease the RBC or PLT counts. To compare the inhibitory

effect of NS-018 on JAK2WT and JAK2V617F in cells, we assessed the antiproliferative activity of NS-018 against Ba/F3 cells expressing murine JAK2WT or murine JAK2V617F. NS-018 suppressed the growth of Ba/F3-JAK2V617F cells with an IC_{50} value of 470 nM, while it suppressed the growth of Ba/F3-JAK2WT cells stimulated with IL-3 with an IC_{50} value of 2000 nM (Table 5-1). Thus, NS-018 showed 4.3-fold selectivity for Ba/F3-JAK2V617F cells over Ba/F3-JAK2WT cells (V617F/WT ratio). Other JAK2 inhibitors also showed selectivity for Ba/F3-JAK2V617F over Ba/F3-JAK2WT cells (Table 5-1), though the selectivity was lower. For example, INCB018424 (ruxolitinib) and TG101348 showed V617F/WT ratios of 2.0 and 1.5, respectively. Thus, among the eight JAK2 inhibitors tested, NS-018 showed the highest selectivity for JAK2V617F cells.

Table 5-1. Antiproliferative activities of NS-018 and other JAK inhibitors in Ba/F3 cells.

Compound	Target kinase	Proliferation IC_{50} (nM)		Selectivity	Interaction with Gly993	
		Ba/F3-JAK2 WT (+IL-3)	Ba/F3-JAK2 V617F	V617F/WT	CH···O	Water-mediated
NS-018	JAK2, Src	2000	470	4.3	Yes	Yes
AZD1480	JAK1/2	2300	1000	2.3	Yes	No
CP-690,550 (tofacitinib)	JAK1/2/3	2200	760	2.9	No	No
INCB018424 (ruxolitinib)	JAK1/2	630	310	2.0		
CYT387 (momelotinib)	JAK1/2	4300	2400	1.8		
TG101209	JAK2	850	550	1.5		
TG101348 (fedratinib)	JAK2	1000	650	1.5		
AT9283	JAK2/3, Aurora	48	48	1.0	No	No

To further evaluate the functional selectivity of NS-018 for JAK2V617F cells, we performed erythroid colony formation assays with bone-marrow cells from JAK2V617F transgenic mice and WT control mice. NS-018 inhibited the formation of erythroid colony-forming units from WT control and JAK2V617F transgenic mice in a dose-dependent manner, but the degree of inhibition was significantly greater in the JAK2V617F transgenic mice (Figure 5-4). Specifically, in JAK2V617F transgenic mice, NS-018 inhibited erythroid colony growth with a mean IC_{50} value of 360 nM, whereas in WT control mice the corresponding IC_{50} value was > 600 nM. These results show that NS-018 preferentially suppressed the growth of cells harboring JAK2V617F.

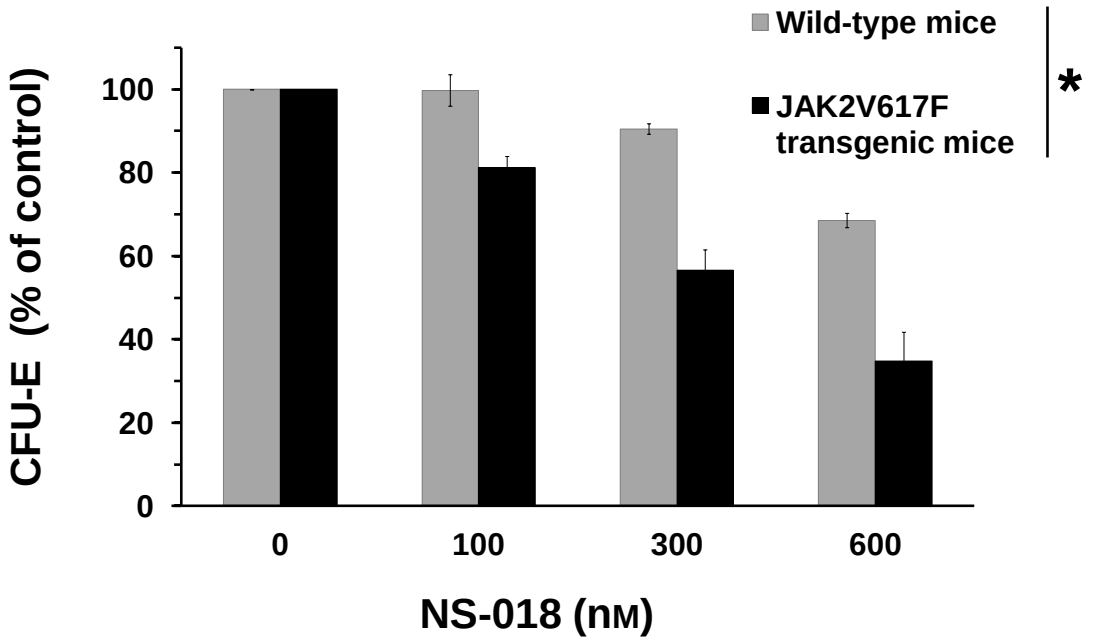

Figure 5-4. Effect of NS-018 on erythroid colony formation in JAK2V617F transgenic mice.

Bone-marrow cells harvested from JAK2V617F transgenic or WT mice were treated with increasing concentrations of NS-018 in a methylcellulose-based medium containing erythropoietin. Erythroid colony-forming units (CFU-E) were counted after incubation for two days. Bars represent the mean ± s.e.m. (n = 4). Statistical significance was assessed by a two-way factorial analysis of variance (*P<0.001).

5-3-3 Unique mode of binding of NS-018 to (flipped) Gly993 of activated JAK2

The JAK2 activation loop, which has a DFG (Asp–Phe–Gly) motif at the start, regulates kinase activity by changing its position. The position of Gly993, located immediately N-terminal to the DFG motif, thus depends on the activation state of the kinase [85]. The X-ray co-crystal structure of JAK2 in complex with NS-018 (Figure 5-5) revealed that NS-018 formed hydrogen bonds with the backbone amino and carbonyl groups of Leu932 in the hinge region. In addition, NS-018 interacted with the carbonyl group of Gly993 through two kinds of hydrogen-bonding interactions. Firstly, there is a hydrogen bond between a nitrogen atom of NS-018 and the water molecule depicted by the red sphere in Figure 5-5. This hydrogen-bonded water molecule forms a second

hydrogen bond with the carbonyl group of Gly993. Thus, there are water-mediated hydrogen-bonding interactions between NS-018 and Gly993. Secondly, there is a CH•••O hydrogen bond between an aromatic CH on the fluorobenzene moiety of NS-018 and the carbonyl group of Gly993 (Figure 5-6a). This type of hydrogen-bonding interaction often plays a role in the binding of kinase inhibitors to their target kinases [109]. Taken together, NS-018 binds in an induced-fit manner to the activated JAK2 through two kinds of hydrogen-bonding interactions with Gly993.

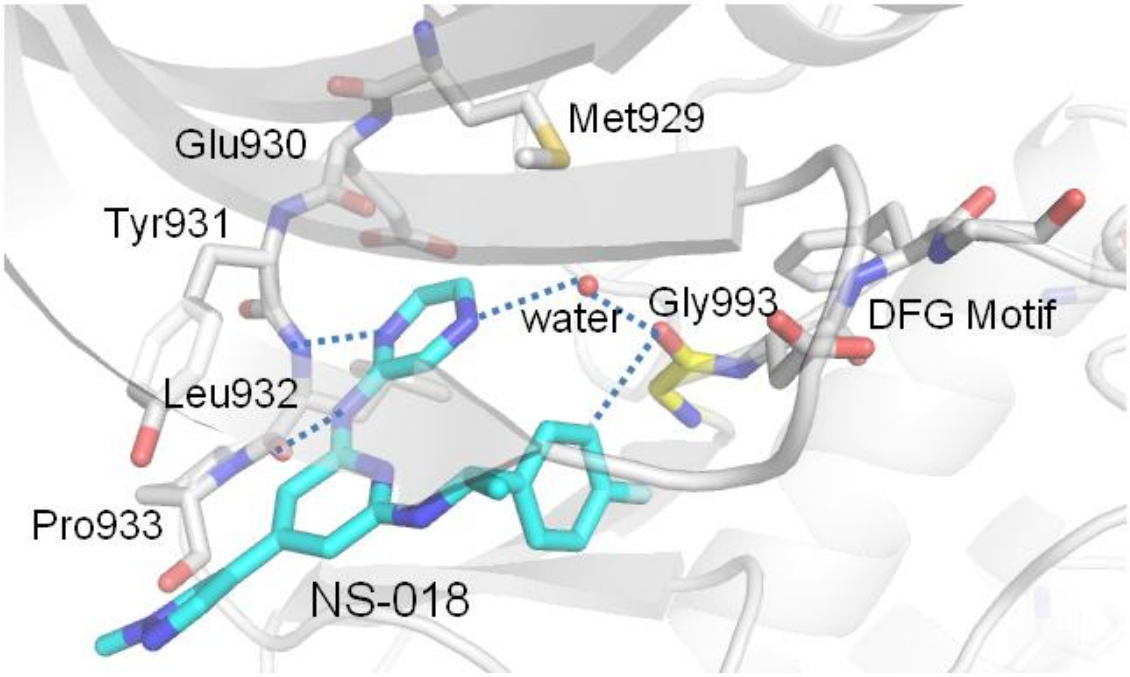

Figure 5-5. Ribbon-and-stick representation of the X-ray co-crystal structure of NS-018 (blue) bound to JAK2 (grey).
Dashed lines represent hydrogen bonds.

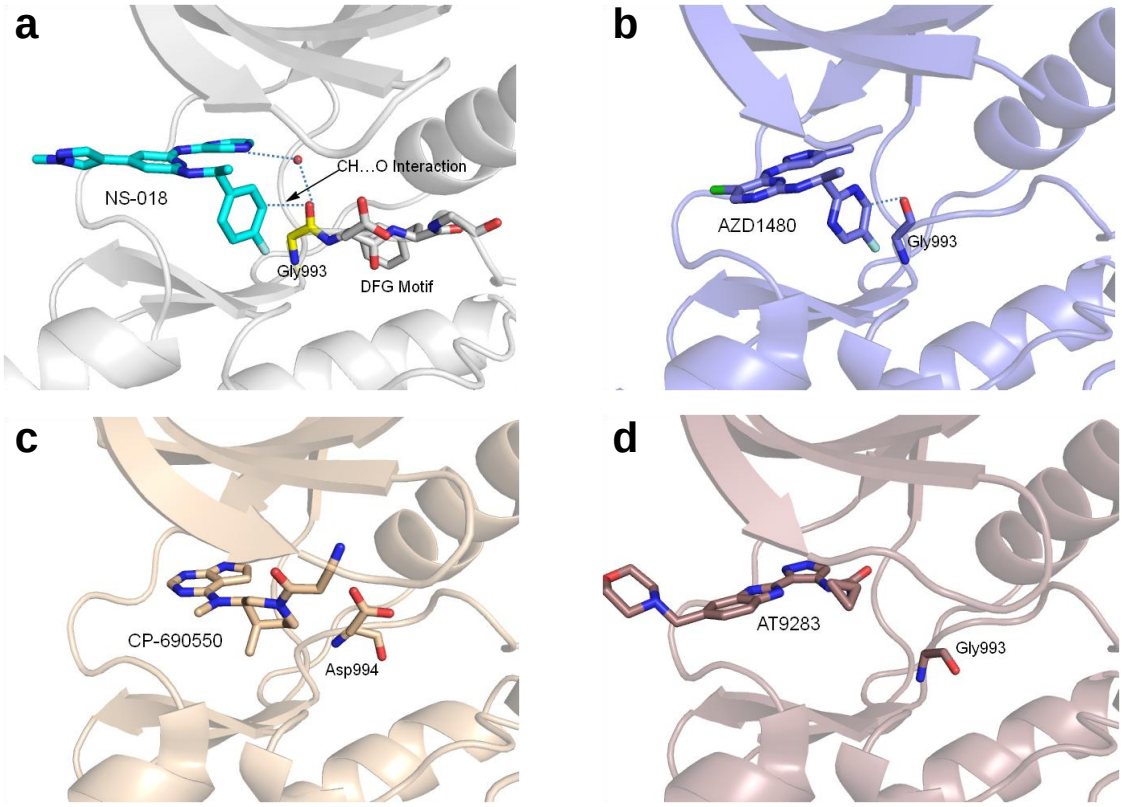

Figure 5-6. X-ray structures of (a) NS-018, (b) AZD1480, (c) CP-690550, and (d) AT9283 in complex with JAK2 kinase.
Protein Data bank IDs for AZD1480, CP-690550, and AT9283 are 2XA4, 3FUP, and 2W1I, respectively.

5-4 Discussion

In our search for a JAK2 inhibitor with reduced hematologic adverse effects, we evaluated the potential of our novel JAK2 inhibitor NS-018 in preclinical models. We first assessed the selective inhibition of the mutant kinase JAK2V617F by NS-018 in Ba/F3 cells. NS-018 showed higher selectivity for JAK2V617F over JAK2WT (a higher V617F/WT ratio) than existing JAK2 inhibitors such as ruxolitinib and TG101348 (Table 5-1). The preferential inhibition of the growth of Ba/F3-JAK2V617F cells by JAK2 inhibitors was unrelated to their target specificity among Jak-family kinases (e.g., selectivity for JAK1/2 or JAK2).

NS-018 shows potent inhibition of Src-family kinases in addition to JAK2 [108], and it could be argued that this contributed to its activity against Ba/F3-JAK2V617F cells.

However, Src-family kinases expressed in Ba/F3-JAK2V617F cells were not phosphorylated (Figure 5-7) and therefore not activated. Furthermore, the Src-family kinase inhibitor dasatinib did not show potent antiproliferative activity against Ba/F3-JAK2V617F cells (IC_{50} = 5000 nM; data not shown). For these reasons, it is unlikely that the Src-inhibitory activity of NS-018 contributed to its antiproliferative activity against Ba/F3-JAK2V617F cells.

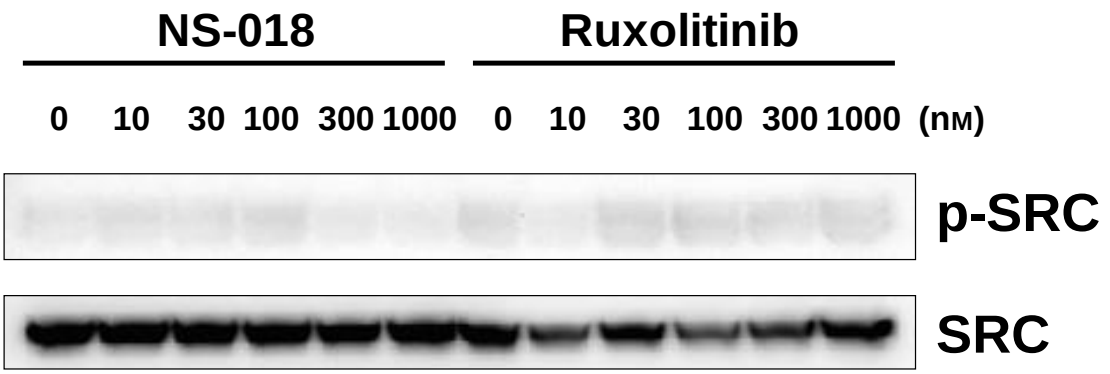

Figure 5-7. Phosphorylation status of Src in Ba/F3-JAK2V617F cells.
Ba/F3-JAK2V617F cells were treated with increasing concentrations of NS-018 or ruxolitinib for 3 h. Total cell lysate was subjected to SDS-PAGE, transferred to a PVDF membrane and probed with antibody specific for phospho-Src family (Tyr416) or Src (Cell Signaling Technology).

The efficacy of several JAK2 inhibitors has been evaluated in JAK2V617F BMT model mice [110,111], but there are phenotypic differences in disease severity among mouse strains [68]. Thus, BMT in BALB/c mice results in more markedly elevated leukocyte counts, a greater degree of splenomegaly and reticulin fibrosis, and higher mortality, than in C57Bl/6 mice. To assess the effect of NS-018 on bone marrow fibrosis, we used the more severely affected strain, BALB/c, to establish a BMT model. Although our model mice showed elevated WBC counts, splenomegaly, high mortality, and bone marrow fibrosis, as previously reported [68], elevated peripheral RBC and PLT counts were not observed (Figure 5-1). Rather, the mice showed thrombopenia 50 days after transplantation (Figure 5-2e). Although the reason for the differences in pathologic phenotype from the previous report is unclear, possible reasons are the difference in the promoters of the retroviral vectors used and the difference in the progenitor cell types infected with retrovirus.

While NS-018 treatment markedly reduced leukocytosis in JAK2V617F BMT model mice (Figure 5-2b), it did not decrease the RBC or PLT counts (Figure 5-2d,e). Because our BMT model had some unusual features, including the absence of polycythemia and thrombocythemia as described above, this apparent lack of effect of NS-018 on the RBC and PLT counts should be interpreted carefully. However, it is consistent with our previous finding that NS-018 prevents the progression of anemia and the decrease in PLT count in JAK2V617F transgenic mice [108]. When we evaluated the another JAK2 inhibitor, R723, in the same model, prevention of progressive anemia was not observed [110]. Because JAK2 signaling plays important roles in erythropoiesis and thrombopoiesis [99-101], JAK2 inhibition is thought to have on-target adverse effects such as a decrease in the RBC and PLT counts. In fact, some JAK2 inhibitors do reduce the RBC or PLT count in mice [110-113]. More importantly, the dose-limiting toxicity of ruxolitinib in MPN patients is thrombocytopenia [80,114]. Thus, a JAK2 inhibitor that produces a smaller reduction in the RBC and PLT counts in the therapeutic window would have clinical benefit. As described here, NS-018 preferentially inhibited the growth of Ba/F3-JAK2V617F cells (Table 5-1) and suppressed erythroid colony formation from bone marrow cells from JAK2V617F transgenic mice (Figure 5-4). Furthermore, NS-018 inhibits erythroid colony formation by peripheral blood mononuclear cells from JAK2V617F^{+} polycythemia vera patients at concentrations significantly lower than those required for healthy controls [108]. These results suggest that NS-018 inhibits the constitutively active JAK2V617F more potently than wild-type JAK2, which is involved in normal erythropoiesis and thrombopoiesis. This preferential inhibition of JAK2V617F by NS-018 could explain the fact that NS-018 does not reduce the RBC or PLT count at therapeutic doses in mouse models. The concentration range over which NS-018 inhibits JAK2V617-dependent cells but not wild-type cells in the model mice might be wider than for other JAK2 inhibitors.

In the present study, NS-018 treatment improved bone marrow fibrosis in JAK2V617F BMT mice (Figure 5-3e–g). This contrasts with our previous study of JAK2V617F transgenic mice in which NS-018 treatment had little effect on the progression of bone marrow fibrosis [108]. However, the fibrosis in the transgenic mice was more severe than in the BMT mice used in the present study. In addition, in the transgenic mice NS-018 was administered on weekdays only, whereas in the BMT mice it was administered every day. The lack of dosing of the transgenic mice over the weekend might have reduced the effect of NS-018 on the fibrosis. Some JAK2 inhibitors, including TG101348 and CYT387, improve bone marrow fibrosis in JAK2V617F BMT mice [110,111], but unfortunately they also produce a decrease in the hematocrit in the

therapeutic dose range in mice. Thus, an important and distinctive feature of NS-018 is its apparent lack of a suppressive effect on the RBC and PLT counts in the therapeutic window in mouse models.

To investigate the structural factors determining the preference of NS-018 for JAK2V617F, we explored the X-ray co-crystal structures of the inhibitors listed in Table 5-1. As shown in Figure 5-5 and Figure 5-6a, NS-018 interacts with the carbonyl group of Gly993, which is located immediately N-terminal to the DFG motif, through two kinds of hydrogen-bonding interactions that are only operative in activated JAK2. These interactions could explain the high V617F/WT ratio of NS-018. While similar CH•••O hydrogen-bonding interactions with Gly993 are found for AZD1480 (Figure 5-6b), the water-mediated interaction is absent. This could account for the lower V617F/WT ratio of AZD1480 compared with NS-018. CP-690,550 interacts with JAK2 in a unique way (Figure 5-6c); specifically, 1) Gly993 does not interact directly with CP-690,550, and Asp994 is located close to CP-690,550, and 2) a unique interaction is found between the terminal CN group of CP-690,550 and the glycine-rich loop (P-loop) [115]. Although the reason for CP-690,550's relatively high V617F/WT ratio is unclear, a different mechanism could contribute to the recognition of the active state of JAK2 by CP-690,550. INCB018424 and CYT387 also have the terminal CN group, so a similar recognition mechanism might be operative for these compounds. A docking model of the interaction of TG101209 with JAK2 has been published [94], but the X-ray structure is still unavailable. It was thus impossible to perform detailed analyses for TG101209 and the structurally similar TG101348. The X-ray structure shows that AT9283 does not interact with Gly993 (Figure 5-6d), and accordingly AT9283 showed no preference for V617F. A recent study of the JAK2 inhibitor LY2784544, which has a high preference for JAK2V617F, also emphasizes the interaction with Gly993 [116]. All these facts point to the importance of considering interactions with Gly993 when the aim is to design inhibitors with higher V617F/WT ratios.

In summary, NS-018 preferentially inhibited the growth of JAK2V617F-harboring cells over JAK2WT-harboring cells. NS-018 was also effective against leukocytosis, splenomegaly, and bone marrow fibrosis, and prolonged survival in JAK2V617F BMT mice with no reduction in the RBC or PLT counts. These characteristic features of NS-018 may be explained at least in part by its unique mode of binding to the activated form of JAK2. This may contribute to a therapeutic benefit for MPN patients by allowing the simultaneous satisfaction of the two requirements of efficacy and reduced hematologic adverse effects. The efficacy and safety of NS-018 for the treatment of MPN is expected to be verified by ongoing clinical trials.

Chapter 6

Evaluation of NS-018 in high-risk myelodysplastic syndrome patient samples

6-1 Introduction

Myelodysplastic syndrome (MDS) is a malignant hematologic disease characterized by variable cytopenia due to ineffective hematopoiesis with dysplastic hematopoietic cells and an increased risk of evolution to acute myelogenous leukemia (AML), and it is highly heterogeneous in that it displays a variety of complex cytogenetic and molecular abnormalities [117–120]. Despite recent advances in the understanding of its molecular features, the treatment outcome of MDS remains unfavorable. In particular, as reflected by the International Prognosis Scoring System (IPSS), revised IPSS (IPSS-R) and WHO Prognosis Scoring System (WPSS), the outlook for MDS patients having poor prognostic cytogenetic abnormalities and advanced disease stage with an increased percentage of abnormal myeloblasts in the bone marrow (BM) and/or peripheral blood is extremely unfavorable [121–124]. Although allogeneic hematopoietic stem cell transplantation (allo-SCT) is a curative treatment approach [125], it can be applied only to younger MDS patients, and its success is limited by the high rate of relapse in patients with high-risk cytogenetics [126]. Conventional combination chemotherapies, including cytarabine and/or anthracyclines, potently induce remission in a proportion of MDS patients by suppressing MDS clones; however, the treatment outcome is frequently hampered by high rates of relapse, delayed recovery of normal hematopoiesis, and related complications such as infection [127,128]. Pharmacologic intervention with novel epigenetic modifiers such as azacitidine (5-Aza) has induced more durable remission in MDS patients compared with conventional cytotoxic therapies or best supportive care; however, 5-Aza induced hematologic complete remission in only 20–30% of patients and rarely cured MDS [129]. Therefore, the development of additional therapeutics which can effectively suppress MDS clones with

less toxicity against normal hematopoiesis is urgently needed for the treatment of MDS, especially in high-risk patients.

Normal hematopoiesis requires the fine tuning of cell signaling networks which regulate hematopoietic stem cell maintenance, survival and differentiation. For instance, activation of the Janus kinase/Signal transducers and activators of transcription (JAK/STAT) pathway promotes hematopoiesis in response to the binding of cytokines such as stem cell factor, granulocyte-colony stimulating factor, erythropoietin, interleukin-3 or thrombopoietin to their respective receptors, while it also induces negative feedback regulators such as SOCS (suppressor of cytokine signaling) or CIS (cytokine-induced STAT inhibitor) family proteins, which silence positive signals to prevent excessive hematopoiesis [130]. The disharmony of the positive and negative signaling is involved in the pathophysiology of hematologic malignancies. In chronic myelogenous leukemia with aberrant constitutively active Abl tyrosine kinase, abnormally upregulated downstream cell-proliferation signals, including those mediated by the JAK/STAT, RAS/MAPK and AKT pathways, override the inhibitory signals despite the over-expression of SOCS-family members [131,132]. Somatic mutations in the JAK2 gene which cause constitutive activation of STATs are involved in the pathogenesis of myeloproliferative neoplasms (MPNs) and refractory anemia with ringed sideroblasts with thrombocytosis, a subtype of MDS/MPN [66,133]. Insufficient inactivation of the JAK/STAT pathway due to the repression of SOCS-1 or SHP-1 through gene hypermethylation is involved in the progression of high-risk MDS and AML [134,135]. These findings prompted us to investigate whether JAK2 inhibition can selectively inhibit the proliferation of MDS clones, especially those with a high potency for clonogenic proliferation. To test this hypothesis, we investigated the effect of a novel highly selective JAK2 inhibitor, NS-018, which is under early phase clinical trial for MPN, on the colony-forming ability and STAT3 phosphorylation status of hematopoietic progenitor cells from high-risk *de novo* MDS patients.

6-2 Materials and Methods

6-2-1 Cells, reagents and colony formation assay

This study was approved by the institutional review boards of Kyoto Prefectural University of Medicine and Kyoto Second Red Cross Hospital. BM mononuclear cells (BMMNCs) from twelve MDS patients and three healthy volunteers were collected with

informed consent in accordance with the Declaration of Helsinki. To investigate the effect of NS-018 on BMMNCs of highly aggressive MDS, we selected MDS patients evaluated as high or very high risk at least by IPSS-R or WPSS at their diagnosis at our institute during the past three years, and 12 samples were available for this study. MDS subtypes of 12 patients included 2 refractory cytopenia with multilineage dysplasia (RCMD), 4 refractory anemia with excess blasts (RAEB)-1, 5 RAEB-2 and 1 MDS-unclassifiable according to the WHO classification [136]. All MDS patients had complex and/or unfavorable cytogenetic abnormalities, and their prognostic risks were defined to be intermediate (n = 1), high (n = 2) or very high(n = 9) in the IPSS-R (Table 6-1) [121–124].

NS-018, is an ATP-competitive small-molecule inhibitor of JAK2. The crystal structure of NS-018 bound to the JAK2 kinase domain and the *in vitro* selective inhibitory activity of NS-018 against JAK2 kinase has been described elsewhere [108,137]. BMMNCs from healthy volunteers and MDS patients were isolated by conventional Ficoll-Paque density gradient centrifugation, and the isolated BMMNCs were incubated in MethoCult GF H4434 methylcellulose medium containing various hematopoietic cytokines (STEMCELL Technologies, Vancouver, Canada) at 1.0 x 10^5 cells/ml with or without NS-018 at 37°C in a humidified atmosphere of 5% CO2. Commercially available purified normal human CD34-positive (CD34+) BM cells (Lonza, Walkersville, MD) were used as a control. Burst-forming unit-erythroid (BFU-E) and colony-forming unit-granulocyte/macrophage (CFU-GM) colonies were counted under an inverted microscope on day 14 of culture.

Table 6-1. Clinical and cytogenetic/epigenetic features of MDS patients.

	Age /Gender	WHO MDS subtype	NCC ($x10^9$/L)	BM Blast (%)	PB Blast (%)	chromosome	IPSS IPSS-R WPSS	Methylation		JAK2 mutation	Treatment	Prognosis
								SOCS-1	*SHIP1*			
1	57/M	RAEB-1	77.0	4.8	2	46, XY, del(7)(q11.2) [6] / 46, sl, del(12)(p?), +14, der(14;18)(q10;q10) [8] / 46, sl, del(7), +der(7)del(7)(p?)del(7) [6]	Int-1 VH VH	+	++	-	Metenolone HC	32M
2	84/F	RAEB-2	25.0	14	3	47, XX, +8 [15] / 48, idem, +8 [1] / 46, XX [4]	H VH VH	++	++	-	BSC	3M+
3	54/M	RCMD	821.0	4.4	0	46, XY, i(17)(q10) [19] / 46, idem, del(2)(q?) [1]	Int-1 H Int	-	++	-	5-Aza R-BMT	10M+
4	61/F	RAEB-1	46.0	5.4	0	45, XX, del(5)(q?), -9, add(21)(p11.2), add(22)(q11.2) [6] / 46, idem, +mar1 [10] / 46,XX [3]	Int-2 VH VH	++	+	-	CTx UR-BMT	17M+
5	70/M	RAEB-1	189.0	3.2	2	44, XY, dic(5;12)(q11.2;p11.2), -7, add(7)(q11.2), -22, +mar1 [5] / 44, idem, add(3)(p11) [2] / 43, idem, add(3)(p11), -mar1 [6] / 46, XY [7]	Int-2 VH VH	-	+	-	5-Aza	10M
6	80/M	RCMD	184.0	3.8	0	46, XY, add(5)(q11.2) [1] / 45, sl, del(1)(p?), -7, -10, add(11)(q23), -13, -15, add(19)(p13), +rl, +mar1, +mar2 [6] / 45, sl, -18, -20, +r2 [2] / 46, XY [1]	H VH H	N.A.	N.A.	N.A.	BSC	7M+
7	67/M	RAEB-2	203.0	10.2	3	45, XX, add(4)(q21), der(5;19)(p10;q10), del(7)(q?), -9, +19, add(21)(q22) [1]/ 45, idem, -add(4), +rl [3]/ 46, XX, der(5;19), der(7;12)(p10;q10), +8, +19 [1]	H VH VH			N.A.	5-Aza	9M
8	63/F	RAEB-2	96.0	14.4	9	46, XX, add(6)(p21) [3]/ 46, XX, del(7)(q?) [3]/ 46, XX, del(12)(p11.2) [1]/ 46, XX, t(21;22)(q22;q11.2) [1]/ 46, XX [8]	Int-2 VH VH			N.A.	CTx UR-BMT 5-Aza+Len	10M+
9	86/M	RAEB-2	154.0	10.1	1	46, XY, t(3;3)(q21;q26.2) [20]	Int-2 VH VH			N.A.	Metenolone	20M+
10	72/M	RAEB-2	165.0	11.6	8	47, XY, +8	Int-2 H H			N.A.	5-Aza +LBH-589	16M+
11	72/M	RAEB-1	25.0	6.4	3	46, XY, +1, der(1;7)(q10;p10) [6]/ 46, idem, inv(7)(q11.2q36) [5]/ 45, X, -Y [3]/ 46, XY [5]	H VH VH			N.A.	5-Aza	4M
12	68/M	MDS-U	51.0	3.4	0	46, XY, +1, der(1;7)(q10;p10) [18]/ 46, XY [2]	Int-2 Int H			N.A.	5-Aza	12M+

M, male; F, female; RAEB, refractory anemia with excess blasts; RCMD, refractory cytopenia with multilineage dysplasia; MDS-U, MDS-unclassifiable; NCC, nucleated cell count; BM, bone marrow; PB, peripheral blood; IPSS, International Prognostic Scoring System; IPSS-R, Revised IPSS; WPSS, WHO Prognostic Scoring System; Int, intermediate; H, high; VH, very high; HC, hydroxycarbonate; BSC, best supportive care; 5-Aza, 5-azacitidine; R-BMT, related bone marrow transplantation; UR-BMT, unrelated bone marrow transplantation; CTx, chemotherapy with cytotoxic agents; Len, lenalidomide; LBH-589, panobinostat. N.A., not available, N.E., not examined.

6-2-2 Western blotting

After the evaluation of colony numbers on day 14 of culture, colony-forming cells were collected, washed twice with phosphate buffered saline (PBS) (−) and resuspended in RPMI 1640 medium supplemented with 10% fetal bovine serum, 2 mM L-glutamate and penicillin/streptomycin. Cells were cultured for 3 h with or without 1 μM NS-018 and then lysed. Western blotting was performed as described elsewhere [138]. Briefly, protein samples were separated by SDS-PAGE and then electroblotted onto a Hybond-P PDVF membrane (Amersham Biosciences, Uppsala, Sweden). The membranes were blocked with 5% (w/v) non-fat dry milk in PBS containing 0.1% (v/v) Tween 20 (Sigma, St Louis, MO). Antibodies (Abs) against STAT3 (Cell Signaling Technology, Beverly, MA), α-tubulin (Sigma) and phosphorylated (phospho-) STAT3 (Cell Signaling Technology) were used. Abs were detected by using horseradish peroxidase-conjugated secondary Abs and the enhanced chemi-luminescence (ECL) or ECL Prime Western Blotting Detection System (Amersham Biosciences).

6-2-3 Detection of genetic abnormalities in BMMNCs from MDS patients

We investigated the methylation status of the SOCS-1 and SHP-1 genes and the JAK2 gene mutation JAK2V617F in MDS-BMMNCs analyzed in this study. For the qualitative detection of methylated cytosine bases in the SOCS-1 and SHP-1 genes, regardless of the methylation level, conventional bisulfite pretreatment and methylation-specific polymerase chain reaction (PCR) was performed as described by [134,135,139]. The JAK2V617F gene mutation was analyzed by using the ipsogen JAK2 MutaScreen Kit (Qiagen, Hilden, Germany) according to the manufacturer's instructions. Briefly, this kit enables the identification of the JAK2V617F gene mutation by a multiplex assay using two TaqMan probes, of which one is specific for the wild-type JAK2 gene and the other for the JAK2V617F gene mutation.

6-2-4 Statistical analysis

All data were analyzed with two-sided, unpaired t-tests, and a P value of 0.05 was considered significant. Values are expressed as the mean ± SD of independent colony-forming assays conducted in triplicate.

6-3 Results

6-3-1 Formation of CFU-GM and BFU-E colonies from MDS-derived BMMNCs

First, we examined the colony-forming ability of normal and MDS-derived BMMNCs (MDS-BMMNCs) in MethoCult medium. The ability of purified CD34+ cells to produce hematopoietic colonies was more than 10-fold that of unpurified normal BMM-NCs. Two of twelve MDS-BMMNCs failed to form hematopoietic colonies, and, even in the ten MDS-BMMNCs which did form hematopoietic colonies, there were significantly fewer colonies than when purified CD34+ cells were used ($P < 0.001$), and they were fewer than when unpurified normal BMMNCs were used ($P = 0.007$). Two of two samples of purified normal CD34+ cells and all three normal BMMNC samples produced hematopoietic colonies with almost equal frequencies for BFU-E and CFU-GM, while in MDS-BMMNC-derived colonies the majority of hematopoietic colonies were CFU-GM (Table 6-2).

Table 6-2. Colony formation by CD34+ bone-marrow mononuclear cells (BMMNCs), BMMNCs from healthy donors and MDS patients.

		BFU-E (colony count)	CFU-GM (colony count)	CFU-GM ratio (%)
$CD34^+$ BM	1	4400	5700	56.4
	2	6200	4900	44.1
	Mean ± SD	5300 ± 1273	5300 ± 566	50
Control	1	200	220	52.4
	2	433	468	51.9
	3	543	688	55.9
	Mean ± SD	433 ± 175	468 ± 234	52
MDS	1	4	27	87.1
	2	0	0	NA
	3	1	162	99.1
	4	3	9	78.3
	5	9	144	94.3
	6	0	0	NA
	7	11	279	96.2
	8	26	321	92.5
	9	4	179	97.8
	10	47	394	89.3
	11	18	29	61.7
	12	16	60	78.9
	Mean ± SD	11.6 ± 13.8	133.7 ± 136.8	87.5

Cells (1 x 10^5 cells/ml) were incubated in MethoCult and the numbers of burst-forming unit-erythroid (BFU-E) and colony-forming unit-granulocyte/macrophage (CFU-GM) colonies were counted after 14 days. N.A.: not applicable.

6-3-2 Methylation status of SOCS-1 and SHP-1 genes and JAK2 gene mutation status of MDS-derived MDS-BMMNCs

We examined the methylation status of the SOCS-1 and SHP-1 genes of MDS-BMMNCs. Genomic DNA samples from eleven of twelve patients were available (the exception was patient 6). Although the degree of methylation differed among the samples, the methylated SOCS-1 gene was detected in four of eleven MDS-BMMNC samples and the methylated SHP-1 gene was detected in seven of eleven MDS-BMMNC samples examined (Figure 6-1A and Table 6-1). No JAK2V617F gene mutation was identified in any of five samples examined (Figure 6-1B).

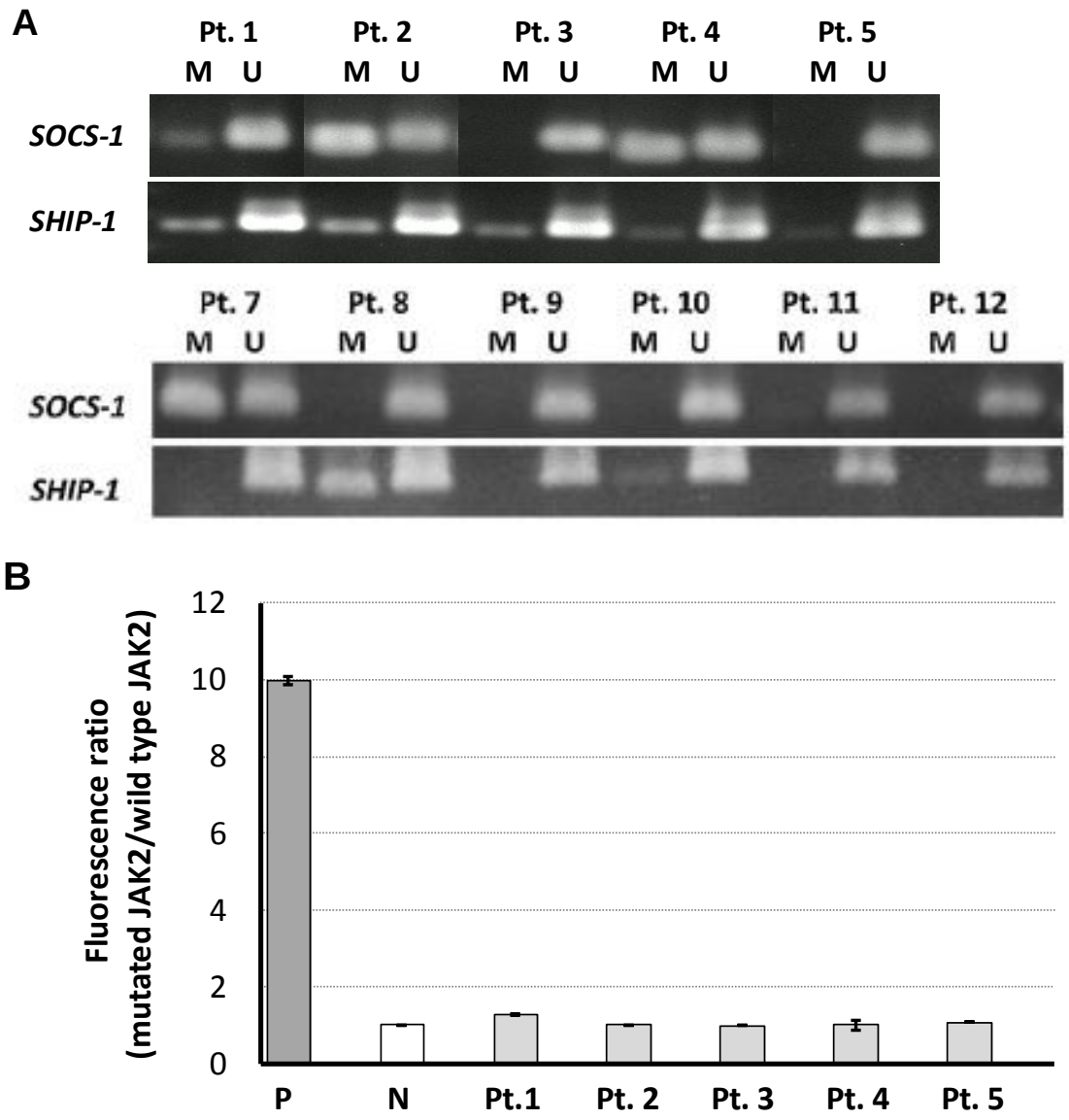

Figure 6-1. Genetic features of MDS patients.

(A) Methylation status of SOCS-1 andSHP-1 genes in bone-marrow mononuclear cells from MDS patients. M, methylated; U, unmethylated. Pt, patient. (B) JAK2V617F gene mutation status in bone-marrow mononuclear cells from MDS patients. Data of Pts. 1 to 5 are representative of eleven patients except for Pt. 6. The Y-axis represents the mean ± SD of the relative fluorescence ratio between mutated and wild type JAK2 genes in the positive control for the mutated JAK2 gene (P), the negative control with the wild type JAK2 gene supplied in the kit, and genes from Pts. 1 to 5.

6-3-3 NS-018 preferentially suppresses CFU-GM formation from MDS-derived BMMNCs

To investigate whether targeting JAK2 activity has therapeutic potential for MDS, we examined the effect of NS-018 on the colony-forming ability of unpurified BMMNCs from healthy controls and MDS-BMMNCs. NS-018 suppressed the CFU-GM colony formation of both normal BMMNCs and MDS-BMMNCS in a dose-dependent manner. Specifically, 0.5 μM NS-018 decreased the numbers of CFU-GM colonies from normal BMMNCs and MDS-BMMNCs to 87.2 ± 8.2% and 45.8 ± 8.8% ($P < 0.001$), respectively, and the corresponding figures for 1.0 μM NS-018 were 61.4 ± 18.6% and 25.1 ± 11.5% ($P = 0.0015$), respectively, compared to untreated MNCs (Figure 6-2A and 6-2B). This result demonstrates that NS-018 preferentially suppressed CFU-GM formation from MDS-BMMNCs over that of normal BMMNCs.

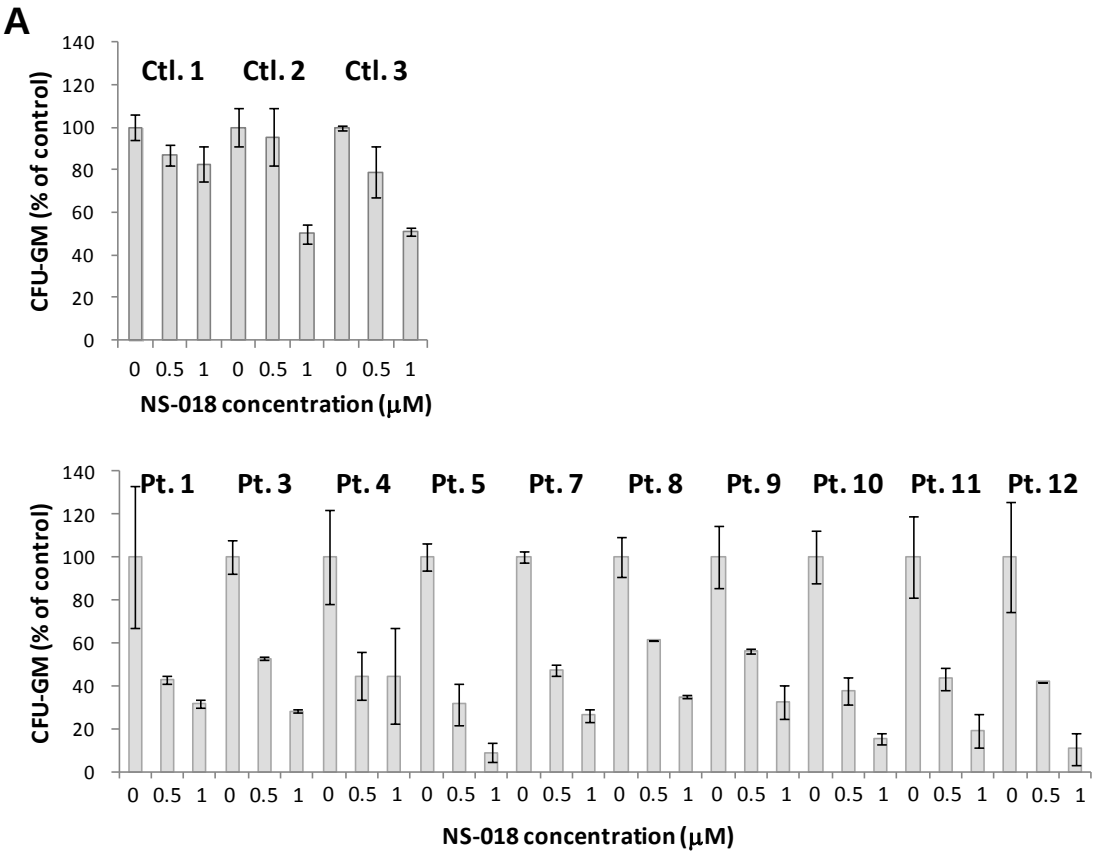

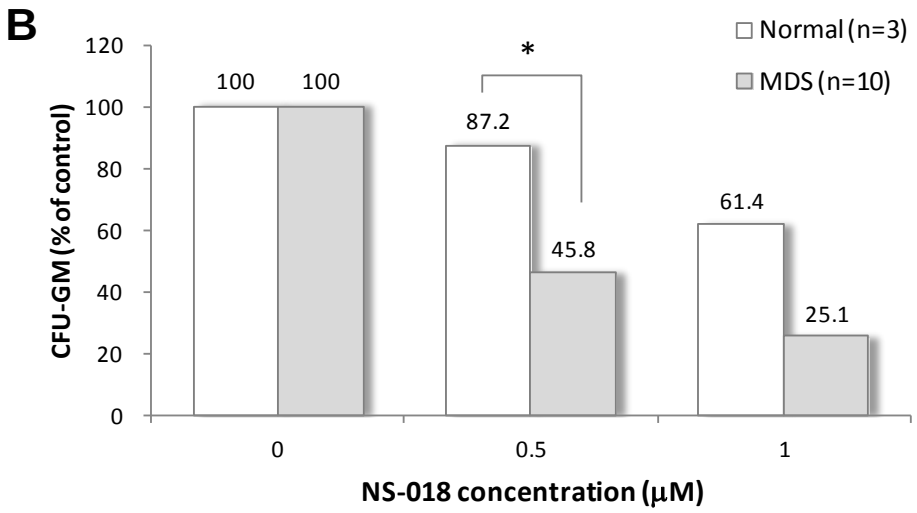

Figure 6-2. Effect of NS-018 on CFU-GM formation by bone-marrow mononuclear cells (BMMNCs) from healthy donors and MDS patients.
(A) Cells (1×10^5 cells/ml) were incubated in MethoCult with or without NS-018 at 0.5 or 1.0 μM and the numbers of colony-forming unit-granulocyte/macrophage (CFU-GM) colonies were counted after14 days. The left panel shows the results in normal BMMNCs (Control; Ctl.) (n = 3), and the right panel shows the results in MDS-BMMNCs (n = 10). No colony formation was observed in patients (Pts) 2 or 6. (B) Effect of NS-018 on CFU-GM formation between by normal BMMNCs from three healthy volunteers and MDS-derived BMMNCs from ten patients (Pts 1–12, except Pts 2 and 6). *P < 0.01.

6-3-4 Effect of NS-018 on STAT3 activity of colony-forming BMMNCs

To test whether NS-018 effectively inhibits JAK2 kinase activity in BMMNCs, we investigated the phosphorylation status ofSTAT3 before and after NS-018 treatment. STAT3 is one of the major target located downstream of JAK2, and it is activated through phosphorylation. Basal STAT3 expression levels were higher in CFU-GM forming cells from one MDS patient (Pt. 5) than in CFU-GM-forming cells from a normal control (Ctl. 3) (Figure 6-3). However, STAT3 was phosphorylated only in CFU-GM-forming cells from MDS patients and not in normal BMMNCs, and treatment with 1.0 μM NS-018 for 3 h almost completely suppressed the phosphorylation of STAT3 in CFU-GM-forming cells from MDS patients (Figure 6-3).

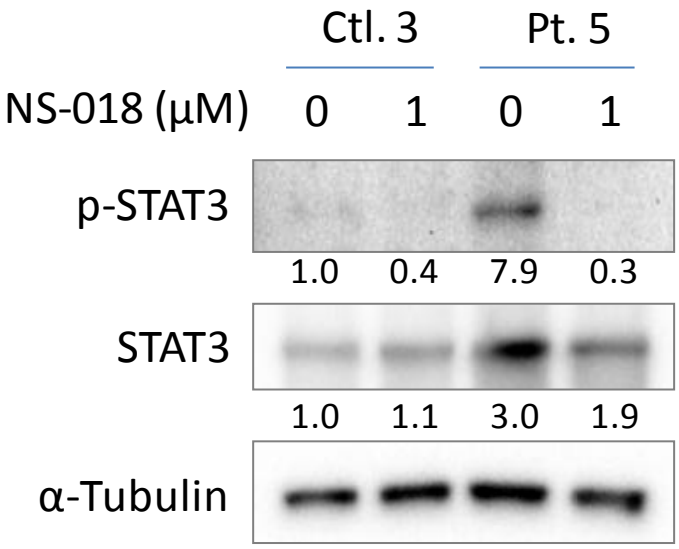

Figure 6-3. Effect of NS-018 on STAT3 activity.

Colony-forming cells from normal and MDS bone-marrow mononuclear cells were cultured with or without 1 μM NS-018 for 3 h, and the levels of total STAT3 and phosphorylated (p-) STAT3 were examined. α-Tubulin was also examined as the internal control. Image Lab software (Ver.4.1) (Bio-Rad Laboratories, Hercules, CA) was used for the quantification of protein expression levels. The expression levels of total STAT3 and p-STAT3 in untreated control cells were taken to be 1.0.

6-4 Discussion

MDS has two major clinical manifestations, cytopenias and leukemic evolution, and it remains a hard-to-treat disease, especially when allo-SCT is not applicable. Pharmacologic intervention with immunosuppressants, such as cyclosporine A, and anabolic steroids is occasionally efficacious for relatively long-term hematopoietic recovery in MDS patients with the major clinical presentation of cytopenias in the absence of blast expansion [140,141], whereas no promising treatment exists once the disease evolves into the aggressive phase with the excess of blasts that results from the acquisition of cell-proliferation potency. Even 5-Aza, the first-line pharmacologic intervention at the time of writing, has only a transient effect and rarely cures MDS [129]. Although recent genome-wide studies have demonstrated the involvement of various types of genetic and epigenetic abnormalities in cell differentiation, cell proliferation, cell

survival and RNA splicing during the development and progression of MDS [142,143], no single mutation or promising molecular target which is universally critical for MDS patients has been identified so far. Therefore, there is an urgent need for a therapeutic agent which can suppress the growth of highly proliferative MDS clones in a wide variety of patients.

Through the analysis of MDS-BMMNCs from high-risk MDS patients with unfavorable karyotypes, this study shows that MDS-BMMNCs from the majority (though not all) MDS patients produced hematopoietic colonies with a lower frequency than did normal BMMNCs. The lower colony-forming ability of MDS-BMMNCs from these patients may reflect the susceptibility of MDS clones to apoptosis, which may be associated with ineffective hematopoiesis. On the other hand, the ability of MDS-BMMNCs from the other patients to form colonies may reflect a more proliferative and highly aggressive phenotype of MDS clones, which may cause the excess of blasts clinically [144]. Our study demonstrates that the inhibition of the kinase activity of JAK2 preferentially suppresses the clonogenic growth of MDS-BMMNCs compared with normal BMMNCs, suggesting that JAK2 inhibition is specifically effective in preventing the overgrowth of leukemogenic clones in MDS, while it preserves more normal hematopoietic progenitor cells than MDS progenitors. A previous study has also shown the anti-cancer activity of erlotinib, an inhibitor of epidermal growth factor receptor, against leukemic and MDS cells through its off-target inhibitory effects on JAK2 and nucleophosmin [145]. NS-018 is highly selective for JAK2 [108], and this study is the first to present evidence for the effect of the specific inhibition of JAK2 by NS-018 on the clonogenic growth of MDS-BMMNCs from high-risk MDS patients. In BMMNCs from patient 5, STAT3 was activated even though these cells had no methylated SOCS-1, weakly methylated SHP-1 and no JAK2V617F gene mutation. This suggests that the hypermethylation of the SOCS-1 and SHP-1 genes and the presence of the JAK2V617F gene mutation, which all cause JAK2 activation, are not a prerequisite for the activation of JAK2/STAT signaling. Therefore, JAK2 could be universally targetable in MDS with a proliferative phenotype regardless of the types of genetic or epigenetic aberration, and NS-018 is a candidate agent for aggressive MDS with proliferative phenotype. Nevertheless, previous clinical trials have shown that myelosuppression was one of the most frequent adverse events with JAK2 inhibitors, such as CEP-701 or INCB018424, in MPNs [80,104,146]. Despite the encouraging results from our *in vitro* study, the extensive caution should be needed for myelosuppression in the use of JAK2 inhibitor for MDS patients with ineffective hematopoiesis.

In conclusion, our results provide the first evidence that a JAK2 inhibitor, NS-018,

potently suppresses the formation of MDS-BMMNCs with relatively low toxicity against normal BMMNCs. NS-018 could be a new therapeutic option for high-risk MDS.

Chapter 7

Conclusion

Although researchers and medical personnel have high expectations for molecularly targeted anticancer drugs, only a few such drugs have been successful. Although the concept of molecularly targeted anticancer drugs is precise and essentially correct, the techniques used to evaluate them are not precise enough. In other words, there are defects in the current strategy of drug discovery. The drug discovery process itself is still incomplete and has many challenges. Although high-throughput screening (HTS) using cells is a great technique, it is only the first step in selecting compounds. The phenotypes of the mutated cells are not identical to that of the disease in human patients. It is critical to use an evaluation system in which the healing process is identical to that in patients. At present, only an appropriate disease model in animals can realize such an evaluation system; it is not currently possible with cells. The current strategy of drug discovery has not taken full advantage of animal models.

To address this problem, I incorporated appropriate animal models into the drug discovery process (Figure 7-1). I constructed animal models that accurately reflect the patient pathology in two types of hematological malignancies, imatinib-resistant CML and MPN, that could not be reproduced in conventional models. The site of action of the drug in these models was the bone marrow, which was the location of the original cancer. There is a high expectation that drugs which can improve the pathology in these model animals can improve the clinical condition of patients. As a result of the improved screening of tyrosine kinase inhibitors using these animal models, it was possible to increase the probability of selecting promising compounds. The selected compounds, NS-187 and NS-018, are in clinical trial for the treatment of CML and MPN, respectively.

In contrast to the imatinib-resistant CML and MPN, a suitable animal model has not been constructed for MDS, although the effectiveness of NS-018 was demonstrated in patient cells. Neither NS-018 nor any other JAK2 inhibitors have reached clinical trial in MDS. This suggests that evaluation in an appropriate disease model animal is important for validation of compounds in the drug discovery process. Although the construction of

appropriate disease model animals rarely attracts attention, it is possible to increase the success rate of drug discovery by strengthening this part of the process.

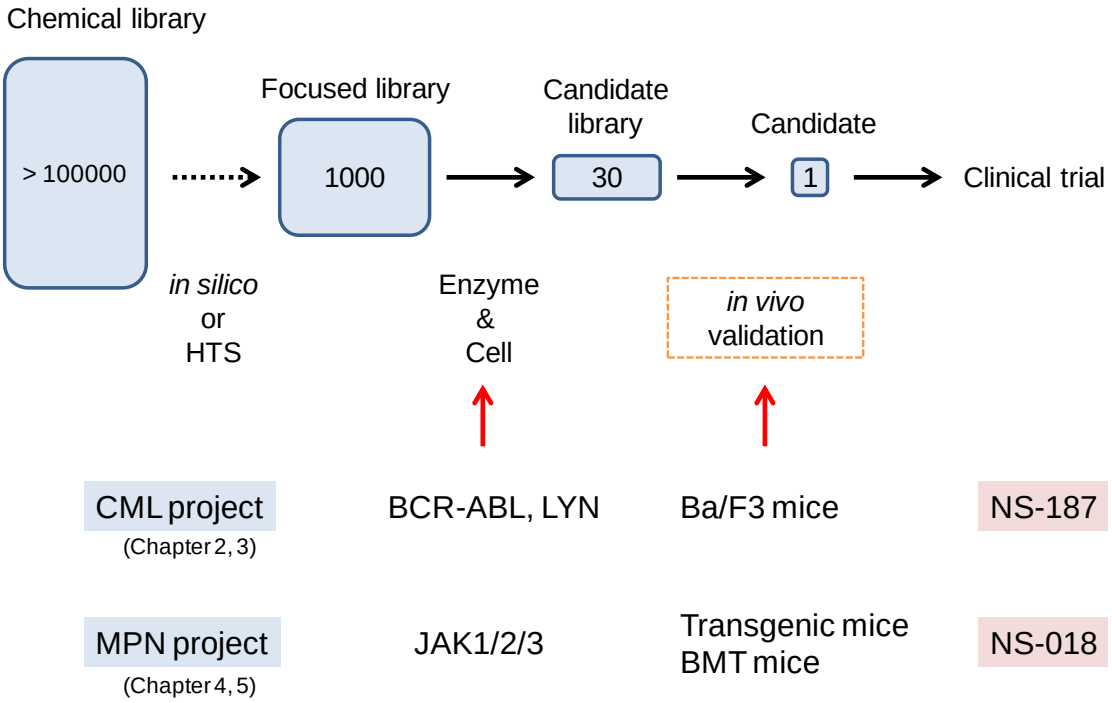

Figure 7-1. Drug discovery process for tyrosine kinase inhibitors in this thesis.

Ba/F3 transplant mice is a disease model of imatinib-resistant CML. Transgenic mice and bone marrow transplantation (BMT) mice are disease models of MPN. NS-187 and NS-018 are the compounds selected by screening in the projects.

It is still unclear whether tyrosine kinase inhibitors, including NS-187 and NS-018, can truly eradicate cancer. Long-term administration of tyrosine kinase inhibitors will stop relapse at least in certain types of cancer. However, tyrosine kinases are obviously not almighty as target molecules: their inhibition is not a sufficient therapy for all types of cancer. The oncogene addiction hypothesis, which provides a rationale for the current strategy, may apply to only specific cancers. Whether or not ideal target molecules really exist is a key question facing researchers. They may not be found in the current approaches. As mentioned in chapter 1, research on cancer has a long history and many concepts and theories have been proposed over the years. New concepts have been created in association with technological developments in fields such as autopsy, microscopy, chemistry, and genetics. I expect that new technologies and concepts will

lead to the development of new approaches and strategies to find ideal target molecules. I also believe that we can find ideal compounds as drug candidates if we use suitable techniques, including appropriate model animals.

To conclude, appropriate disease model animals for drug discovery of tyrosine kinase inhibitors have been successfully developed, and promising compounds for clinical trials have been selected. The probability of selecting promising drug candidates can be increased by evaluating compounds in appropriate animal models during the drug discovery process.

References

1. Sudhakar A. History of Cancer, Ancient and Modern Treatment Methods. J Cancer Sci Ther. 2009;1:1-4.
2. Weinstein IB, Joe A. Oncogene addiction. Cancer Res. 2008;68:3077-3080.
3. Center for Cancer Control and Information Services. CANCER STATISTICS IN JAPAN 2012.
4. Matsuda A, Matsuda T, Shibata A, Katanoda K, Sobue T, Nishimoto H, The Japan Cancer Surveillance Research Group. Cancer Incidence and Incidence Rates in Japan in 2008: A Study of 25 Population-based Cancer Registries for the Monitoring of Cancer Incidence in Japan (MCIJ) Project. Japanese Journal of Clinical Oncology. 2013;44:388-396.
5. Hahn WC, Weinberg RA. A subway map of cancer pathways. Nature Reviews Cancer. http://www.nature.com/nrc/poster/subpathways/index.html.
6. McCubrey JA, Steelman LS, Abrams SL, Bertrand FE, Ludwigb DE, Bäsecke J, Libra M, Stivala F, Milella M, Tafuri A, Lunghi P, Bonati A, Martelli AM. Targeting survival cascades induced by activation of Ras/Raf/MEK/ERK, PI3K/PTEN/Akt/mTOR and Jak/STAT pathways for effective leukemia therapy. Leukemia. 2008;22:708-722.
7. Chartier M, Chénard T, Barker J, Najmanovich R. Kinome Render: a stand-alone and web-accessible tool to annotate the human protein kinome tree. PeerJ. 2013;1:e126.
8. Hakoshima T. Recent progress in structural biology of AGC protein kinases. Tanpakushitsu Kakusan Koso. 2006;51:1557-1568.
9. Deininger MW, Druker BJ. Specific targeted therapy of chronic myelogenous leukemia with imatinib. Pharmacol Rev. 2003;55:401-423.
10. Levine RL, Pardanani A, Tefferi A, Gilliland DG. Role of JAK2 in the pathogenesis and therapy of myeloproliferative disorders. Nat Rev Cancer. 2007;7:673-683.
11. Tamaoki T, Nomoto H, Takahashi I, Kato Y, Morimoto M, Tomita F. Staurosporine, a potent inhibitor of phospholipid/Ca++dependent protein kinase. Biochem Biophys Res Commun. 1986;135:397-402.
12. Deininger MW, Goldman JM, Lydon N, Melo JV. The tyrosine kinase inhibitor CGP57148B selectively inhibits the growth of BCR-ABL-positive cells. Blood.

1997;90:3691-3698.
13. Johnson JI, Decker S, Zaharevitz D, Rubinstein LV, Venditti JM, Schepartz S, Kalyandrug S, Christian M, Arbuck S, Hollingshead M, Sausville EA. Relationships between drug activity in NCI preclinical in vitro and in vivo models and early clinical trials. Br J Cancer. 2001;84:1424-1431.
14. Teicher BA. Tumor models for efficacy determination. Mol Cancer Ther. 2006;5:2435-2443.
15. Frese KK, Tuveson DA. Maximizing mouse cancer models. Nat Rev Cancer. 2007;7:645-658.
16. Cortes JE, Talpaz M, Beran M, et al. Philadelphia chromosome-negative chronic myelogenous leukemia with rearrangement of the breakpoint cluster region: long-term follow-up results. Cancer. 1995;75:464-470.
17. Clark SS, McLaughlin J, Timmons M, et al. Expression of a distinctive BCR-ABL oncogene in Ph1-positive acute lymphocytic leukemia (ALL). Science. 1988;239:775-777.
18. O'Brien SG, Guilhot F, Larson RA, et al. Imatinib compared with interferon and low-dose cytarabine for newly diagnosed chronic-phase chronic myeloid leukemia. N Engl J Med. 2003:348:994-1004.
19. Goldman JM, Melo JV. Chronic myeloid leukemia: advances in biology and new approaches to treatment. N Engl J Med. 2003;349:1451-1464.
20. Druker BJ, Sawyers CL, Kantarjian H, et al. Activity of a specific inhibitor of the BCR-ABL tyrosine kinase in the blast crisis of chronic myeloid leukemia and acute lymphoblastic leukemia with the Philadelphia chromosome. N Engl J Med. 2001; 344:1038-1042.
21. Ottmann OG, Druker BJ, Sawyers CL, et al. A phase 2 study of imatinib in patients with relapsed or refractory Philadelphia chromosome-positive acute lymphoid leukemias. Blood. 2002;100:1965-1971.
22. Gorre ME, Mohammed M, Ellwood K, et al. Clinical resistance to STI-571 cancer therapy caused by BCR-ABL gene mutation or amplification. Science. 2001;293:876-880.
23. Hofmann WK, Jones LC, Lemp NA, et al. Ph(+) acute lymphoblastic leukemia resistant to the tyrosine kinase inhibitor STI571 has a unique BCRABL gene mutation. Blood. 2002;99:1860-1862.
24. Nardi V, Azam M, Daley GQ. Mechanisms and implications of imatinib resistance mutations in BCR-ABL. Curr Opin Hematol. 2004;11:35-43.
25. Deininger M, Buchdunger E, Druker BJ. The development of imatinib as a

therapeutic agent for chronic myeloid leukemia. Blood. 2005;105:2640-2653.
26. Cortes J, Giles F, O'Brien S, et al. Result of high dose imatinib mesylate in patients with Philadelphia chromosome-positive chronic myeloid leukemia after failure of interferon-alpha. Blood. 2003;102:83-86.
27. Kantarjian H, Talpaz M, O'Brien S, et al. High dose imatinib mesylate therapy in newly diagnosed Philadelphia chromosome-positive chronic phase chronic myeloid leukemia. Blood. 2004;103:2873-2878.
28. O'Brien S, Giles F, Talpaz M, et al. Results of triple therapy with interferon-alpha, cytarabine, and homoharringtonine, and the impact of adding imatinib to the treatment sequence in patients with Philadelphia chromosome-positive chronic myelogenous leukemia in early chronic phase. Cancer. 2003;98:888-893.
29. Wisniewski D, Lambek CL, Liu C, et al. Characterization of potent inhibitors of the Bcr-Abl and the c-kit receptor tyrosine kinases. Cancer Res. 2002;62:4244-4255.
30. Golas JM, Arndt K, Etienne C, et al. SKI-606, a 4-anilino-3-quinolinecarbonitrile dual inhibitor of Src and Abl kinases, is a potent antiproliferative agent against chronic myelogenous leukemia cells in culture and causes regression of K562 xenografts in nude mice. Cancer Res. 2003;63:375-381.
31. O'Hare T, Pollock R, Stoffregen EP, et al. Inhibition of wild-type and mutant Bcr-Abl by AP23464, a potent ATP-based oncogenic protein kinase inhibitor: implications for CML. Blood. 2004;104:2532-2539.
32. Shah NP, Tran C, Lee FY, Chen P, Norris D, Sawyers CL. Overriding imatinib resistance with a novel ABL kinase inhibitor. Science. 2004;305:399-401.
33. Lombardo LJ, Lee FY, Chen P, et al. Discovery of N-(2-chloro-6-methyl-phenyl)-2-(6-(4-(2-hydroxyethyl)-piperazin-1-yl)-2-methylpyri midin-4-ylamino)thiazole-5-carboxamide (BMS-354825), a dual Src/Abl kinase inhibitor with potent antitumor activity in preclinical assays. J Med Chem. 2004;47:6658-6661.
34. Donato NJ, Wu JY, Stapley J, et al. BCR-ABL independence and LYN kinase overexpression in chronic myelogenous leukemia cells selected for resistance to STI571. Blood. 2003;101:690-698.
35. Dai Y, Rahmani M, Corey SJ, Dent P, Grant S. A Bcr/Abl-independent, Lyn-dependent form of imatinib mesylate (STI-571) resistance is associated with altered expression of Bcl-2. J Biol Chem. 2004;279:34227-34239.
36. Ptasznik A, Nakata Y, Kalota A, Emerson SG, Gewirtz AM. Short interfering RNA (siRNA) targeting the Lyn kinase induces apoptosis in primary, and drug-resistant, BCR-ABL1(+) leukemia cells. Nat Med. 2004;10:1187-1189.

37. Tanaka S, Amling M, Neff L, et al. c-Cbl is downstream of c-Src in a signalling pathway necessary for bone resorption. Nature. 1996;383:528-531.
38. Touyz RM, Wu XH, He G, et al. Role of c-Src in the regulation of vascular contraction and Ca^{2+} signaling by angiotensin II in human vascular smooth muscle cells. J Hypertens. 2001;19:441-449.
39. Davis ME, Cai H, McCann L, Fukai T, Harrison DG. Role of c-Src in regulation of endothelial nitric oxide synthase expression during exercise training. Am J Physiol Heart Circ Physiol. 2003;284:1449-1453.
40. Cary LA, Klinghoffer RA, Sachsenmaier C, Cooper JA. SRC catalytic but not scaffolding function is needed for integrin-regulated tyrosine phosphorylation, cell migration, and cell spreading. Mol Cell Biol. 2002;22:2427-2440.
41. Luton F, Verges M, Vaerman JP, Sudol M, Mostov KE. The SRC family protein tyrosine kinase p62yes controls polymeric IgA transcytosis in vivo. Mol Cell. 1999;4:627-632.
42. Schindler T, Bornmann W, Pellicena P, Miller WT, Clarkson B, Kuriyan J. Structural mechanism for STI-571 inhibition of abelson tyrosine kinase. Science. 2000;289:1938-1942.
43. Nagar B, Bornmann WG, Pellicena P, et al. Crystal structures of the kinase domain of c-Abl in complex with the small molecule inhibitors PD173955 and imatinib (STI-571). Cancer Res. 2002;62:4236-4243.
44. Halgren TA. Merck Molecular Force Field, I: extension of MMFF94 using experimental data, additional computational data, and empirical rules. J Comput Chem. 1996;17:490-512.
45. Dan S, Naito M, Tsuruo T. Selective induction of apoptosis in Philadelphia chromosome-positive chronic myelogenous leukemia cells by an inhibitor of BCR-ABL tyrosine kinase, CGP 57148. Cell Death Differ. 1998;5:710-715.
46. Hochhaus A, La Rosee P. Imatinib therapy in chronic myelogenous leukemia: strategies to avoid and overcome resistance. Leukemia. 2004;18:1321-1331.
47. Plattner R, Kadlec L, DeMali KA, Kazlauskas A, Pendergast AM. c-Abl is activated by growth factors and Src family kinases and has a role in the cellular response to PDGF. Genes Dev. 1999;13:2400-2411.
48. Nagar B, Hantschel O, Young MA, et al. Structural basis for the autoinhibition of c-Abl tyrosine kinase. Cell. 2003;112:859-871.
49. Sonoyama J, Matsumura I, Ezoe S, et al. Functional cooperation among Ras, STAT5, and phosphatidylinositol 3-kinase is required for full oncogenic activities of BCR/ABL in K562 cells. J Biol Chem. 2002;277:8076-8082.

50. Daley GQ. Towards combination target-directed chemotherapy for chronic myeloid leukemia: role of farnesyl transferase inhibitors. Semin Hematol. 2003;40:11-14.
51. Kuroda J, Kimura S, Segawa H, et al. The thirdgeneration bisphosphonate Zoledronate synergistically augments the anti-Ph leukemia activity of imatinib mesylate. Blood. 2003;102:2229-2235.
52. Tsao AS, Kantarjian H, Cortes J, O'Brien S, Talpaz M. Imatinib mesylate causes hypopigmentation in the skin. Cancer. 2003;98:2483-2487.
53. Weisberg E, Manley PW, Breitenstein W, et al. Characterization of AMN107, a selective inhibitor of native and mutant Bcr-Abl. Cancer Cell. 2005;7:129-141.
54. O'Hare T, Walters DK, Stoffregen EP, et al. In vitro activity of Bcr-Abl inhibitors AMN107 and BMS-354825 against clinically relevant imatinibresistant Abl kinase domain mutants. Cancer Res. 2005;65:4500-4505.
55. Abraham MH, Platts JA. Hydrogen bond structural group constants. J Org Chem. 2001;66:3484-3491.
56. Gumireddy K, Baker SJ, Cosenza SC, et al. A non-ATP-competitive inhibitor of BCR-ABL overrides imatinib resistance. Proc Natl Acad Sci USA. 2005;102:1992-1997.
57. Kimura S, Naito H, Segawa H, Kuroda J, Yuasa T, Sato K, et al. NS-187, a potent and selective dual Bcr-Abl/Lyn tyrosine kinase inhibitor, is a novel agent for imatinib-resistant leukemia. Blood. 2005;106:3948–3954.
58. Asaki T, Sugiyama Y, Hamamoto T, Higashioka M, Umehara M, Naito H, et al. Design and synthesis of 3-substituted benzamide derivatives as Bcr-Abl kinase inhibitors. Bioorg Med Chem Lett. 2006;16:1421–1425.
59. Miething C, Mugler C, Grundler R, Hoepfl J, Bai RY, Peschel C, et al. Phosphorylation of tyrosine 393 in the kinase domain of Bcr-Abl influences the sensitivity towards imatinib in vivo. Leukemia. 2003;17:1695–1699.
60. Campbell PJ, Green AR. The myeloproliferative disorders. N Engl J Med. 2006;355:2452–2466.
61. Tefferi A, Thiele J, Orazi A, Kvasnicka HM, Barbui T, Hanson CA, et al. Proposals and rationale for revision of the World Health Organization diagnostic criteria for polycythemia vera, essential thrombocythemia, and primary myelofibrosis: recommendations from an ad hoc international expert panel. Blood. 2007;110:1092–1097.
62. Tefferi A. Essential thrombocythemia, polycythemia vera, and myelofibrosis: current management and the prospect of targeted therapy. Am J Hematol. 2008;83:491–497.

63. Baxter EJ, Scott LM, Campbell PJ, East C, Fourouclas N, Swanton S, et al. Acquired mutation of the tyrosine kinase JAK2 in human myeloproliferative disorders. Lancet. 2005;365:1054–1061.
64. James C, Ugo V, Le Couedic JP, Staerk J, Delhommeau F, Lacout C, et al. A unique clonal JAK2 mutation leading to constitutive signalling causes polycythaemia vera. Nature. 2005;434:1144–1148.
65. Kralovics R, Passamonti F, Buser AS, Teo SS, Tiedt R, Passweg JR, et al. A gain-of-function mutation of JAK2 in myeloproliferative disorders. N Engl J Med. 2005;352:1779–1790.
66. Levine RL, Wadleigh M, Cools J, Ebert BL, Wernig G, Huntly BJ, et al. Activating mutation in the tyrosine kinase JAK2 in polycythemia vera, essential thrombocythemia, and myeloid metaplasia with myelofibrosis. Cancer Cell. 2005;7:387–397.
67. Zhao R, Xing S, Li Z, Fu X, Li Q, Krantz SB, et al. Identification of an acquired JAK2 mutation in polycythemia vera. J Biol Chem. 2005;280:22788–22792.
68. Wernig G, Mercher T, Okabe R, Levine RL, Lee BH, Gilliland DG. Expression of Jak2V617F causes a polycythemia vera-like disease with associated myelofibrosis in a murine bone marrow transplant model. Blood. 2006;107:4274–4281.
69. Lacout C, Pisani DF, Tulliez M, Gachelin FM, Vainchenker W, Villeval JL. JAK2V617F expression in murine hematopoietic cells leads to MPD mimicking human PV with secondary myelofibrosis. Blood. 2006;108:1652–1660.
70. Bumm TG, Elsea C, Corbin AS, Loriaux M, Sherbenou D, Wood L, et al. Characterization of murine JAK2V617F-positive myeloproliferative disease. Cancer Res. 2006;66:11156–11165.
71. Zaleskas VM, Krause DS, Lazarides K, Patel N, Hu Y, Li S, et al. Molecular pathogenesis and therapy of polycythemia induced in mice by JAK2 V617F. PLoS One. 2006;1:e18.
72. Tiedt R, Hao-Shen H, Sobas MA, Looser R, Dirnhofer S, Schwaller J, et al. Ratio of mutant JAK2-V617F to wild-type Jak2 determines the MPD phenotypes in transgenic mice. Blood. 2008;111:3931–3940.
73. Xing S, Wanting TH, Zhao W, Ma J, Wang S, Xu X, et al. Transgenic expression of JAK2V617F causes myeloproliferative disorders in mice. Blood. 2008;111: 5109–5117.
74. Shide K, Shimoda HK, Kumano T, Karube K, Kameda T, Takenaka K, et al. Development of ET, primary myelofibrosis and PV in mice expressing JAK2 V617F. Leukemia. 2008;22:87–95.

75. Akada H, Yan D, Zou H, Fiering S, Hutchison RE, Mohi MG. Conditional expression of heterozygous or homozygous Jak2V617F from its endogenous promoter induces a polycythemia vera–like disease. Blood. 2010;115:3589–3596.
76. Marty C, Lacout C, Martin A, Hasan S, Jacquot S, Birling MC, et al. Myeloproliferative neoplasm induced by constitutive expression of JAK2V617F in knock-in mice. Blood. 2010;116:783–787.
77. Li J, Spensberger D, Ahn JS, Anand S, Beer PA, Ghevaert C, et al. JAK2 V617F impairs hematopoietic stem cell function in a conditional knock-in mouse model of JAK2 V617F–positive essential thrombocythemia. Blood. 2010;116:1528–1538.
78. Scott LM, Tong W, Levine RL, Scott MA, Beer PA, Stratton MR, et al. JAK2 exon 12 mutations in polycythemia vera and idiopathic erythrocytosis. N Engl J Med. 2007;356:459–468.
79. Pikman Y, Lee BH, Mercher T, McDowell E, Ebert BL, Gozo M, et al. MPLW515L is a novel somatic activating mutation in myelofibrosis with myeloid metaplasia. PLoS Med. 2006;3:e270.
80. Verstovsek S, Kantarjian H, Mesa RA, Pardanani AD, Cortes-Franco J, Thomas DA, et al. Safety and efficacy of INCB018424, a JAK1 and JAK2 inhibitor, in myelofibrosis. N Engl J Med. 2010;363:1117–1127.
81. Pardanani A, Gotlib JR, Jamieson C, Cortes JE, Talpaz M, Stone RM, et al. Safety and efficacy of TG101348, a selective JAK2 inhibitor, in myelofibrosis. J Clin Oncol. 2011;29:789–796.
82. Lucet IS, Fantino E, Styles M, Bamert R, Patel O, Broughton SE, et al. The structural basis of Janus kinase 2 inhibition by a potent and specific pan-Janus kinase inhibitor. Blood. 2006;107:176–183.
83. Otwinowski Z, Minor W. Processing of X-ray diffraction data collected in oscillation mode. Methods Enzymol. 1997;276:307–326.
84. McCoy AJ, Grosse-Kunstleve RW, Adams PD, Winn MD, Storoni LC, Read RJ. Phaser crystallographic software. J. Appl. Cryst. 2007;40,658–674.
85. Lindauer K, Loerting T, Liedl KR, Kroemer RT. Prediction of the structure of human Janus kinase 2 (JAK2) comprising the two carboxy-terminal domains reveals a mechanism for autoregulation. Protein Eng. 2001;14:27–37.
86. Tyner JW, Walters DK, Willis SG, Luttropp M, Oost J, Loriaux M, et al. RNAi screening of the tyrosine kinome identifies therapeutic targets in acute myeloid leukemia. Blood. 2008;111:2238–2245.
87. Huang D, Zhou T, Lafleur K, Nevado C, Caflisch A. Kinase selectivity potential for inhibitors targeting the ATP binding site: a network analysis. Bioinformatics.

2010;26:198–204.
88. Ingley E, Klinken SP. Cross-regulation of JAK and Src kinases. Growth Factors. 2006;24:89–95.
89. Garcia R, Bowman TL, Niu G, Yu H, Minton S, Muro-Cacho CA, et al. Constitutive activation of Stat3 by the Src and JAK tyrosine kinases participates in growth regulation of human breast carcinoma cells. Oncogene. 2001;20:2499–2513.
90. Tanaka H, Takeuchi M, Takeda Y, Sakai S, Abe D, Ohwada C, et al. Identification of a novel TEL–Lyn fusion gene in primary myelofibrosis. Leukemia. 2010;24:197–200.
91. Wappl M, Jaeger E, Streubel B, Gisslinger H, Schwarzinger I, Valent P, et al. Dasatinib inhibits progenitor cell proliferation from polycythaemia vera. Eur J Clin Invest. 2008;38:578–584.
92. Ugo V, Marzac C, Teyssandier I, Larbret F, Lécluse Y, Debili N, et al. Multiple signaling pathways are involved in erythropoietin-independent differentiation of erythroid progenitors in polycythemia vera. Exp Hematol. 2004;32:179–187.
93. Randi ML, Brunati AM, Scapin M, Frasson M, Deana R, Magrin E, et al. Src tyrosine kinase preactivation is associated with platelet hypersensitivity in essential thrombocythemia and polycythemia vera. Blood. 2010;115:667–676.
94. Pardanani A, Hood J, Lasho T, Levine RL, Martin MB, Noronha G, et al. TG101209, a small molecule JAK2-selective kinase inhibitor potently inhibits myeloproliferative disorder-associated JAK2V617F and MPLW515L/K mutations. Leukemia. 2007;21:1658–1668.
95. Liu PCC, Caulder E, Li J, Waeltz P, Margulis A, Wynn R, et al. Combined inhibition of Janus kinase 1/2 for the treatment of JAK2V617F-driven neoplasms: selective effects on mutant cells and improvements in measures of disease severity. Clin Cancer Res. 2009;15:6891–6900.
96. Quintás-Cardama A, Vaddi K, Liu P, Manshouri T, Li J, Scherle PA, et al. Preclinical characterization of the selective JAK1/2 inhibitor INCB018424: therapeutic implications for the treatment of myeloproliferative neoplasms. Blood. 2010;115:3109–3117.
97. Cervantes F, Arellano-Rodrigo E, Alvarez-Larrán A. Blood cell activation in myeloproliferative neoplasms. Haematologica, 2009;94:1484–1488.
98. Mishchenko E, Tefferi A. Treatment options for hydroxyurea-refractory disease complications in myeloproliferative neoplasms: JAK2 inhibitors, radiotherapy, splenectomy and transjugular intrahepatic portosystemic shunt. Eur J Haematol. 2010;85:192–199.

99. Parganas E, Wang D, Stravopodis D, Topham DJ, Marine JC, Teglund S, et al. Jak2 is essential for signaling through a variety of cytokine receptors. Cell. 1998;93:385–395.
100. Neubauer H, Cumano A, Müller M, Wu H, Huffstadt U, Pfeffer K. Jak2 deficiency defines an essential developmental checkpoint in definitive hematopoiesis. Cell. 1998;93:397–409.
101. Park SO, Wamsley HL, Bae K, Hu Z, Li X, Choe SW, et al. Conditional deletion of Jak2 reveals an essential role in hematopoiesis throughout mouse ontogeny: implications for Jak2 inhibition in humans. PLoS One. 2013;8:e59675.
102. Verstovsek S, Mesa RA, Gotlib J, Levy RS, Gupta V, DiPersio JF, et al. A double-blind, placebo-controlled trial of ruxolitinib for myelofibrosis. N Engl J Med. 2012;366:799–807.
103. Harrison C, Kiladjian JJ, Al-Ali HK, Gisslinger H, Waltzman R, Stalbovskaya V, et al. JAK inhibition with ruxolitinib versus best available therapy for myelofibrosis. N Engl J Med. 2012;366:787–798.
104. Santos FP, Kantarjian HM, Jain N, Manshouri T, Thomas DA, Garcia-Manero G, et al. Phase 2 study of CEP-701, an orally available JAK2 inhibitor, in patients with primary or postpolycythemia vera/essential thrombocythemia myelofibrosis. Blood. 2010;115:1131–1136.
105. Pardanani A, Vannucchi AM, Passamonti F, Cervantes F, Barbui T, Tefferi A. JAK inhibitor therapy for myelofibrosis: critical assessment of value and limitations. Leukemia. 2011;25:218–225.
106. Tefferi A. JAK inhibitors for myeloproliferative neoplasms: clarifying facts from myths. Blood. 2012;119:2721–2730.
107. Tam CS, Verstovsek S. Investigational Janus kinase inhibitors. Expert Opin Investig Drugs. 2013;22:687–699.
108. Nakaya Y, Shide K, Niwa T, Homan J, Sugahara S, Horio T, et al. Efficacy of NS-018, a potent and selective JAK2/Src inhibitor, in primary cells and mouse models of myeloproliferative neoplasms. Blood Cancer J. 2011;1:e29.
109. Pierce AC, ter Haar E, Binch HM, Kay DP, Patel SR, Li P. CH···O and CH···N hydrogen bonds in ligand design: a novel quinazolin-4-ylthiazol-2-ylamine protein kinase inhibitor. J Med Chem. 2005;48:1278–1281.
110. Shide K, Kameda T, Markovtsov V, Shimoda HK, Tonkin E, Fang S, et al. R723, a selective JAK2 inhibitor, effectively treats JAK2V617F-induced murine myeloproliferative neoplasm. Blood. 2011;117:6866–6875.
111. Wernig G, Kharas MG, Okabe R, Moore SA, Leeman DS, Cullen DE, et al.

Efficacy of TG101348, a selective JAK2 inhibitor, in treatment of a murine model of JAK2V617F-induced polycythemia vera. Cancer Cell. 2008;13:311–320.

112. Tyner JW, Bumm TG, Deininger J, Wood L, Aichberger KJ, Loriaux MM, et al. CYT387, a novel JAK2 inhibitor, induces hematologic responses and normalizes inflammatory cytokines in murine myeloproliferative neoplasms. Blood. 2010;115:5232–5240.

113. Wernig G, Kharas MG, Mullally A, Leeman DS, Okabe R, George T, et al. EXEL-8232, a small-molecule JAK2 inhibitor, effectively treats thrombocytosis and extramedullary hematopoiesis in a murine model of myeloproliferative neoplasm induced by MPLW515L. Leukemia. 2012;26:720–727.

114. Ostojic A, Vrhovac R, Verstovsek S. Ruxolitinib for the treatment of myelofibrosis: its clinical potential. Ther Clin Risk Manag. 2012;8:95–103.

115. Williams NK, Bamert RS, Patel O, Wang C, Walden PM, Wilks AF, et al. Dissecting specificity in the Janus kinases: the structures of JAK-specific inhibitors complexed to the JAK1 and JAK2 protein tyrosine kinase domains. J Mol Biol. 2009;387:219–232.

116. Ma L, Clayton JR, Walgren RA, Zhao B, Evans RJ, Smith MC, et al. Discovery and characterization of LY2784544, a small-molecule tyrosine kinase inhibitor of JAK2V617F. Blood Cancer J. 2011;3:e109.

117. Haferlach T. Molecular genetics in myelodysplastic syndromes. Leuk Res. 2012;36:1459–1462.

118. Nagoshi H, Horiike S, Kuroda J, Taniwaki M. Cytogenetic and molecular abnormalities in myelodysplastic syndrome. Curr Mol Med. 2011;11:678–685.

119. Garcia-Manero G. Myelodysplastic syndromes: 2011 update on diagnosis, risk-stratification, and management. Am J Hematol. 2011;86:490–498.

120. Voso MT, Fenu S, Latagliata R, Buccisano F, Piciocchi A, Aloe-Spiriti MA, Breccia M, Criscuolo M, Andriani A, Mancini S, Niscola P, Naso V, Nobile C, Piccioni AL, D'Andrea M, D'Addosio A, Leone G, Venditti A. Revised International Prognostic Scoring System (IPSS) Predicts Survival and Leukemic Evolution of Myelodysplastic Syndromes Significantly Better Than IPSS and WHO Prognostic Scoring System: Validation by the Gruppo Romano Mielodisplasie Italian Regional Database. J Clin Oncol. 2013;31:2671-2677.

121. Park MJ, Kim HJ, Kim SH, Kim DH, Kim SJ, Jang JH, Kim K, Kim WS, Jung CW. Is International Prognostic Scoring System (IPSS) still standard in predicting prognosis in patients with myelodysplastic syndrome? External validation of the

WHO Classification-Based Prognostic Scoring System (WPSS) and comparison with IPSS. Eur J Haematol. 2008;81:364-373.

122. Germing U, Lauseker M, Hildebrandt B, Symeonidis A, Cermak J, Fenaux P, Kelaidi C, Pfeilstöcker M, Nösslinger T, Sekeres M, Maciejewski J, Haase D, Schanz J, Seymour J, Kenealy M, Weide R, Lübbert M, Platzbecker U, Valent P, Götze K, Stauder R, Blum S, Kreuzer KA, Schlenk R, Ganser A, Hofmann WK, Aul C, Krieger O, Kündgen A, Haas R, Hasford J, Giagounidis A. Survival, prognostic factors and rates of leukemic transformation in 381 untreated patients with MDS and del(5q): a multicenter study. Leukemia. 2012;26:1286-1292.

123. Greenberg PL, Tuechler H, Schanz J, Sanz G, Garcia-Manero G, Solé F, Bennett JM, Bowen D, Fenaux P, Dreyfus F, Kantarjian H, Kuendgen A, Levis A, Malcovati L, Cazzola M, Cermak J, Fonatsch C, Le Beau MM, Slovak ML, Krieger O, Luebbert M, Maciejewski J, Magalhaes SM, Miyazaki Y, Pfeilstöcker M, Sekeres M, Sperr WR, Stauder R, Tauro S, Valent P, Vallespi T, van de Loosdrecht AA, Germing U, Haase D. Revised international prognostic scoring system for myelodysplastic syndromes. Blood. 2012;120:2454-2465.

124. Schlegelberger B, Göhring G, Thol F, Heuser M. Update on cytogenetic and molecular changes in myelodysplastic syndromes. Leuk Lymphoma. 2012;53:525-536.

125. Cutler C. Allogeneic hematopoietic stem-cell transplantation for myelodysplastic syndrome. Hematology Am Soc Hematol Educ Program. 2010;2010:325-329.

126. van der Straaten HM, van Biezen A, Brand R, Schattenberg AV, Egeler RM, Barge RM, Cornelissen JJ, Schouten HC, Ossenkoppele GJ, Verdonck LF; Netherlands Stem Cell Transplant Registry "TYPHON". Allogeneic stem cell transplantation for patients with acute myeloid leukemia or myelodysplastic syndrome who have chromosome 5 and/or 7 abnormalities. Haematologica. 2005;90:1339-1345.

127. Mühlemann K, Wenger C, Zenhäusern R, Täuber MG. Risk factors for invasive aspergillosis in neutropenic patients with hematologic malignancies. Leukemia. 2005;19:545-550.

128. Kume H, Yamazaki T, Abe M, Tanuma H, Okudaira M, Okayasu I. Increase in aspergillosis and severe mycotic infection in patients with leukemia and MDS: comparison of the data from the Annual of the Pathological Autopsy Cases in Japan in 1989, 1993 and 1997. Pathol Int. 2003;53:744-750.

129. Fenaux P, Mufti GJ, Hellstrom-Lindberg E, Santini V, Finelli C, Giagounidis A, Schoch R, Gattermann N, Sanz G, List A, Gore SD, Seymour JF, Bennett JM, Byrd J, Backstrom J, Zimmerman L, McKenzie D, Beach C, Silverman LR; International Vidaza High-Risk MDS Survival Study Group. Efficacy of azacitidine compared with that of conventional care regimens in the treatment of higher-risk myelodysplastic syndromes: a randomised, open-label, phase III study. Lancet Oncol. 2009;10:223-232.

130. Starr R, Willson TA, Viney EM, Murray LJ, Rayner JR, Jenkins BJ, Gonda TJ, Alexander WS, Metcalf D, Nicola NA, Hilton DJ. A family of cytokine-inducible inhibitors of signalling. Nature. 1997;387:917-921.

131. Schultheis B, Carapeti-Marootian M, Hochhaus A, Weisser A, Goldman JM, Melo JV. Overexpression of SOCS-2 in advanced stages of chronic myeloid leukemia: possible inadequacy of a negative feedback mechanism. Blood. 2002;99:1766-1775.

132. Kuroda J, Yamamoto M, Sasaki N, Taniwaki M. Multifaceted Mechanisms for Cell Survival in Chronic Myelogenous Leukemia. Curr Cancer Drug Targets. 2013;13:69-79.

133. Schmitt-Graeff AH, Teo SS, Olschewski M, Schaub F, Haxelmans S, Kirn A, Reinecke P, Germing U, Skoda RC. JAK2V617F mutation status identifies subtypes of refractory anemia with ringed sideroblasts associated with marked thrombocytosis. Haematologica. 2008;93:34-40.

134. Brakensiek K, Länger F, Schlegelberger B, Kreipe H, Lehmann U. Hypermethylation of the suppressor of cytokine signalling-1 (SOCS-1) in myelodysplastic syndrome. Br J Haematol. 2005;130:209-217.

135. Zhang Y, Zhao D, Zhao H, Wu X, Zhao W, Wang Y, Xia B, Da W. Hypermethylation of SHP-1 promoter in patient with high-risk myelodysplastic syndrome and it predicts poor prognosis. Med Oncol. 2012;29:2359-2363.

136. Harris NL, Jaffe ES, Diebold J, Flandrin G, Muller-Hermelink HK, Vardiman J, Lister TA, Bloomfield CD. World Health Organization classification of neoplastic diseases of the hematopoietic and lymphoid tissues: report of the Clinical Advisory Committee meeting-Airlie House, Virginia, November 1997. J Clin Oncol. 1999;17:3835-3849.

137. Nakaya Y, Shide K, Naito H, Niwa T, Horio T, Miyake J, Shimoda K. Effect of NS-018, a selective JAK2V617F inhibitor, in a murine model of myelofibrosis. Blood Cancer J, 2014;4:e174.

138. Kuroda J, Puthalakath H, Cragg MS, Kelly PN, Bouillet P, Huang DC, Kimura S, Ottmann OG, Druker BJ, Villunger A, Roberts AW, Strasser A. Bim and Bad mediate imatinib-induced killing of Bcr/Abl+ leukemic cells, and resistance due to their loss is overcome by a BH3 mimetic. Proc Natl Acad Sci U S A. 2006;103:14907-10412.
139. Tsutsumi Y, Chinen Y, Sakamoto N, Nagoshi H, Nishida K, Kobayashi S, Yokokawa Y, Taki T, Sasaki N, Yamamoto-Sugitani M, Kobayashi T, Matsumoto Y, Horiike S, Kuroda J, Taniwaki M. Deletion or methylation of CDKN2A/2B and PVT1 rearrangement occur frequently in highly aggressive B-cell lymphomas harboring 8q24 abnormality. Leuk Lymphoma. 2013;54:2760-2764.
140. Jonásova A, Neuwirtová R, Cermák J, Vozobulová V, Mociková K, Sisková M, Hochová I. Cyclosporin A therapy in hypoplastic MDS patients and certain refractory anaemias without hypoplastic bone marrow. Br J Haematol. 1998;100:304-309.
141. Asano Y, Maeda M, Uchida N, Yokoyama T, Osaki K, Shimoda K, Gondo H, Okamura T, Okamura S, Niho Y. Immunosuppressive therapy for patients with refractory anemia. Ann Hematol. 2001;80:634-638.
142. Sanada M, Ogawa S. Genome-wide analysis of myelodysplastic syndromes. Curr Pharm Des. 2012;18:3163-3169.
143. Ogawa S. Splicing factor mutations in myelodysplasia. Int J Hematol. 2012;96:438-442.
144. Pang WW, Pluvinage JV, Price EA, Sridhar K, Arber DA, Greenberg PL, Schrier SL, Park CY, Weissman IL. Hematopoietic stem cell and progenitor cell mechanisms in myelodysplastic syndromes. Proc Natl Acad Sci U S A. 2013;110:3011-3016.
145. Boehrer S, Adès L, Braun T, Galluzzi L, Grosjean J, Fabre C, Le Roux G, Gardin C, Martin A, de Botton S, Fenaux P, Kroemer G. Erlotinib exhibits antineoplastic off-target effects in AML and MDS: a preclinical study. Blood. 2008;111:2170-2180.
146. Verstovsek S, Tam CS, Wadleigh M, Sokol L, Smith CC, Bui LA, Song C, Clary DO, Olszynski P, Cortes J, Kantarjian H, Shah NP. Phase I evaluation of XL019, an oral, potent, and selective JAK2 inhibitor. Leuk Res. 2014;38:316-322.

Acknowledgements

All the experiments presented in this thesis was carried out in the discovery research laboratory in Nippon Shinyaku Co,.Ltd. The study as an engineering science was performed in the laboratory of Professor Jun Miyake, in the Department of Mechanical Science and Bioengineering, the Graduate School of Engineering Science, Osaka University. Completion of this thesis is impossible without the support of many people.

The first and foremost, I wish to express my deepest gratitude to Professor Jun Miyake for his invaluable guidance and cordial encouragement to my research.

I would like to thank Professor Masahito Taya and Professor Tsutomu Araki in the Graduate School of Engineering Science, Osaka University, and Professor Nobuhiko Yamamoto in the Graduate School of Frontier Biosciences, Osaka University, for reviewing my dissertation carefully.

I would also like to thank Professor Fujio Murakami in the Graduate School of Frontier Biosciences, Osaka University, for his support and encouragement.

I express my appreciation to Professor Shinya Kimura (Saga University) and Professor Kazuya Shimoda (Miyazaki University) for the collaboration and guidance to my research.

I would like to acknowledge Dr. Junya Kuroda (Kyoto Prefectural University of Medicine) and Dr. Kotaro Shide (Miyazaki University) for their advice, support, and encouragement. The discussion with them always motivates me.

I would also like to thank my colleagues in Nippon Shinyaku for their support, assistance, and advice in my research and daily life. Especially, Dr. Haruna Naito always supported my research. I give thanks to Dr. Tomoko Niwa for her support. I give thanks to Dr. Gerald E Smyth for English language editing of the manuscript.

I was financially supported by the Doctor degree support system in Nippon Shinyaku Co,.Ltd. I would like to thank the system.

Finally, I am deeply grateful to my family, especially my wife Iku, who made my studies possible by her support at home.

<u>Copyright permission</u>

Publication list

Original papers

1. Shinya Kimura, Haruna Naito, Hidekazu Segawa, Junya Kuroda, Takeshi Yuasa, Kiyoshi Sato, Asumi Yokota, Yuri Kamitsuji, Eri Kawata, Eishi Ashihara, Yohei Nakaya, Haruna Naruoka, Tatsushi Wakayama, Kimio Nasu, Tetsuo Asaki, Tomoko Niwa, Kazuko Hirabayashi, Taira Maekawa. NS-187, a potent and selective dual Bcr-Abl/Lyn tyrosine kinase inhibitor, is a novel agent for imatinib-resistant leukemia. Blood. 2005; 106(12): 3948–3954.
   http://dx.doi.org/10.1182/blood-2005-06-2209

2. Haruna Naito, Shinya Kimura, Yohei Nakaya, Haruna Naruoka, Sachie Kimura, Shinsaku Ito, Tatsushi Wakayama, Taira Maekawa, Kazuko Hirabayashi. In vivo antiproliferative effect of NS-187, a dual Bcr-Abl/Lyn tyrosine kinase inhibitor, on leukemic cells harbouring Abl kinase domain. Leukemia Research. 2006; 30(11): 1443–1446.
   http://dx.doi.org/10.1016/j.leukres.2006.01.006

3. Yohei Nakaya, Kotaro Shide, Tomoko Niwa, Junko Homan, Seishi Sugahara, Tatsuya Horio, Kazuya Kuramoto, Takashi Kotera, Hiroshi Shibayama, Katsutoshi Hori, Haruna Naito, Kazuya Shimoda. Efficacy of NS-018, a potent and selective JAK2/Src inhibitor, in primary cells and mouse models of myeloproliferative neoplasms. Blood Cancer Journal. 2011; 1: e29.
   http://dx.doi.org/10.1038/bcj.2011.29

4. Yohei Nakaya, Kotaro Shide, Haruna Naito, Tomoko Niwa, Tatsuya Horio, Jun Miyake, Kazuya Shimoda. Effect of NS-018, a selective JAK2V617F inhibitor, in a murine model of myelofibrosis. Blood Cancer Journal. 2014; 4: e174.
   http://dx.doi.org/10.1038/bcj.2013.73

5. Junya Kuroda, Ayumi Kodama, Yoshiaki Chinen, Yuji Shimura, Shinsuke Mizutani, Hisao Nagoshi, Tsutomu Kobayashi, Yosuke Matsumoto, Yohei Nakaya, Ayako Tamura, Yutaka Kobayashi, Haruna Naito, Masafumi Taniwaki. NS-018, a selective

JAK2 inhibitor, preferentially inhibits CFU-GM colony formation by bone marrow mononuclear cells from high-risk myelodysplastic syndrome patients. Leukemia Research. 2014; 38(5): 619–624.
http://dx.doi.org/10.1016/j.leukres.2014.03.001

International conferences

1. Naito H, Kimura S, Nakaya Y, Naruoka H, Wakayama T, Kimura S, Ito S, Ashihara E, Maekawa T, Hirabayashi K. Simultaneous Targeting of Lyn and Bcr-Abl Kinases by NS-187 Cures Mice Bearing Imatinib-Resistant Leukemic Cells. 47th American Society of Hematology Annual Meeting. December 2005, Atlanta, USA. (Blood Abstracts 2005,106:1518.)

2. Nakaya Y, Naito H, Homan J, Sugahara S, Horio T, Niwa T, Shide K, Shimoda K. Preferential Inhibition of an Activated Form of Janus Kinase 2 (JAK2) by a Novel JAK2 Inhibitor, NS-018. 52nd American Society of Hematology Annual Meeting. December 2010, Orlando, USA. (Blood Abstracts 2010,116:4107.)

3. Shide K, Nakaya Y, Kameda T, Shimoda H, Hidaka T, Katayose K, Kubuki Y, Matsunaga T, Homan J, Kotera T, Shibayama H, Naito H, Shimoda K. NS-018, a Potent Novel JAK2 Inhibitor, Effectively Treats MurineMPN Induced by the JAK2V617F mutant. 52nd American Society of Hematology Annual Meeting. December 2010, Orlando, USA. (Blood Abstracts 2010,116:4106.)

4. Nakaya Y, Shide K, Naito H, Niwa T, Horio T, Miyake J, Shimoda K. NS-018, a Selective JAK2V617F Inhibitor, Improves JAK2V617F-induced Murine Myelofibrosis without Decreasing the Erythrocyte or Platelet Count. 55th American Society of Hematology Annual Meeting. December 2013, New Orleans, USA. (Blood Abstracts 2013,122:3847.)

5. Kodama A, Naito H, Nakaya Y, Tamura A, Chinen Y, Taki T, Kuroda J, Taniwaki M. The JAK2-Selective Inhibitor NS-018 Preferentially Suppresses CFU-GM Colony Formation by Bone-Marrow Cells from High-risk Myelodysplastic Syndrome Patients. 55th American Society of Hematology Annual Meeting. December 2013, New Orleans, USA. (Blood Abstracts 2013,122:1286.)